Climate4you update June 2020

Contents:

June 2020 global surface air temperature overview

General: This newsletter contains graphs and diagrams showing a selection of key meteorological variables, if possible updated to the most recent past month. All temperatures are given in degrees Celsius.

In the maps on pages 3-4, showing the geographical pattern of surface air temperature anomalies, the last previous 10 years are used as reference period.

The rationale for comparing with this recent period instead of the official WMO so-called 'normal' period 1961-1990, is that the latter period is affected by the cold period 1945-1980. Most comparisons with this period will inevitably appear as warm, and it will be difficult to decide if modern temperatures are increasing or decreasing. Comparing instead with the last previous 10 years overcomes this problem and clearer displays the modern dynamics of ongoing change. This decadal approach also corresponds well to the typical memory horizon for many people and is now also adopted as reference period by other institutions, e.g. the Danish Meteorological Institute (DMI).

In addition, most temperature databases display temporal instability for data before the turn of the century (see, e.g., p. 8). Any comparison with the WMO reference period 1961-1990 will therefore be influenced by such ongoing monthly changes of mainly administrative nature. An unstable value is clearly not suited as reference value. Simply comparing with the last previous 10 years is more useful as reference for modern changes. See also additional reflections on page 47.

The different air temperature records have been divided into three quality classes, QC1, QC2 and QC3, respectively, as described on page 8.

In many diagrams shown in this newsletter the thin line represents the monthly global average value, and the thick line indicate a simple running average, in most cases a simple moving 37-month average, nearly corresponding to a three-year average. The 37-month average is calculated from values covering a range from 18 months before to 18 months after, with equal weight given to all individual months.

The year 1979 has been chosen as starting point in many diagrams, as this roughly corresponds to both the beginning of satellite observations and the onset of the late 20th century warming period. However, several of the data series have a much longer record length, which may be inspected in greater detail on www.climate4you.com.

June 2020 Remote Sensed Surface Temperature

General: For June 2020 AIRS supplied 16200 interpolated surface air data points, obtained from the GISS data portal. According to most surface temperature databases, the June 2020 global average air temperature anomaly was somewhat lower than estimated for the previous month.

The Northern Hemisphere 10-yr temperature anomality pattern (p.3) was characterised by regional contrasts, mainly controlled by the dominant jet stream configuration. Northern Siberia, eastern Canada and the Nordic countries were relatively warm, while much of Asia, western North America and most of Europe were relatively cold, compared to the average for the previous 10 years. Ocean wise, much of northern Pacific was relatively warm, as was large parts of the Norwegian Sea. In contrast southern and central North Atlantic was relatively cold. In the Arctic relatively low temperatures dominated in NW Russia, Greenland and over much of Canada and Alaska, while the remaining central arctic regions were relatively warm.

Near the Equator temperatures were mostly near or slightly below the 10-year average.

The Southern Hemisphere temperatures were largely near or below the average for the previous 10 years. Parts of Australia and central South America were relatively warm, while most other regions were relatively cold or near the 10-yr average. A zone of relatively low surface air temperatures dominated between 20°S and 60°S, affecting ocean as well as land areas. In the Antarctic, regional surface air temperatures were mainly above the 10-year average, although several coastal regions had below average temperatures.

June 2020 global surface air temperature overview versus average June last 10 years

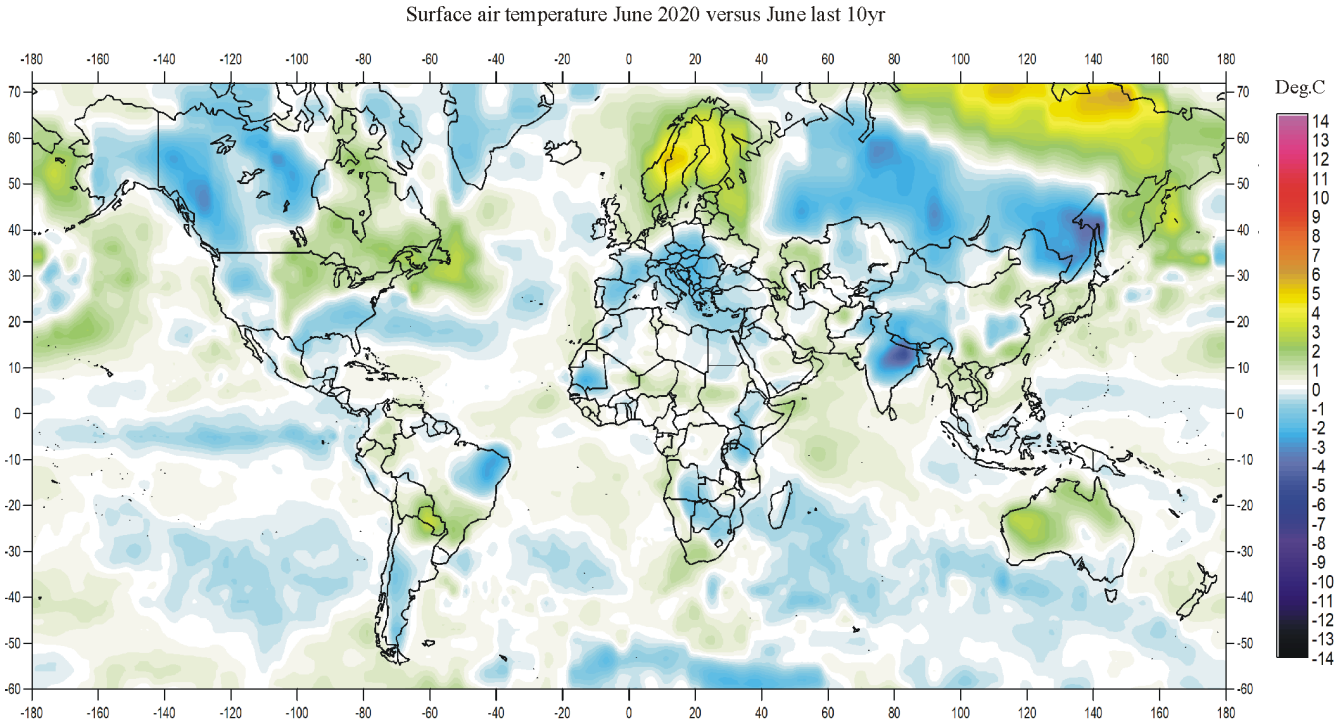

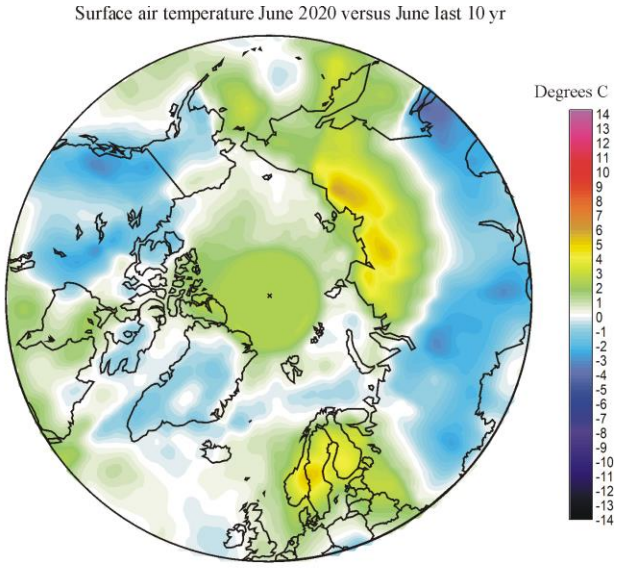

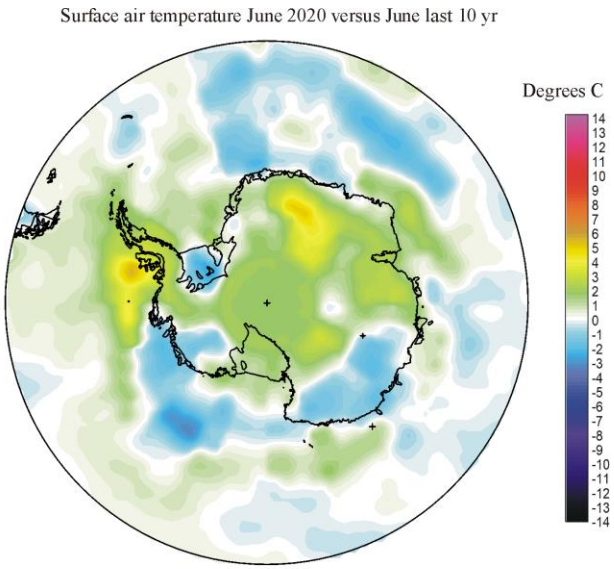

June 2020 surface air temperature compared to the average of June over the last 10 years. Green-yellow-red colours indicate areas with higher temperature than the 10-year average, while blue colours indicate lower than average temperatures. Data source: Remote Sensed Surface Temperature Anomaly, AIRS/Aqua L3 Monthly Standard Physical Retrieval 1 degree x 1 degree V006 (https://airs.jpl.nasa.gov/), obtained from the GISS data portal (https://data.giss.nasa.gov/gistemp/maps/index_v4.html).

June 2020 global surface air temperature compared to June 2019

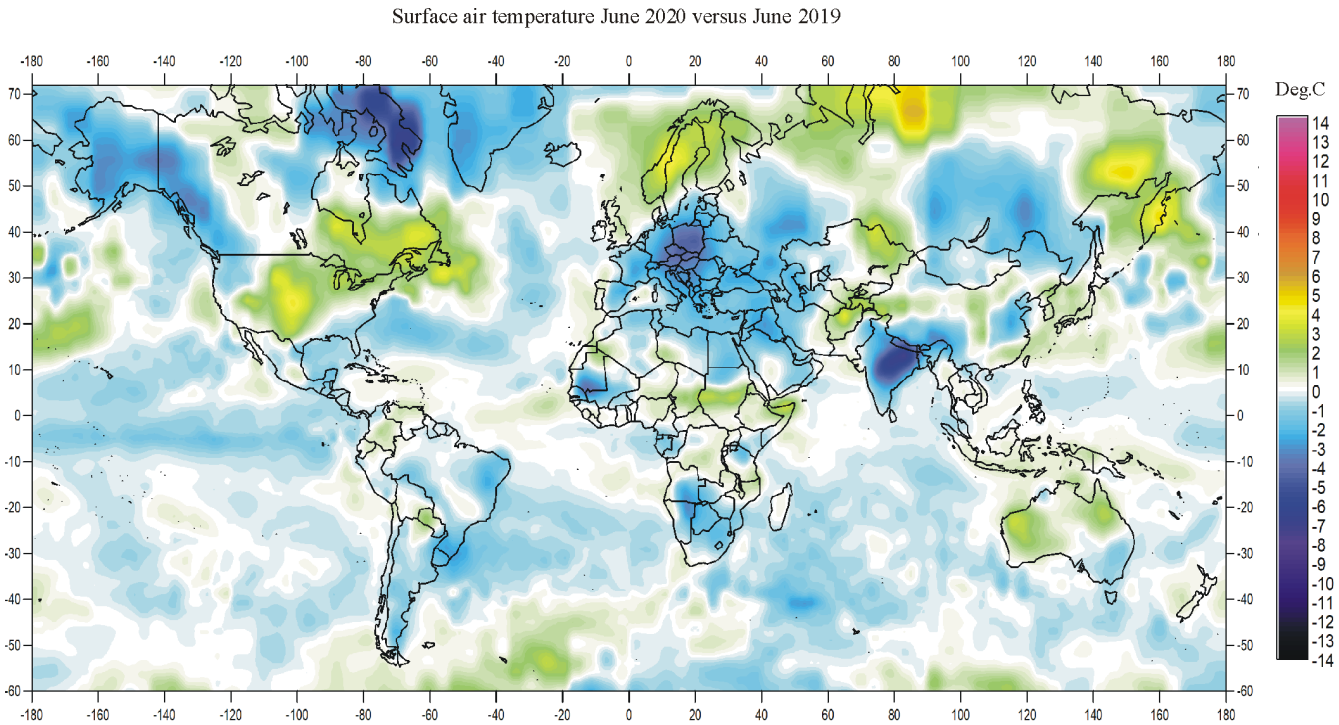

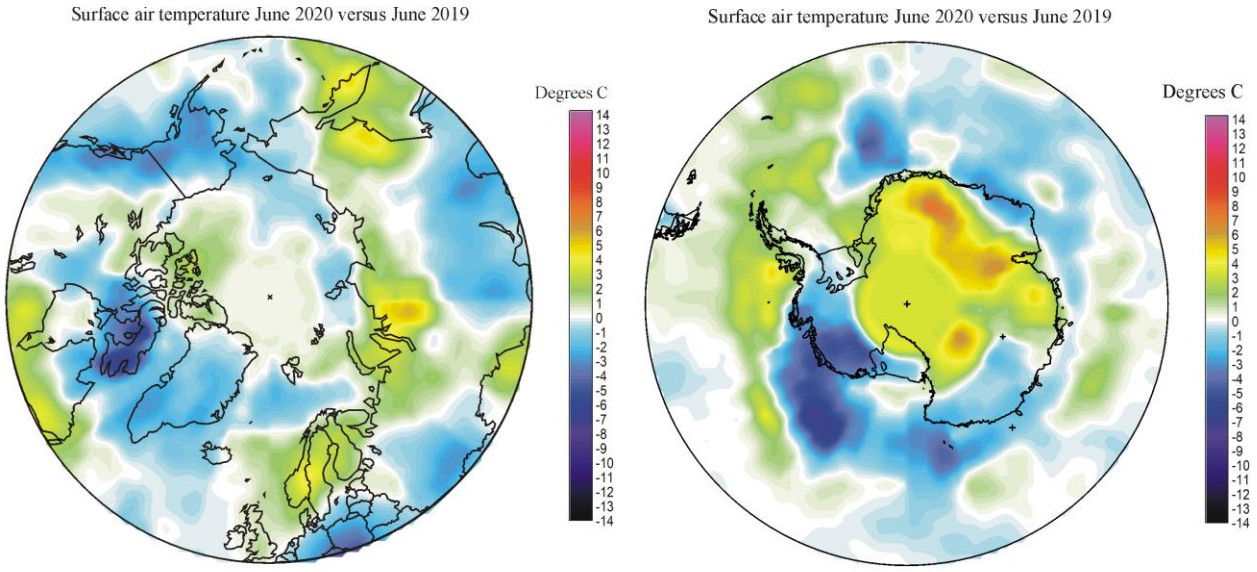

June 2020 surface air temperature compared to June 2019. Green-yellow-red colours indicate regions where the present month was warmer than last year, while blue colours indicate regions where the present month was cooler than one year ago. Variations in monthly temperature from one year to the next has no tangible climatic importance but may nevertheless be interesting to study. Data source: Remote Sensed Surface Temperature Anomaly, AIRS/Aqua L3 Monthly Standard Physical Retrieval 1 degree x 1 degree V006 (https://airs.jpl.nasa.gov/), obtained from the GISS data portal (https://data.giss.nasa.gov/gistemp/maps/index_v4.html).

Temperature quality class 1: Lower troposphere temperature from satellites, updated to June 2020

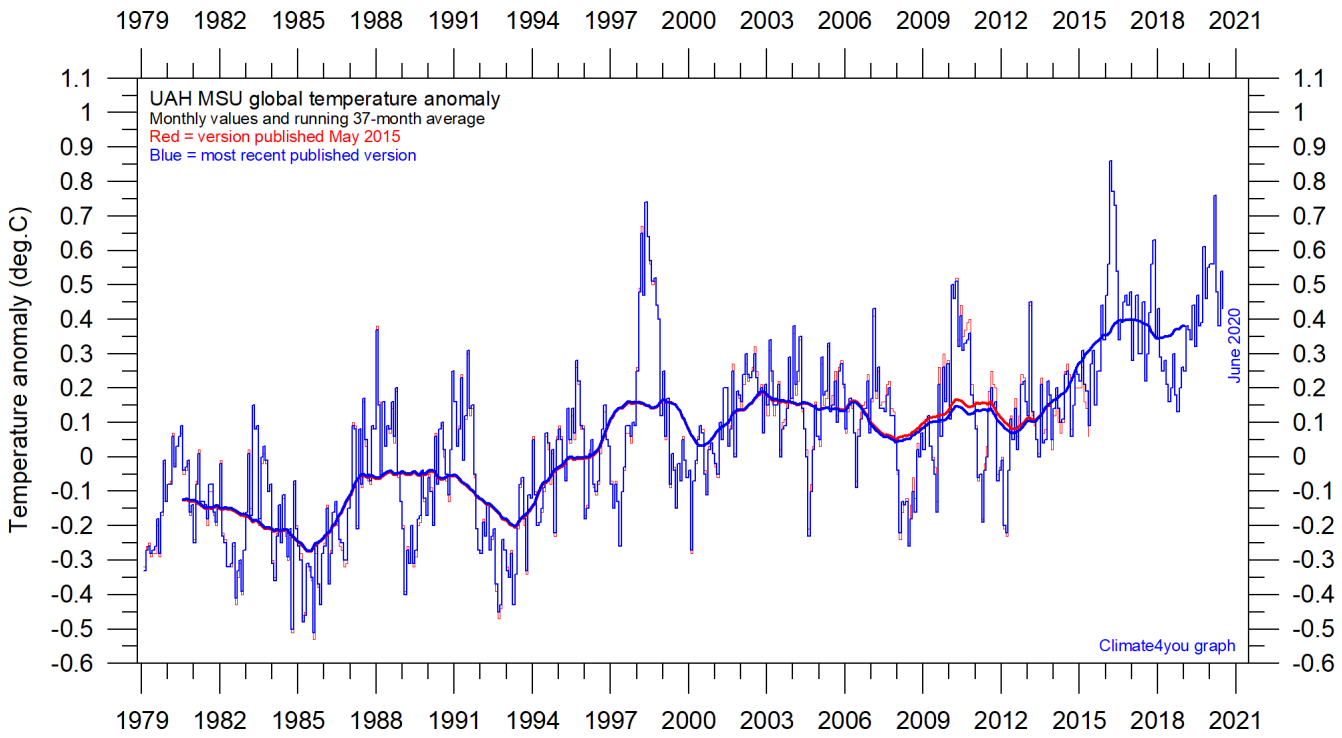

Global monthly average lower troposphere temperature (thin line) since 1979 according to University of Alabama at Huntsville, USA. The thick line is the simple running 37-month average.

5

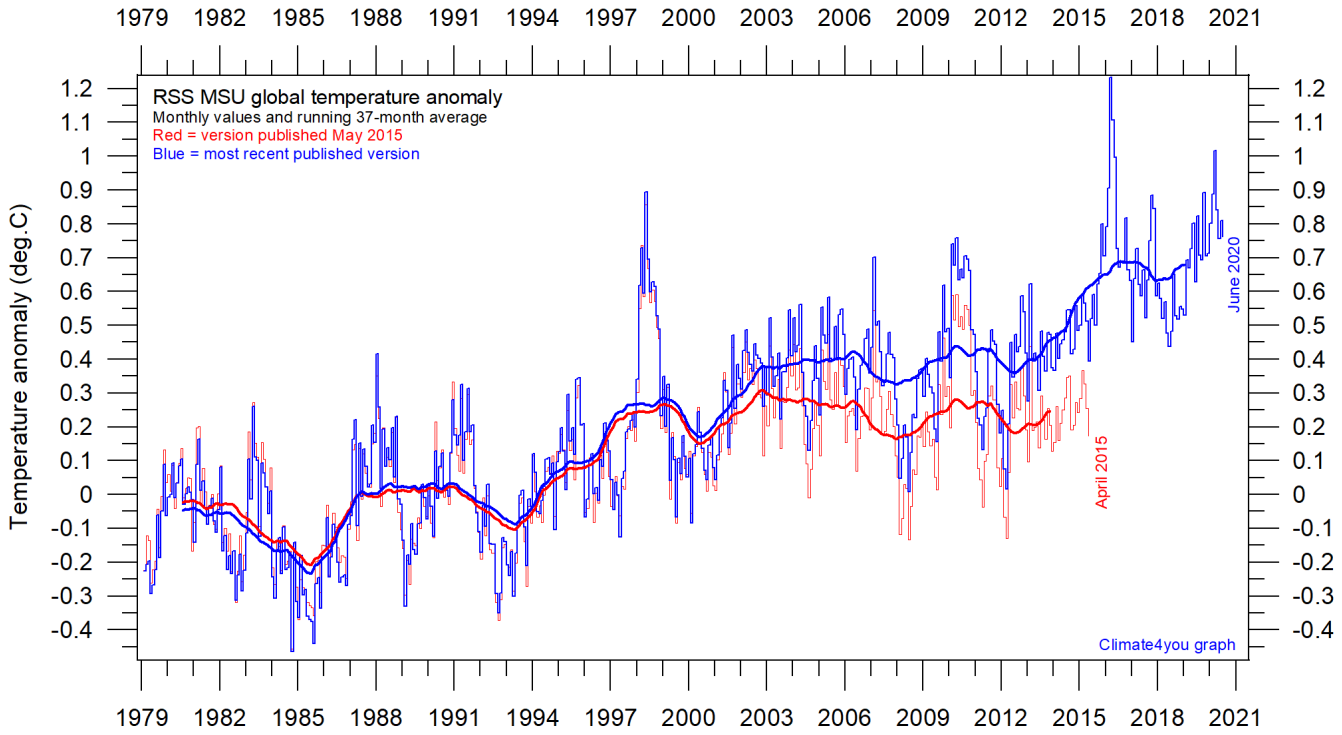

Global monthly average lower troposphere temperature (thin line) since 1979 according to according to Remote Sensing Systems (RSS), USA. The thick line is the simple running 37-month average.

Temperature quality class 2: HadCRUT global surface air temperature, updated to May 2020

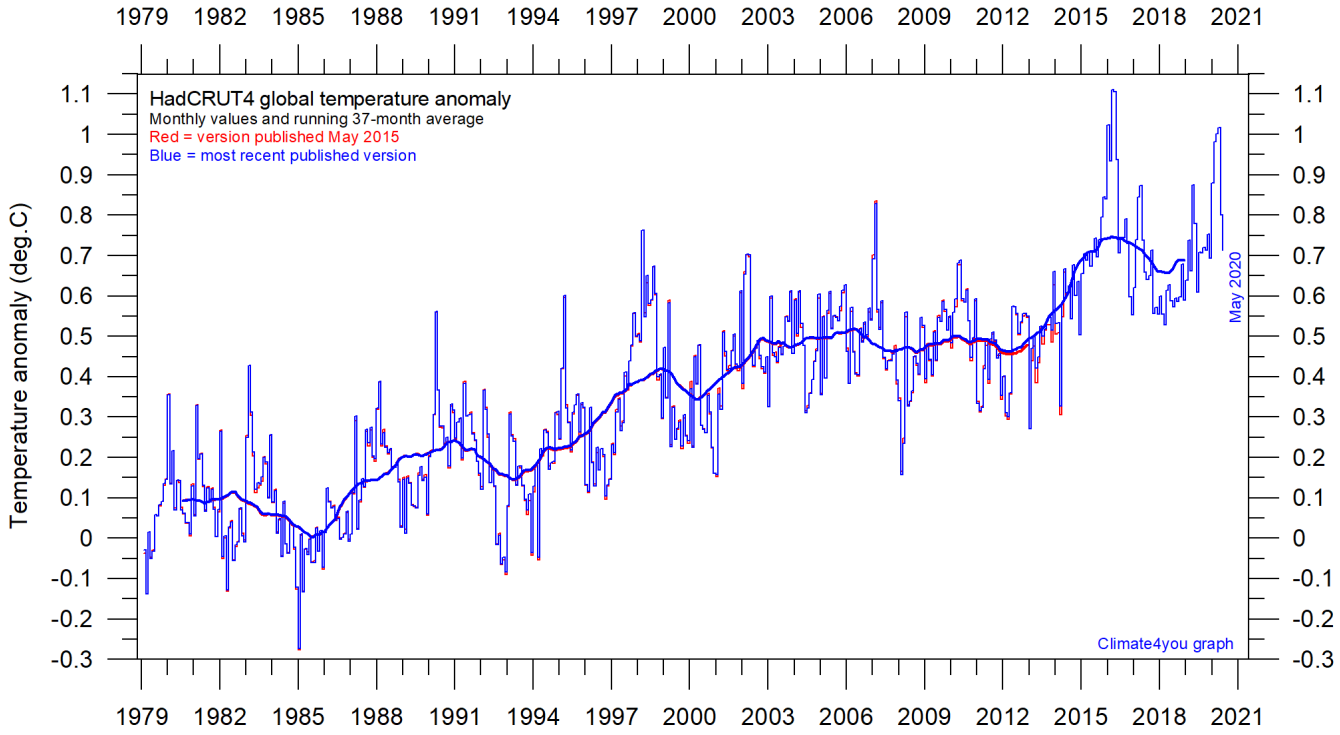

Global monthly average surface air temperature (thin line) since 1979 according to according to the Hadley Centre for Climate Prediction and Research and the University of East Anglia's Climatic Research Unit (CRU), UK. The thick line is the simple running 37-month average.

Temperature quality class 3: GISS and NCDC global surface air temperature, updated to June 2020

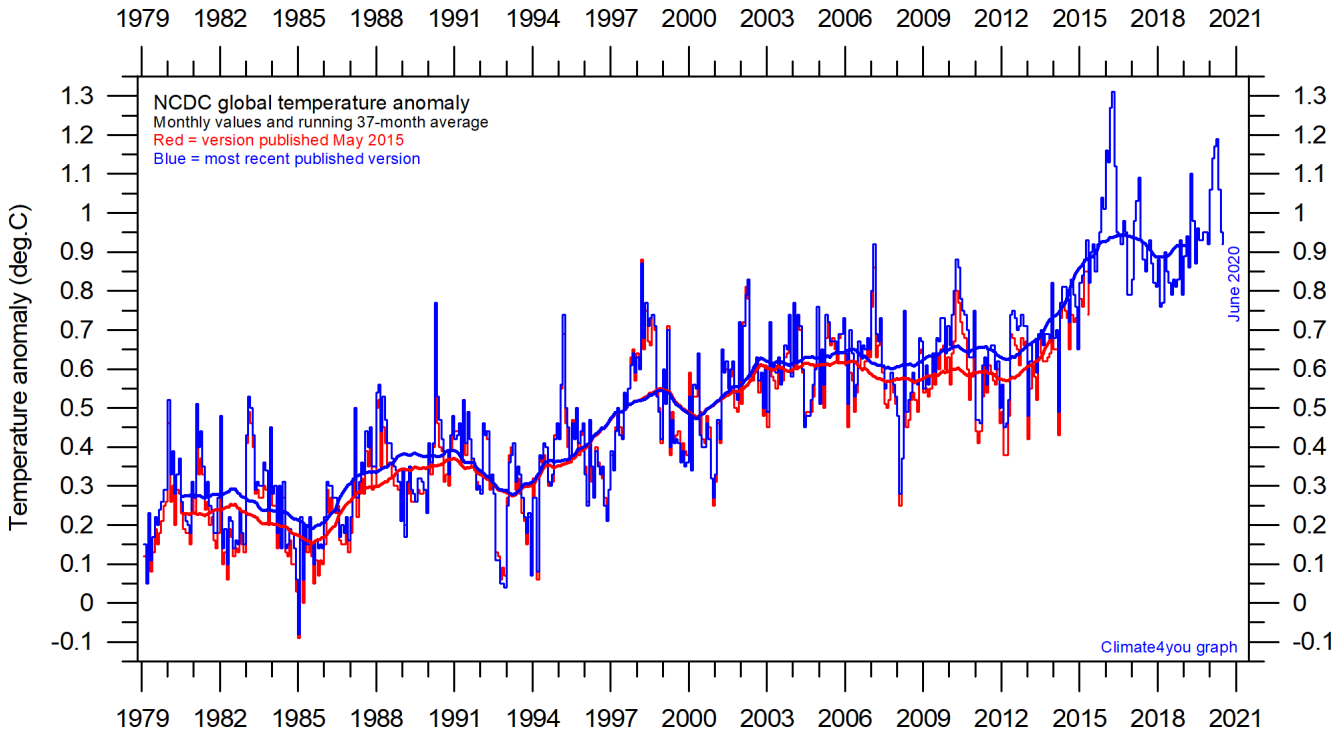

Global monthly average surface air temperature since 1979 according to according to the National Climatic Data Center (NCDC), USA. The thick line is the simple running 37-month average.

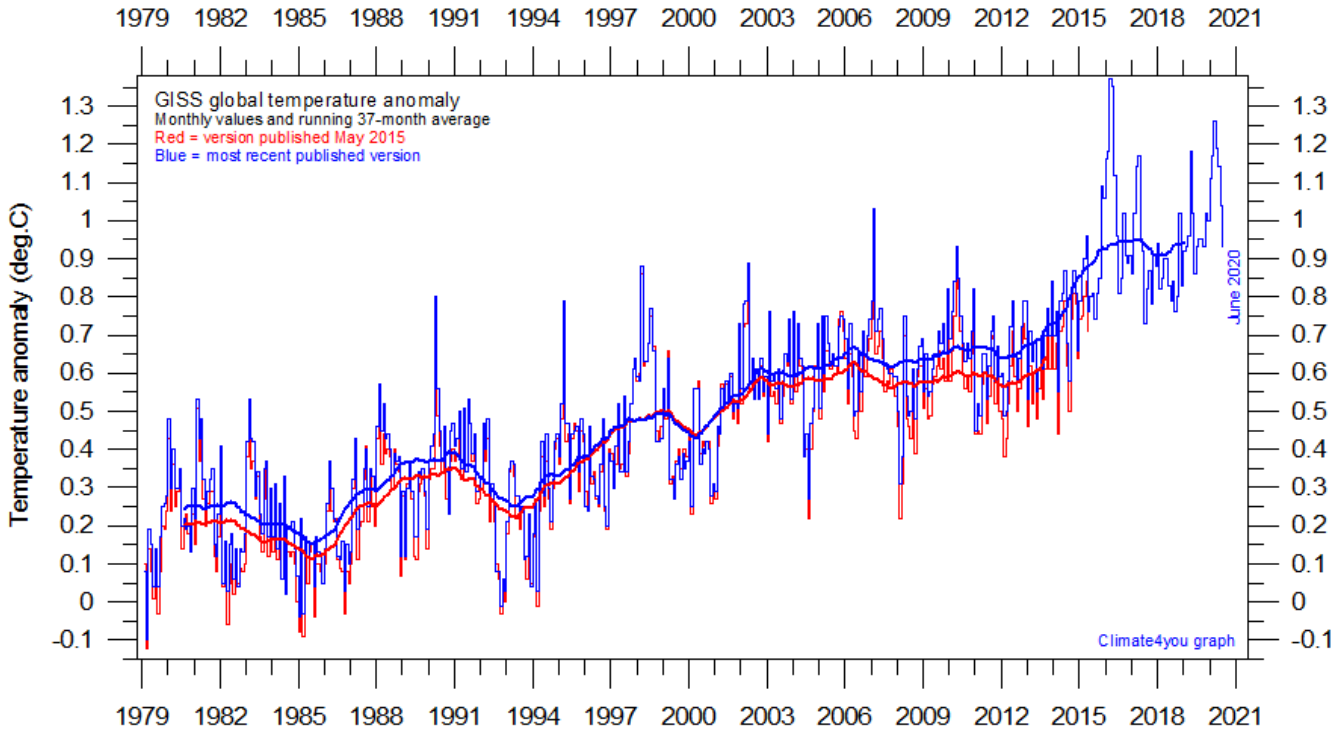

Global monthly average surface air temperature (thin line) since 1979 according to according to the Goddard Institute for Space Studies (GISS), at Columbia University, New York City, USA, using ERSST_v4 ocean surface temperatures. The thick line is the simple running 37-month average.

A note on data record stability and -quality:

The temperature diagrams shown above all have 1979 as starting year. This roughly marks the beginning of the recent episode of global warming, after termination of the previous episode of global cooling from about 1940. In addition, the year 1979 also represents the starting date for the satellite-based global temperature estimates (UAH and RSS). For the three surface air temperature records (HadCRUT, NCDC and GISS), they begin much earlier (in 1850 and 1880, respectively), as can be inspected on www.climate4you.com.

For all three surface air temperature records, but especially NCDC and GISS, administrative changes to anomaly values are quite often introduced, even affecting observations many years back in time. Some changes may be due to the delayed addition of new station data or change of station location, while others probably have their origin in changes of the technique adopted to calculate average values. It is clearly impossible to evaluate the validity of such administrative changes for the outside user of these records; it is only possible to note that such changes quite often are introduced (se example diagram next page).

In addition, the three surface records represent a blend of sea surface data collected by moving ships or by other means, plus data from land stations of partly unknown quality and unknown degree of representativeness for their region. Many of the land stations also has been moved geographically during their period of operation, instrumentation have been changed, and they are influenced by changes in their near surroundings (vegetation, buildings, etc.).

The satellite temperature records also have their problems, but these are generally of a more technical nature and therefore better correctable. In addition, the temperature sampling by satellites is more regular and complete on a global basis than that represented by the surface records. It is also important that the sensors on satellites measure temperature directly by emitted radiation, while most modern surface temperature measurements are indirect, using electronic resistance.

Everybody interested in climate science should gratefully acknowledge the big efforts put into maintaining the different temperature databases referred to in the present newsletter. At the same time, however, it is also important to realise that all temperature records cannot be of equal scientific quality. The simple fact that they to some degree differ shows that they cannot all be correct.

On this background, and for practical reasons, Climate4you therefore operates with three quality classes (1-3) for global temperature records, with 1 representing the highest quality level:

Quality class 1: The satellite records (UAH and RSS).

Quality class 2: The HadCRUT surface record.

Quality class 3: The NCDC and GISS surface records.

The main reason for discriminating between the three surface records is the following:

While both NCDC and GISS often experience quite large administrative changes (see example on p.8), and therefore essentially are unstable temperature records, the changes introduced to HadCRUT are fewer and smaller. For obvious reasons, as the past does not change, any record undergoing continuing changes cannot describe the past correctly all the time. Frequent and large corrections in a database of cause signal a fundamental doubt about what is likely to represent the correct values.

You can find more on the issue of lack of temporal stability on www.climate4you.com (go to: *Global Temperature*, and then proceed to *Temporal Stability*).

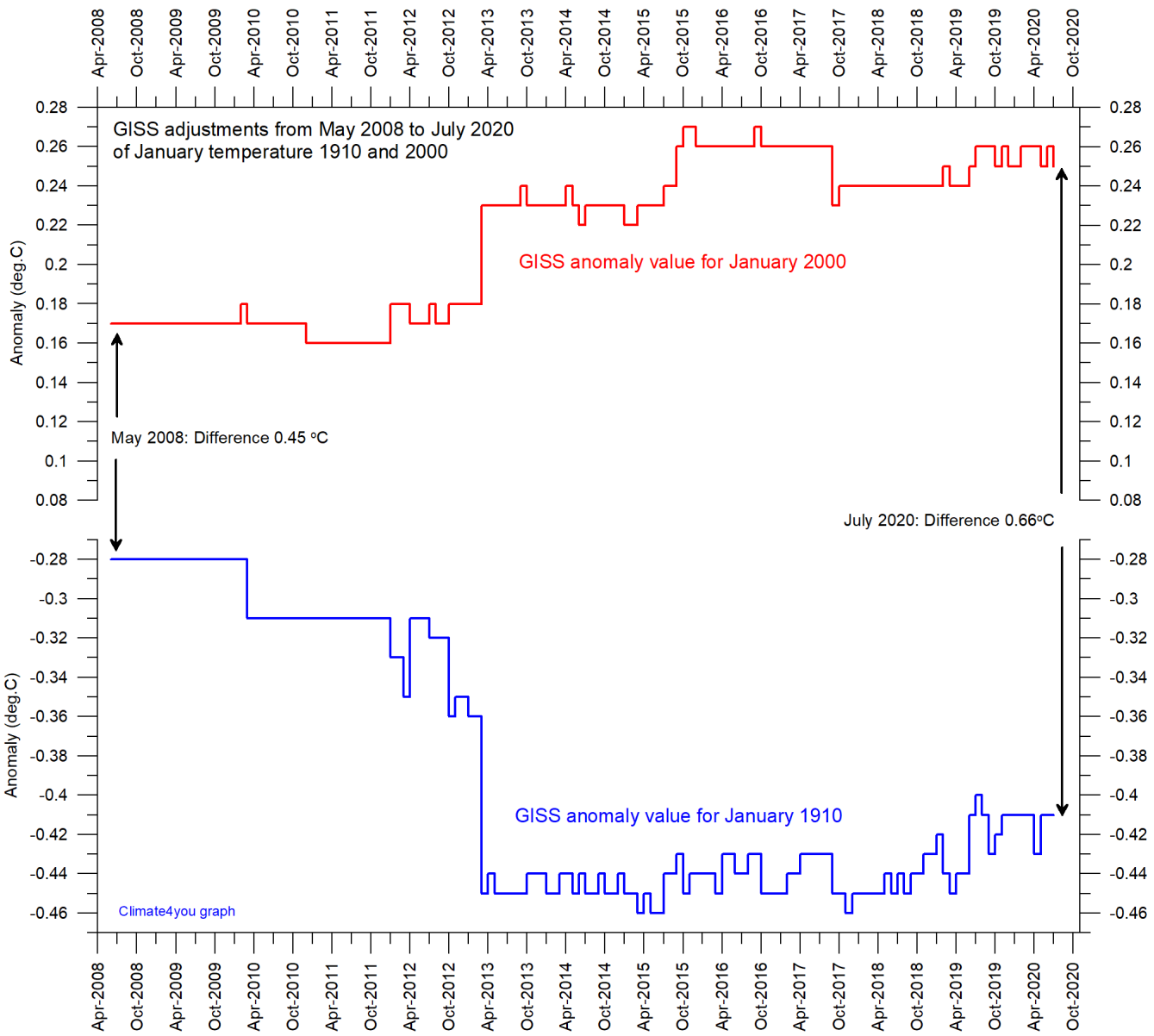

Diagram showing the adjustments made since May 2008 by the [Goddard Institute for Space Studies](#) (GISS), USA, in published anomaly values for the months January 1910 and January 2000.

The administrative upsurge of the temperature increase from January 1915 to January 2000 has grown from 0.45 (reported May 2008) to 0.66°C (reported July 2020). This represents an about 47% administrative temperature increase over this period, meaning that nearly half of the apparent global temperature increase from January 1910 to January 2000 (as reported by GISS) is due to administrative changes of the original data since May 2008.

Comparing global surface air temperature and lower troposphere satellite temperatures; updated to May 2020

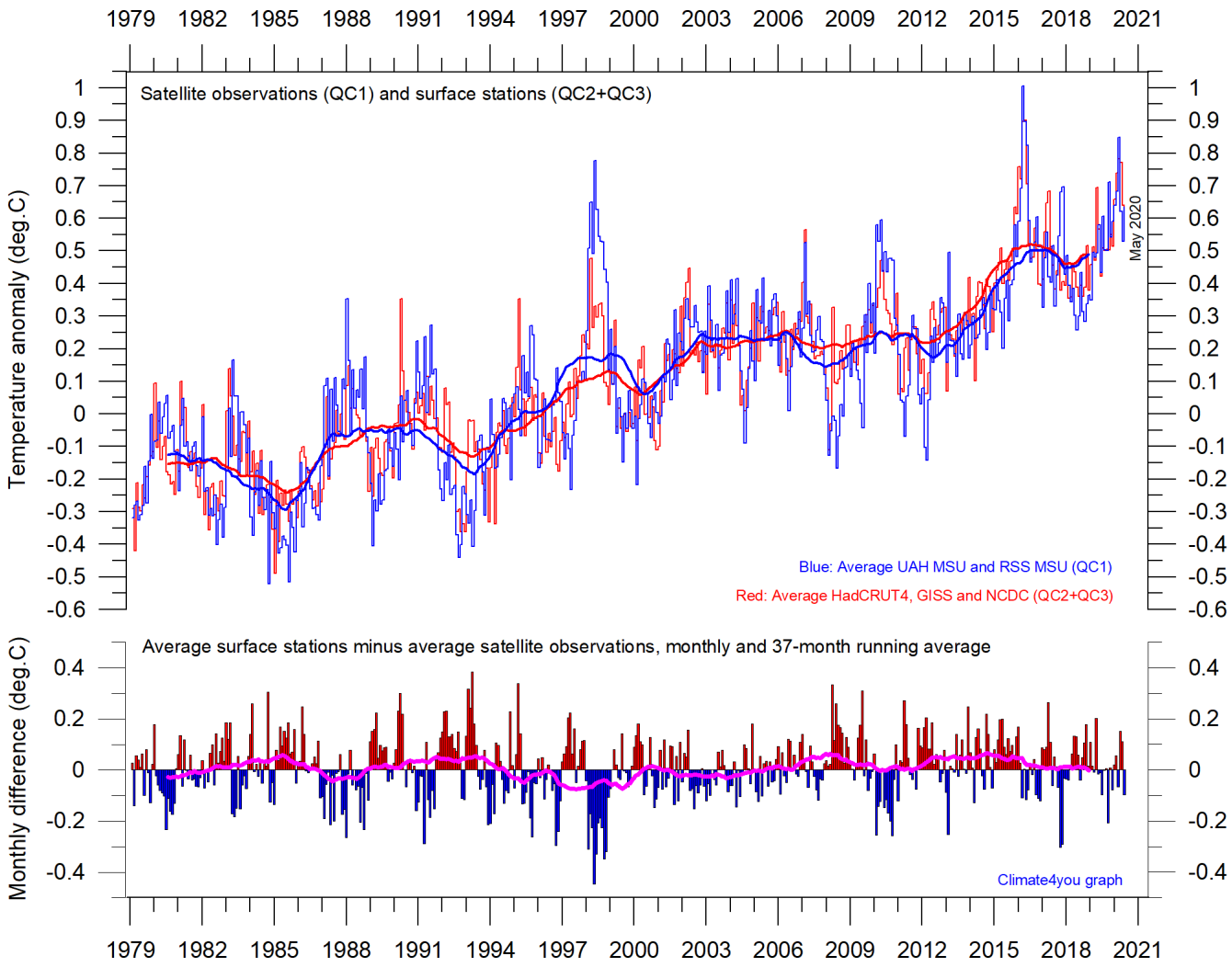

Plot showing the average of monthly global surface air temperature estimates (HadCRUT4, GISS and NCDC) and satellite-based temperature estimates (RSS MSU and UAH MSU). The thin lines indicate the monthly value, while the thick lines represent the simple running 37-month average, nearly corresponding to a running 3-yr average. The lower panel shows the monthly difference between average surface air temperature and satellite temperatures. As the base period differs for the different temperature estimates, they have all been normalised by comparing to the average value of 30 years from January 1979 to December 2008.

Global air temperature linear trends updated to May 2020

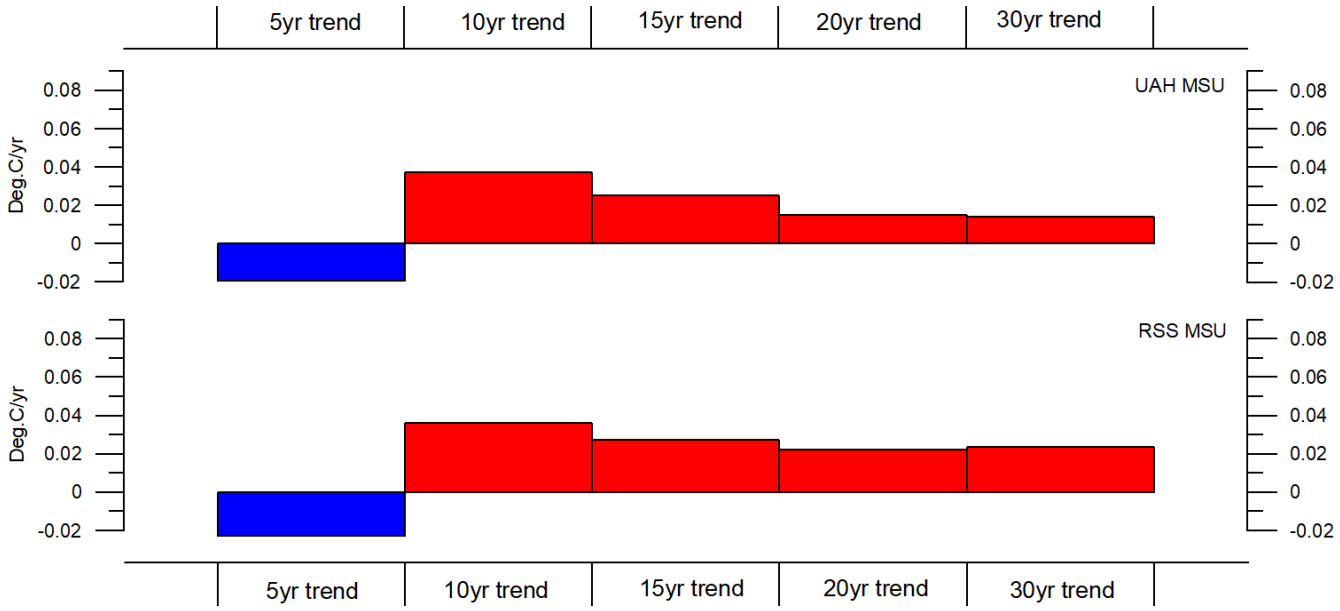

Diagram showing the latest 5, 10, 20 and 30-yr linear annual global temperature trend, calculated as the slope of the linear regression line through the data points, for two satellite-based temperature estimates (UAH MSU and RSS MSU).

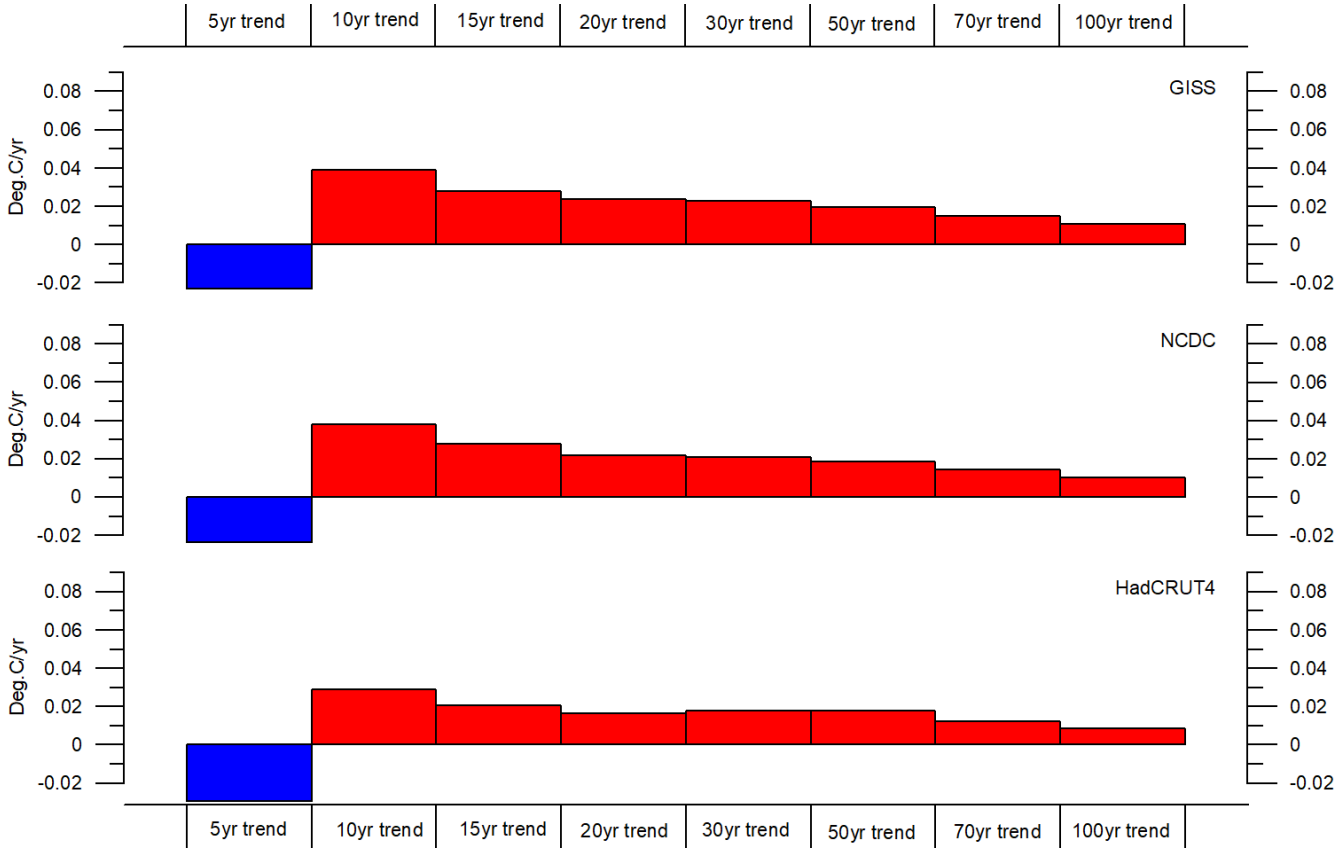

Diagram showing the latest 5, 10, 20, 30, 50, 70 and 100-year linear annual global temperature trend, calculated as the slope of the linear regression line through the data points, for three surface-based temperature estimates (GISS, NCDC and HadCRUT4).

All in one, Quality Class 1, 2 and 3; updated to May 2020

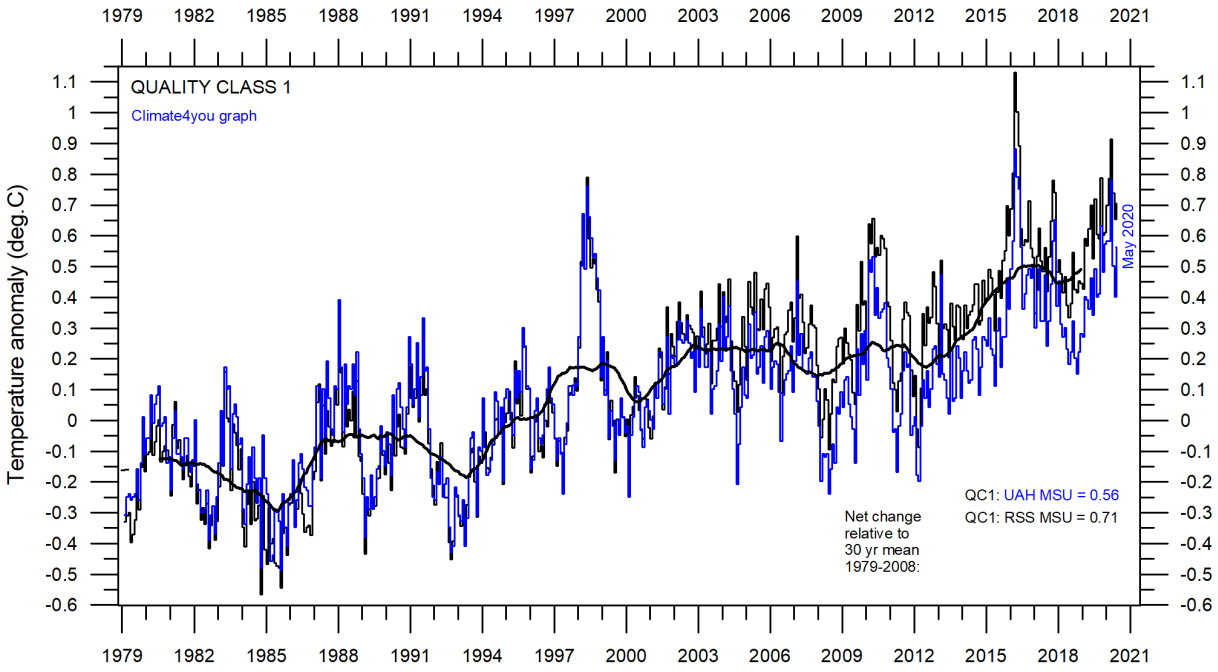

Superimposed plot of Quality Class 1 (UAH and RSS) global monthly temperature estimates. As the base period differs for the individual temperature estimates, they have all been normalised by comparing with the average value of the initial 120 months (30 years) from January 1979 to December 2008. The heavy black line represents the simple running 37 month (c. 3 year) mean of the average of both temperature records. The numbers shown in the lower right corner represent the temperature anomaly relative to the individual 1979-2008 averages.

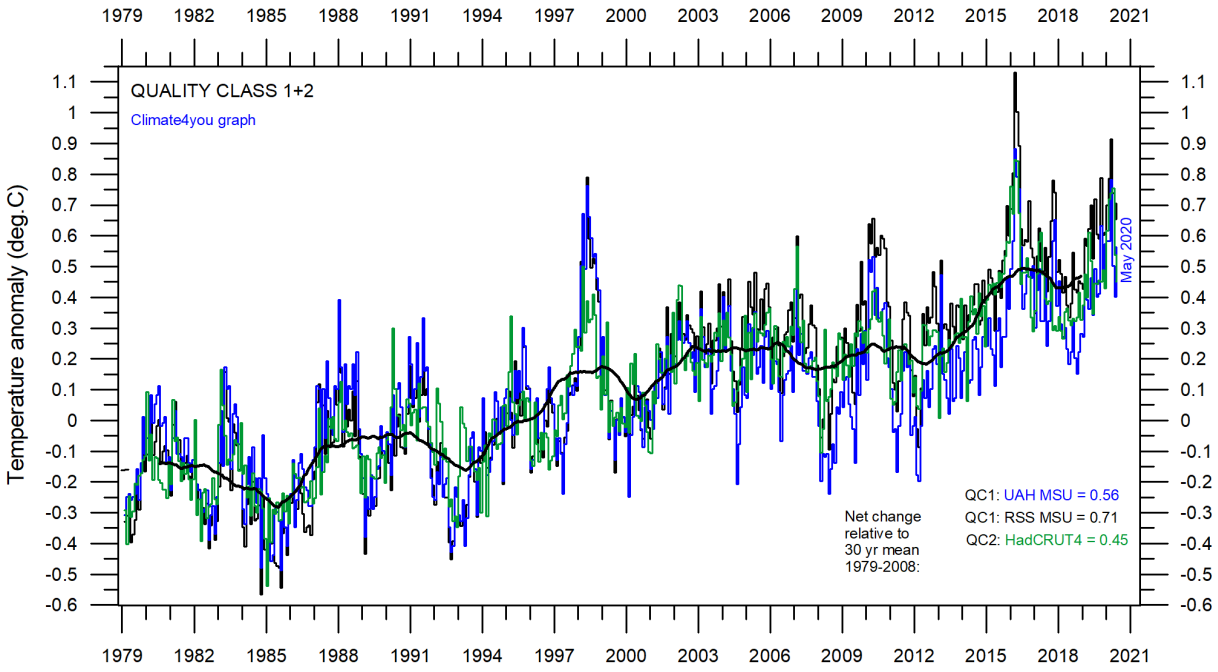

Superimposed plot of Quality Class 1 and 2 (UAH, RSS and HadCRUT4) global monthly temperature estimates. As the base period differs for the individual temperature estimates, they have all been normalised by comparing with the average value of the initial 120 months (30 years) from January 1979 to December 2008. The heavy black line represents the simple running 37 month (c. 3 year) mean of the average of all three temperature records. The numbers shown in the lower right corner represent the temperature anomaly relative to the individual 1979-2008 averages.

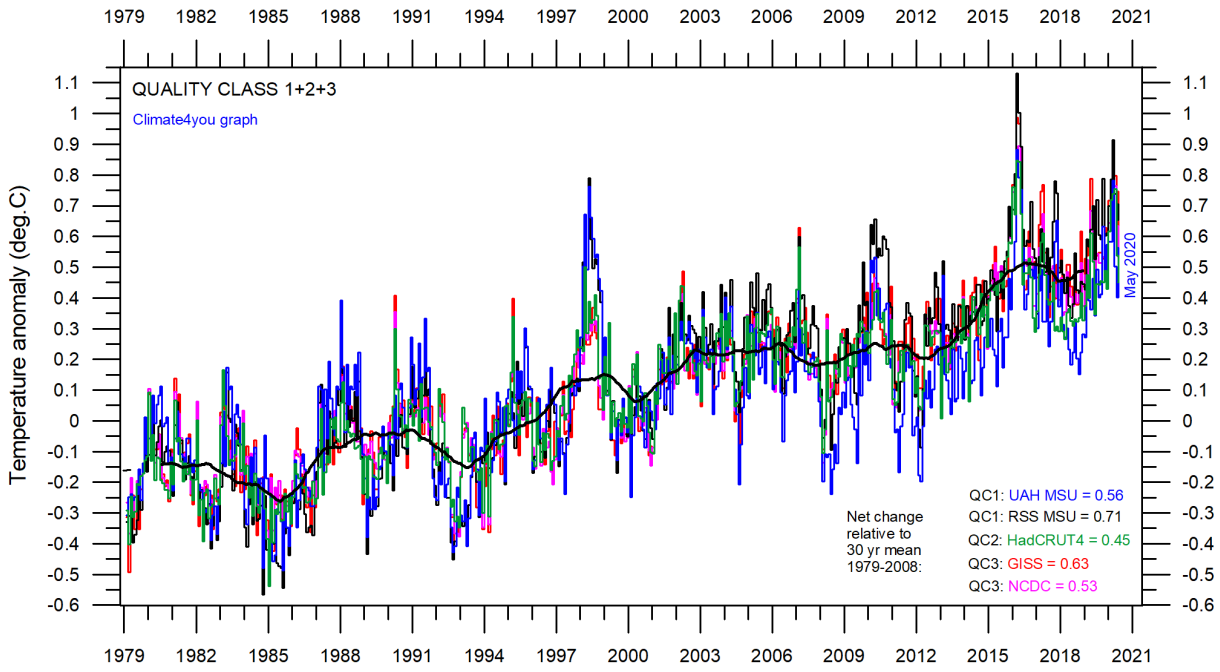

Superimposed plot of Quality Class 1, 2 and 3 global monthly temperature estimates (UAH, RSS, HadCRUT4, GISS and NCDC). As the base period differs for the individual temperature estimates, they have all been normalised by comparing with the average value of the initial 120 months (30 years) from January 1979 to December 2008. The heavy black line represents the simple running 37 month (c. 3 year) mean of the average of all five temperature records. The numbers shown in the lower right corner represent the temperature anomaly relative to the individual 1979-2008 averages.

Please see notes on page 8 relating to the above three quality classes.

Satellite- and surface-based temperature estimates are derived from different types of measurements, and that comparing them directly as done in the diagrams above therefore may be questionable.

However, as both types of estimate often are discussed together, the above composite diagrams may nevertheless be of interest. In fact, the different types of temperature estimates appear to agree as to the overall temperature variations on a 2-3-year scale, although on a shorter time scale there are often considerable differences between the individual records. However, since about 2003 the surface records are slowly drifting towards higher temperatures than the combined satellite record (see p. 10), although this difference recently was much reduced by the adjustment of the RSS satellite series (see lower diagram on page 5).

The combined records (diagram on p. 13) suggest a modest global air temperature increase since 1998, about 0.15°C per decade. The year 1998 was, however, affected by a strong oceanographic El Niño event. Likewise, the recent (2015-16) strong El Niño event probably also represents a relatively short-lived spike on a longer development. It should also be noted that the apparent temperature increase since about 2003 at least partly is the result of ongoing administrative adjustments (page 5-9). At the same time, the temperature records considered here do not indicate any temperature decrease over the last 20 years. See also diagram on page 48.

The present temperature development does not exclude the possibility that global temperatures may begin to increase significantly later. On the other hand, it also remains a possibility that Earth just now is passing an overall temperature peak, and that global temperatures may begin to decrease during the coming years. As always, time will show which of these possibilities is correct.

Global sea surface temperature, updated to June 2020

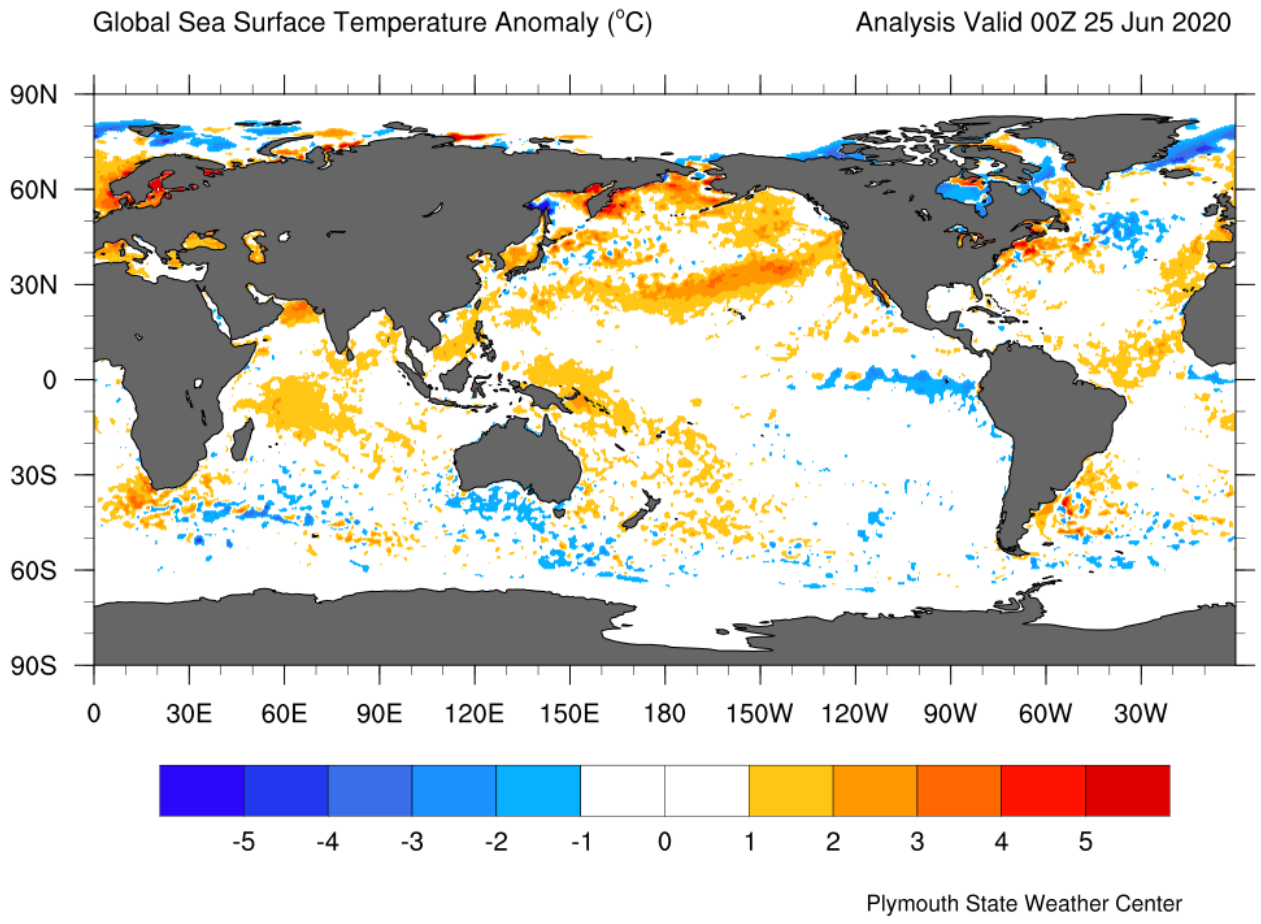

Sea surface temperature anomaly on 25 June 2020. Map source: Plymouth State Weather Center. Reference period: 1977-1991.

Because of the large surface areas near Equator, the temperature of the surface water in these regions is especially important for the global atmospheric temperature (p. 5-7). In fact, no less than 50% of planet Earth's surface area is located within 30°N and 30°S.

A mixture of relatively warm and cold water dominates much of the ocean surface, but with notable differences from month to month. All such ocean surface temperature changes will be influencing global air temperatures in the months to come.

The significance of any short-term cooling or warming reflected in air temperatures should not be overstated. Whenever Earth experiences cold La Niña or warm El Niño episodes (Pacific Ocean, see p.23) major heat exchanges take place between the Pacific Ocean and the atmosphere above, sooner or later showing up in estimates of the global air temperature.

However, this does not necessarily reflect similar changes in the total heat content of the atmosphere-ocean system. In fact, global net changes can be small and such heat exchanges may mainly reflect redistribution of energy between ocean and atmosphere. What matters is the overall temperature development when seen over several years.

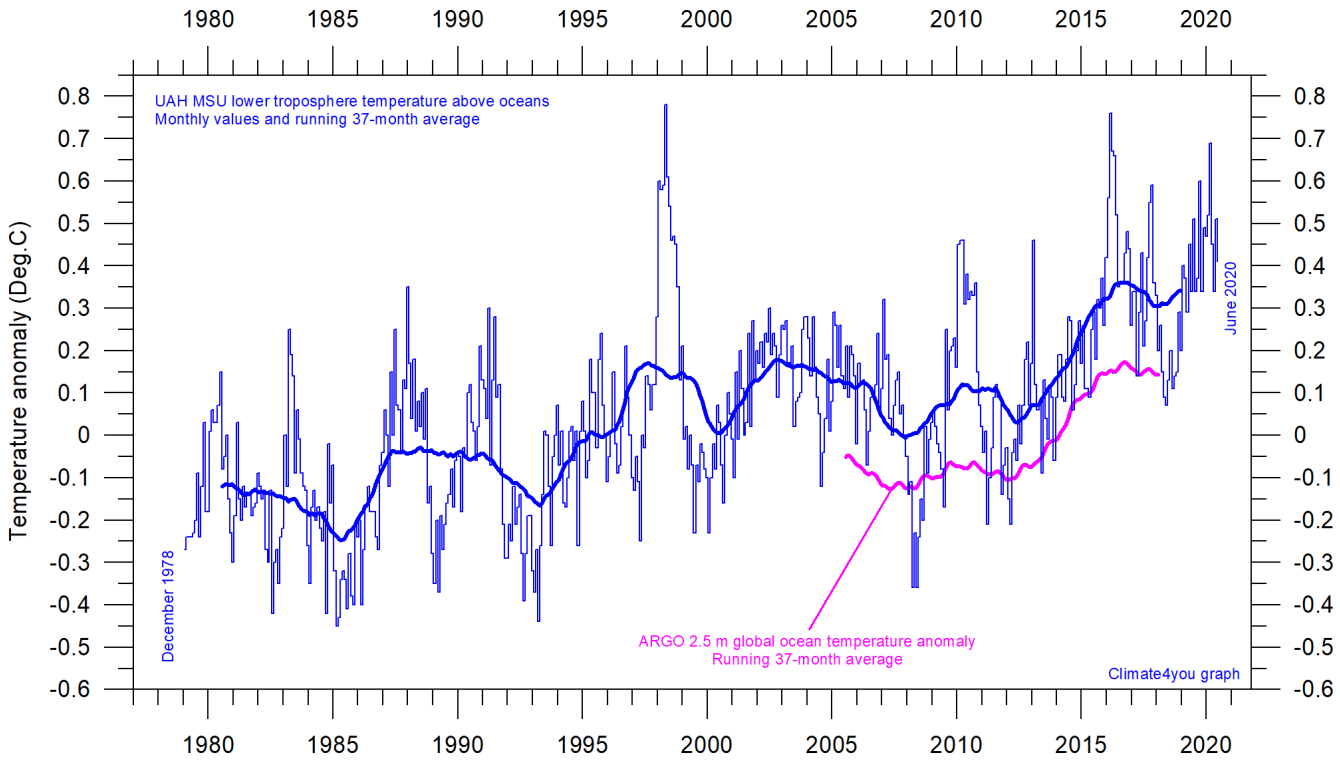

Global monthly average lower troposphere temperature over oceans (thin line) since 1979 according to University of Alabama at Huntsville, USA. The thick line is the simple running 37-month average. Insert: Argo global ocean temperature anomaly from floats, displaced vertically to make visual comparison easier.

15

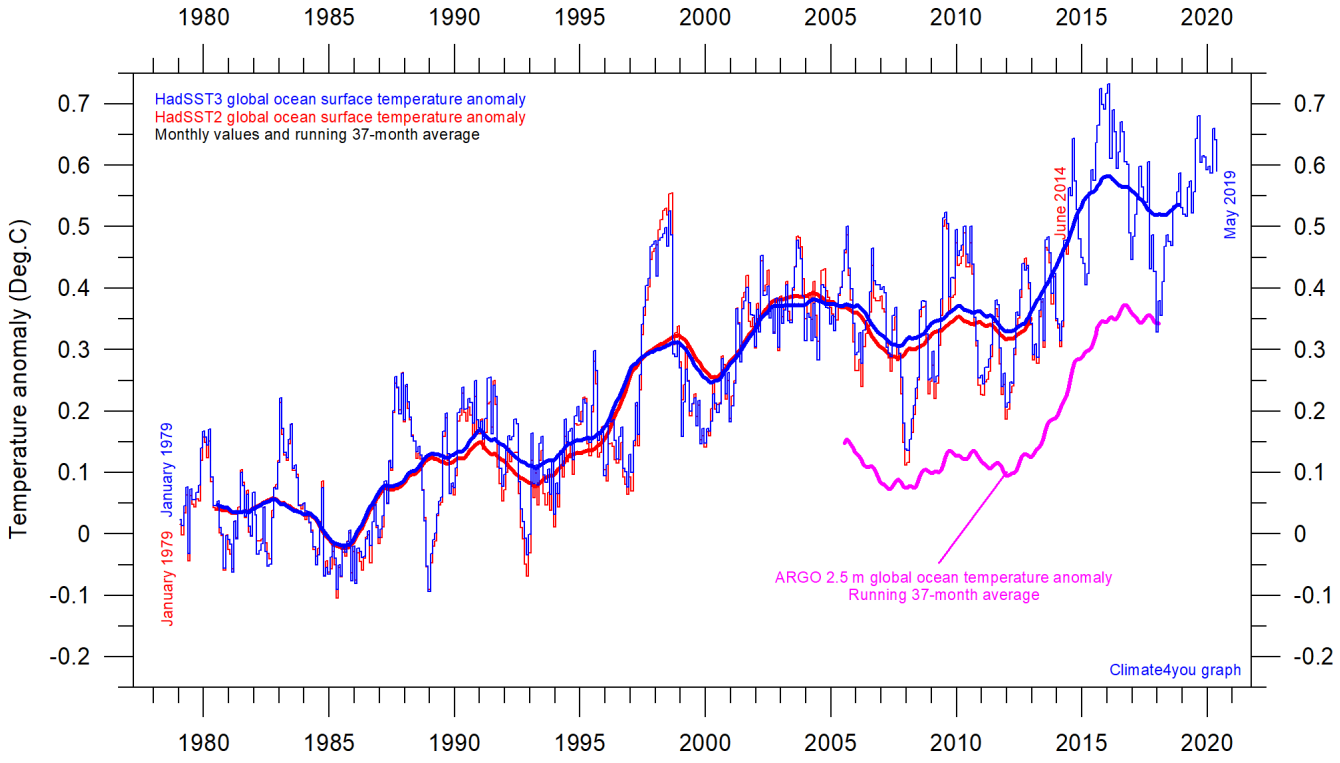

Global monthly average sea surface temperature since 1979 according to University of East Anglia's Climatic Research Unit (CRU), UK. Base period: 1961-1990. The thick line is the simple running 37-month average. Insert: Argo global ocean temperature anomaly from floats, displaced vertically to make visual comparison easier.

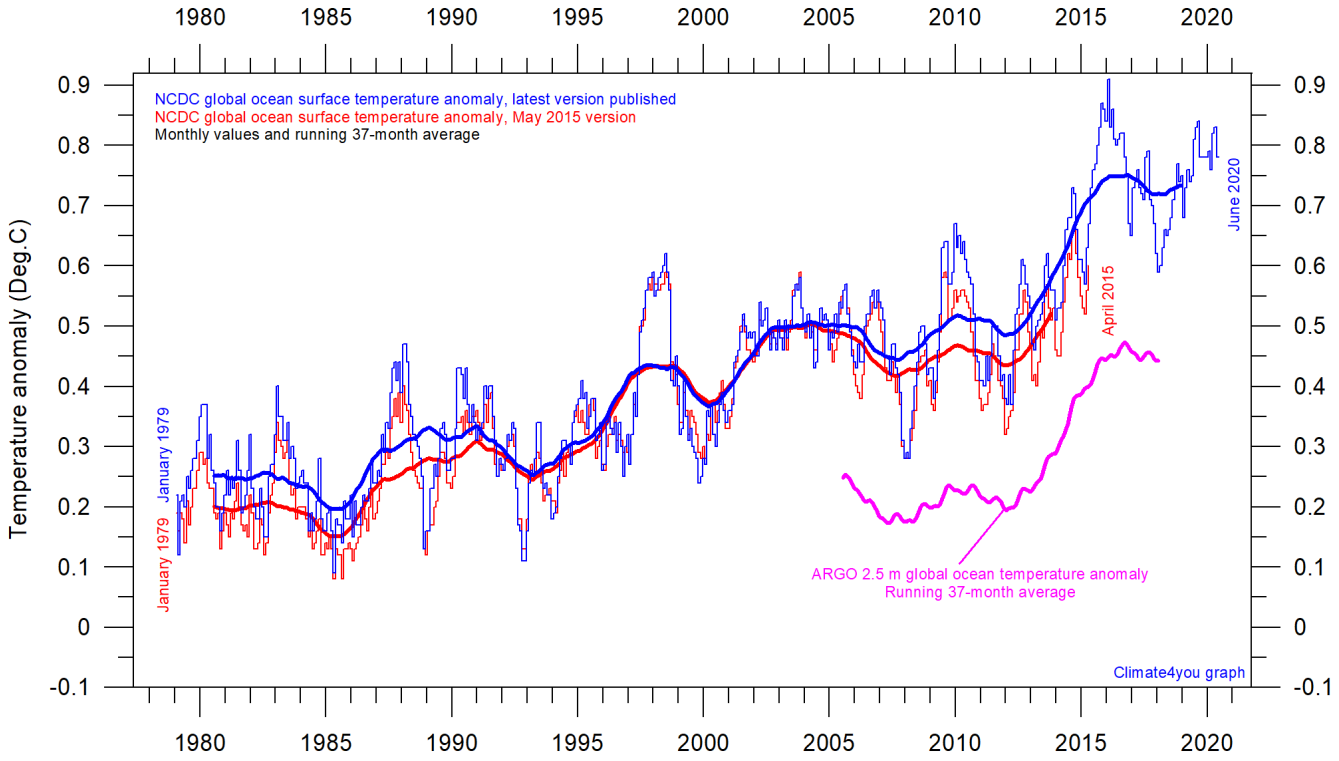

Global monthly average sea surface temperature since 1979 according to the National Climatic Data Center (NCDC), USA. Base period: 1901-2000. The thick line is the simple running 37-month average. Insert: Argo global ocean temperature anomaly from floats, displaced vertically to make visual comparison easier.

June 18, 2015: *NCDC has introduced several rather large administrative changes to their sea surface temperature record. The overall result is to produce a record giving the impression of a continuous temperature increase, also in the 21st century. As the oceans cover about 71% of the entire surface of planet Earth, the effect of this adjustment is clearly reflected in the NCDC record for global surface air temperature (p. 7). The pre-adjustment record is shown in red in the above diagram.*

Ocean temperature in uppermost 100 m, updated to March 2020

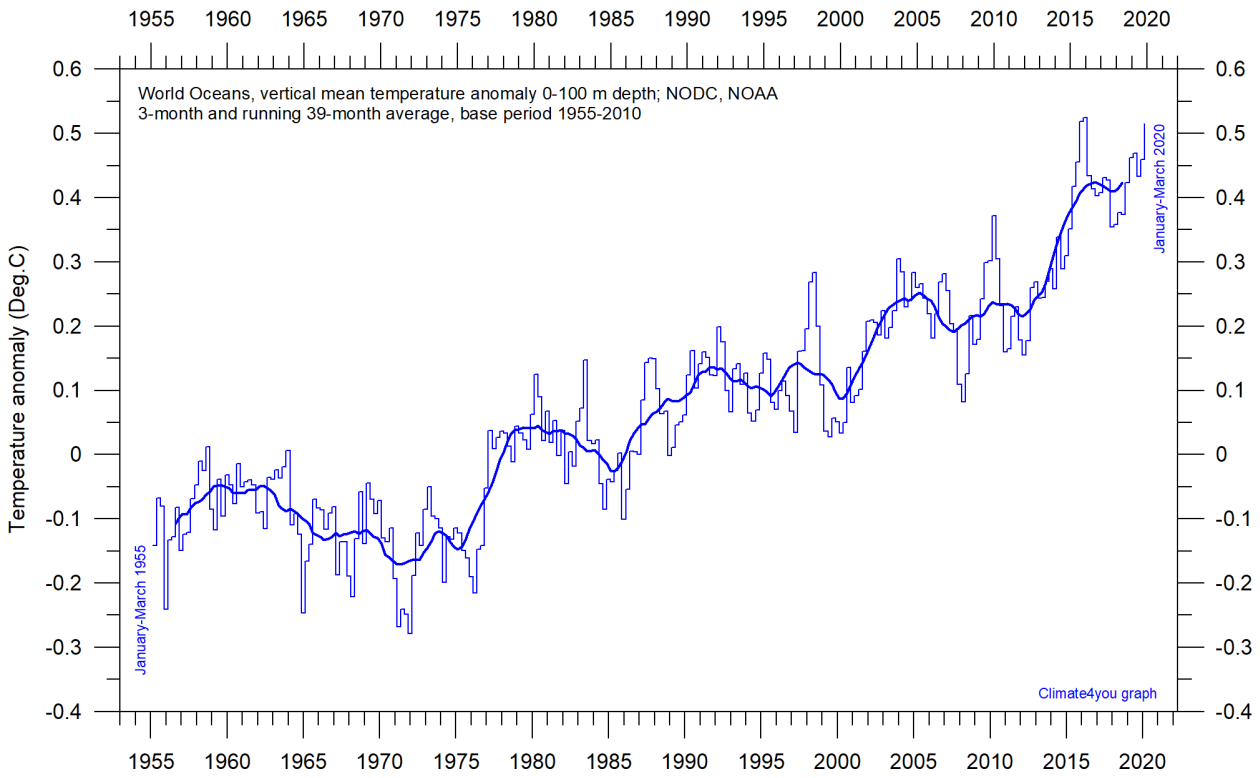

World Oceans vertical average temperature 0-100 m depth since 1955. The thin line indicates 3-month values, and the thick line represents the simple running 39-month (c. 3 year) average. Data source: NOAA National Oceanographic Data Center (NODC). Base period 1955-2010.

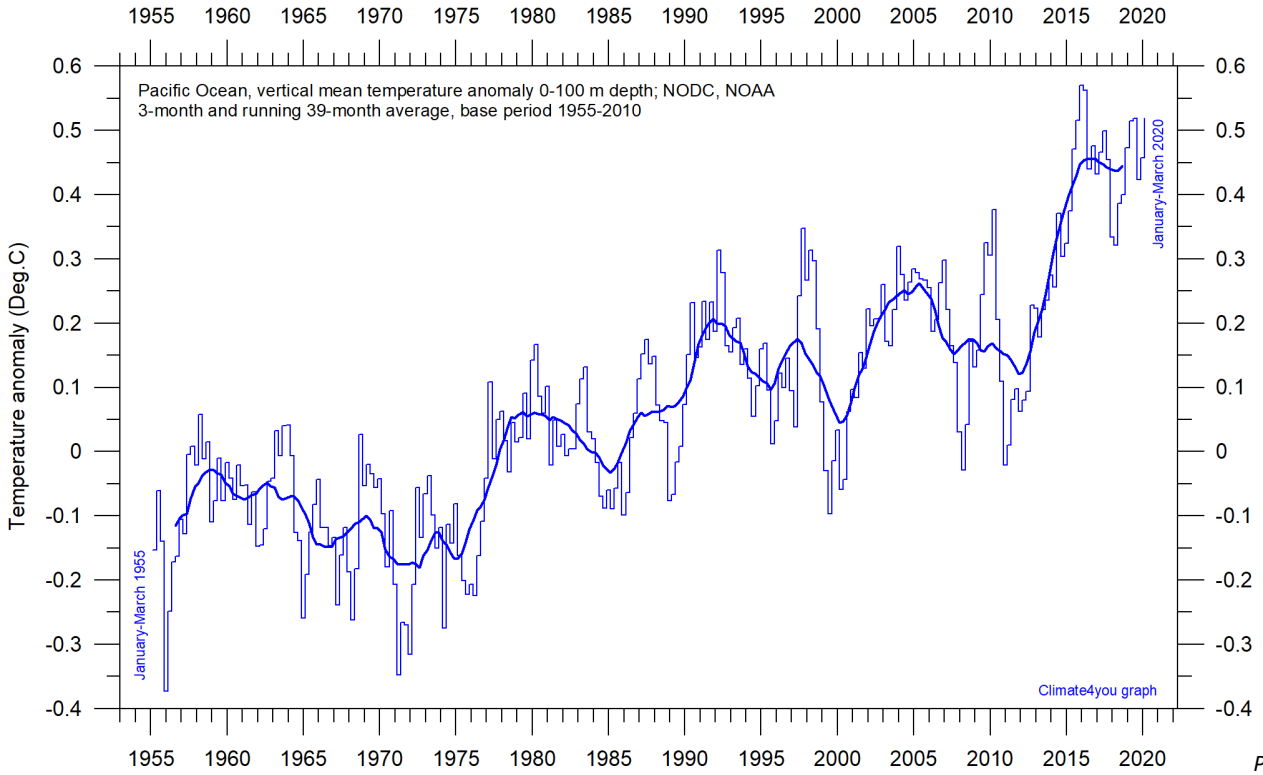

Pacific Ocean vertical average temperature 0-100 m depth since 1955. The thin line indicates 3-month values, and the thick line represents the simple running 39-month (c. 3 year) average. Data source: NOAA National Oceanographic Data Center (NODC). Base period 1955-2010.

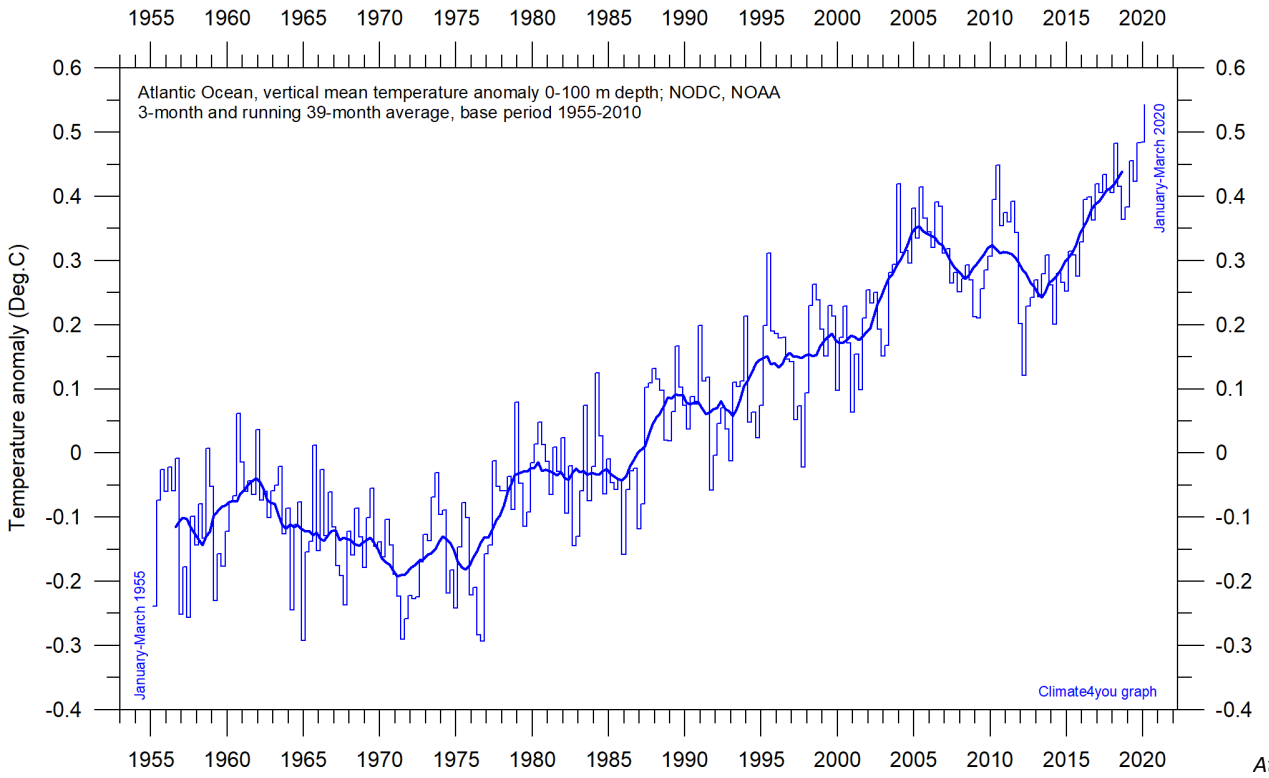

Ocean vertical average temperature 0-100 m depth since 1955. The thin line indicates 3-month values, and the thick line represents the simple running 39-month (c. 3 year) average. Data source: NOAA National Oceanographic Data Center (NODC). Base period 1955-2010.

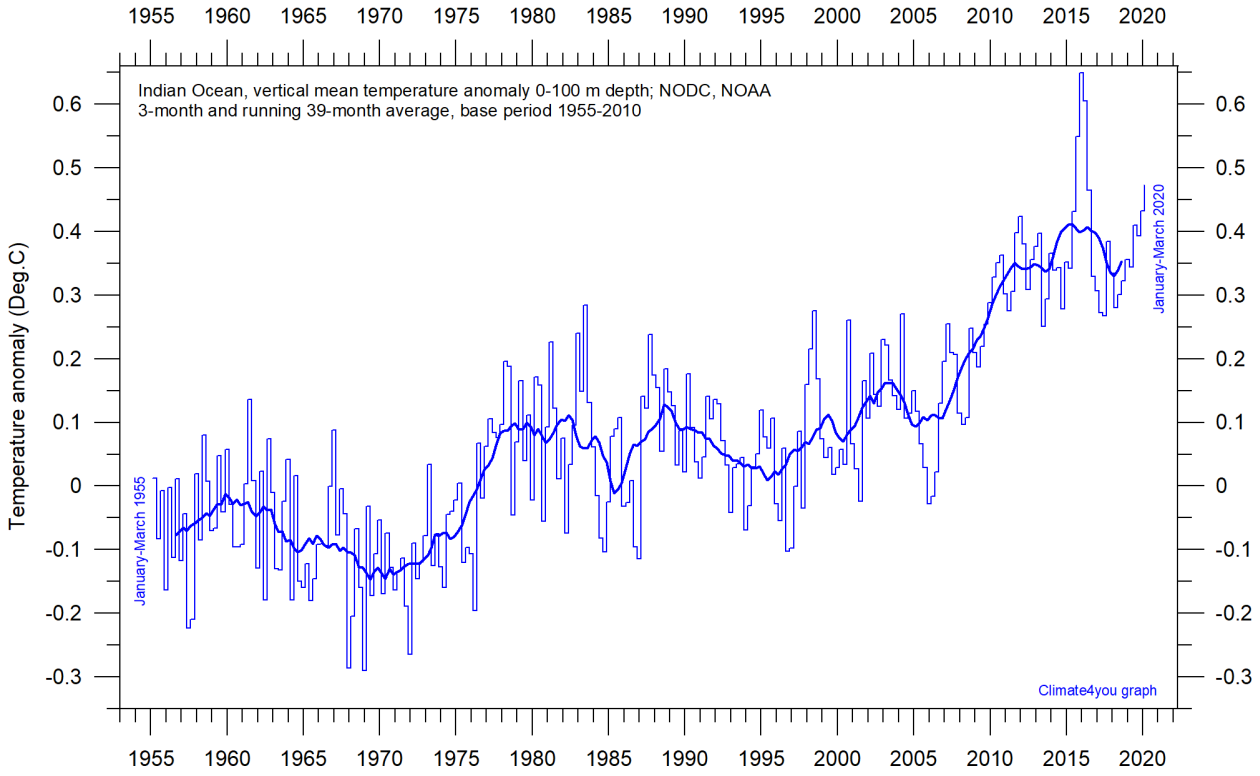

Indian Ocean vertical average temperature 0-100 m depth since 1955. The thin line indicates 3-month values, and the thick line represents the simple running 39-month (c. 3 year) average. Data source: NOAA National Oceanographic Data Center (NODC). Base period 1955-2010.

North Atlantic heat content uppermost 700 m, updated to March 2020

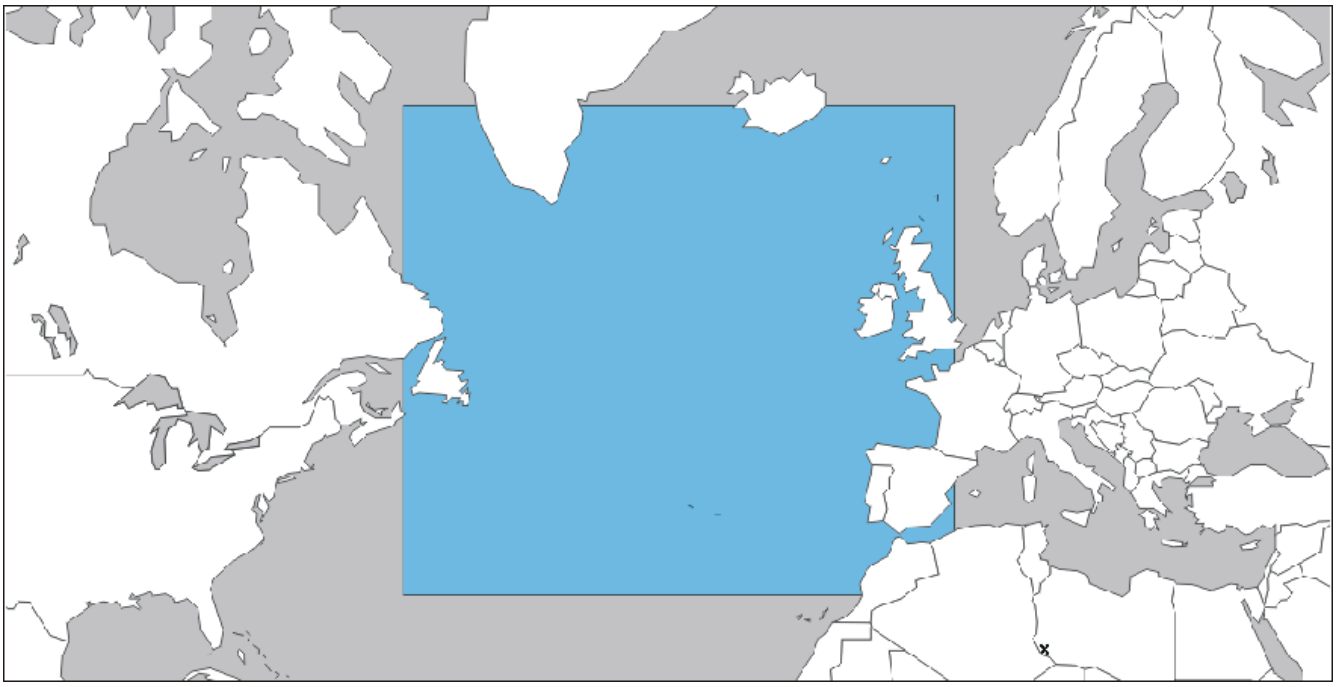

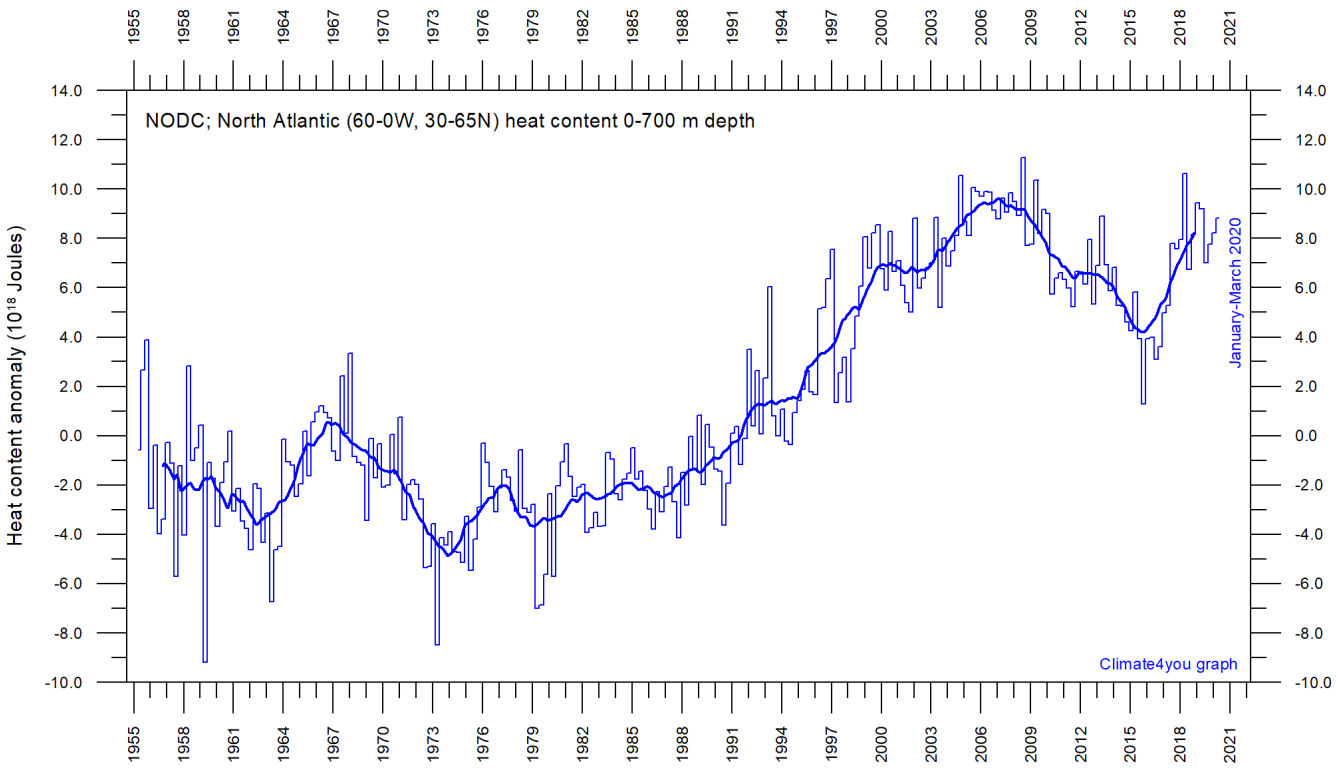

Global monthly heat content anomaly (10^{18} Joules) in the uppermost 700 m of the North Atlantic (60-0W, 30-65N; see map above) *ocean since January 1955. The thin line indicates monthly values, and the thick line represents the simple running 37-month (c. 3 year) average. Data source: National Oceanographic Data Center (NODC).*

North Atlantic temperatures 0-800 m depth along 59°N, 30-0W, updated to July 2019

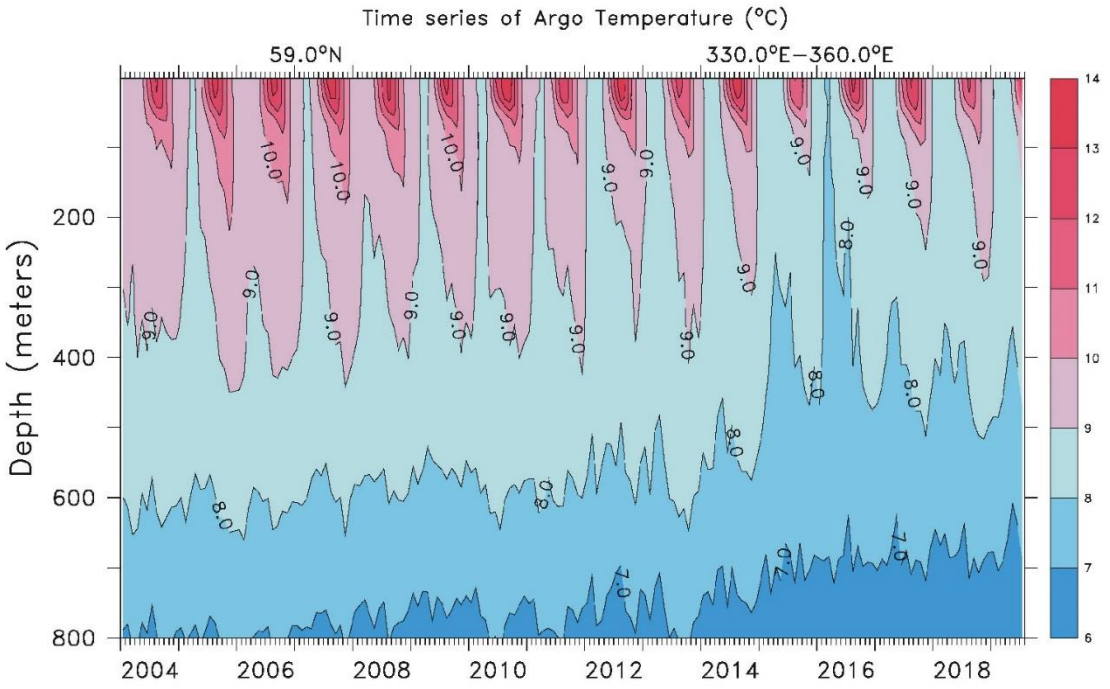

Time series depth-temperature diagram along 59 N across the North Atlantic Current from 30°W to 0°W, from surface to 800 m depth. Source: Global Marine Argo Atlas. See also the diagram below.

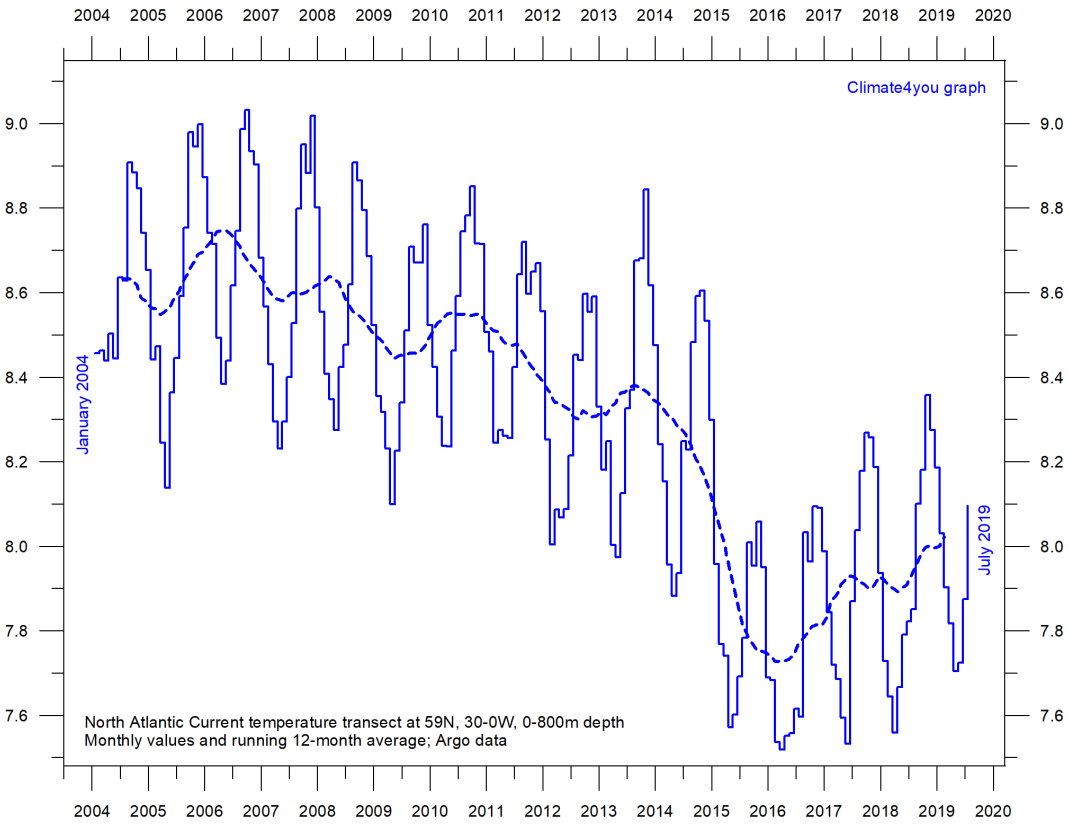

Average temperature along 59 N, 30-0W, 0-800m depth, corresponding to the main part of the North Atlantic Current, using Argo-data. Source: Global Marine Argo Atlas. Additional information can be found in: Roemmich, D. and J. Gilson, 2009. The 2004-2008 mean and annual cycle of temperature, salinity, and steric height in the global ocean from the Argo Program. Progress in Oceanography, 82, 81-100.

Global ocean temperature 0-1900 m depth summary, updated to July 2019

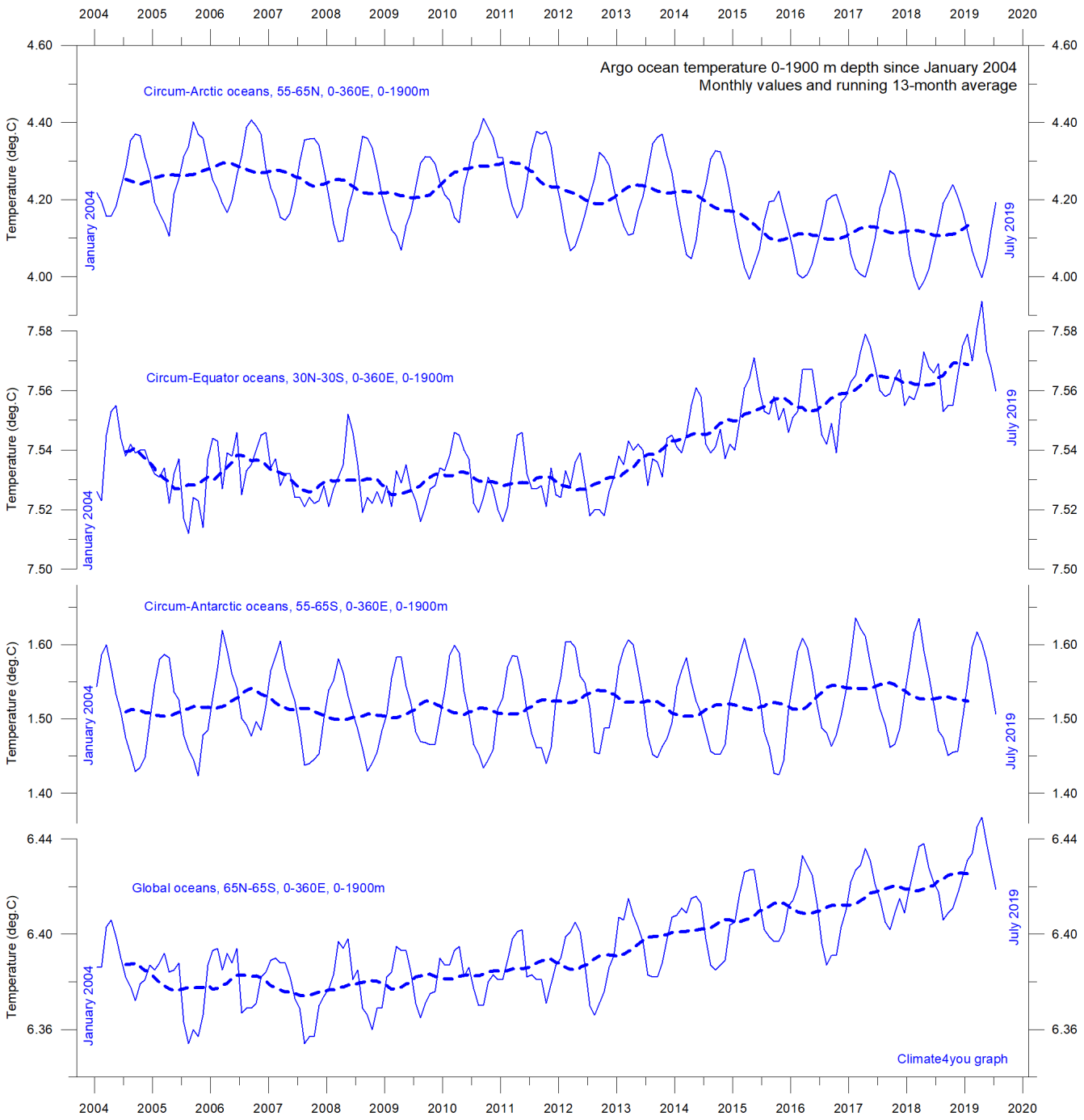

Summary of average temperature in uppermost 1900 m in different parts of the global oceans, using Argo-data. Source: Global Marine Argo Atlas. Additional information can be found in: Roemmich, D. and J. Gilson, 2009. The 2004-2008 mean and annual cycle of temperature, salinity, and steric height in the global ocean from the Argo Program. Progress in Oceanography, 82, 81-100.

The global summary diagram above shows that, on average, the temperature of the global oceans down to 1900 m depth has been increasing since about 2011. It is also seen that this increase since 2013 dominantly is due to oceanic changes occurring near the Equator, between 30°N and 30°S. In contrast, for the circum-Arctic oceans north of 55°N, depth-integrated ocean temperatures have been decreasing since 2011. Near the Antarctic, south of 55°S, temperatures have essentially been stable. At most latitudes, a clear annual rhythm is seen.

Global ocean net temperature change since 2004 at different depths, updated to July 2019

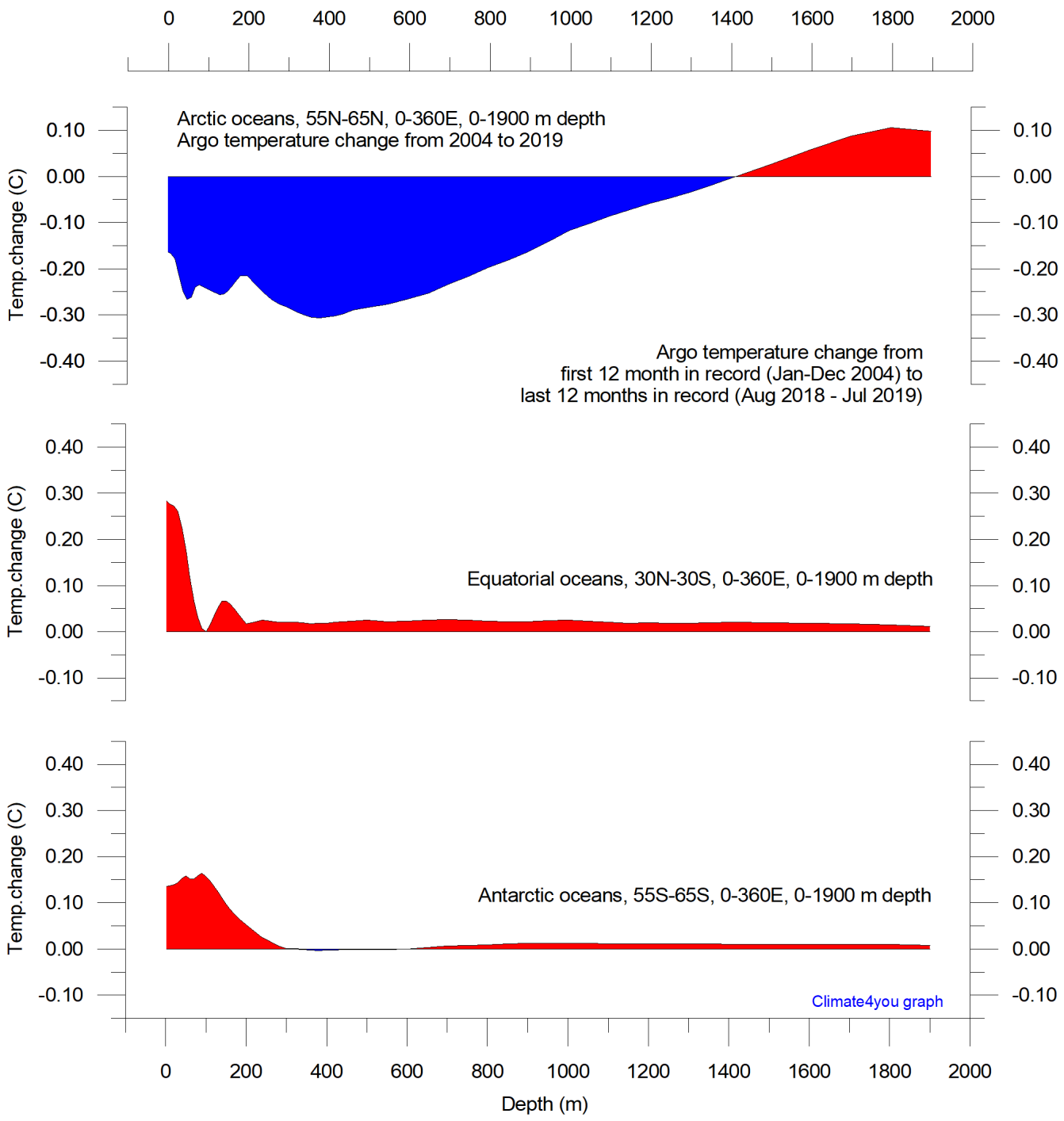

Net temperature change since 2004 from surface to 1900 m depth in different parts of the global oceans, using Argo-data. Source: Global Marine Argo Atlas. Additional information can be found in: Roemmich, D. and J. Gilson, 2009. The 2004-2008 mean and annual cycle of temperature, salinity, and steric height in the global ocean from the Argo Program. Progress in Oceanography, 82, 81-100. Please note that due to the spherical form of Earth, northern and southern latitudes represent only small ocean volumes, compared to latitudes near the Equator.

La Niña and El Niño episodes, updated to June 2020

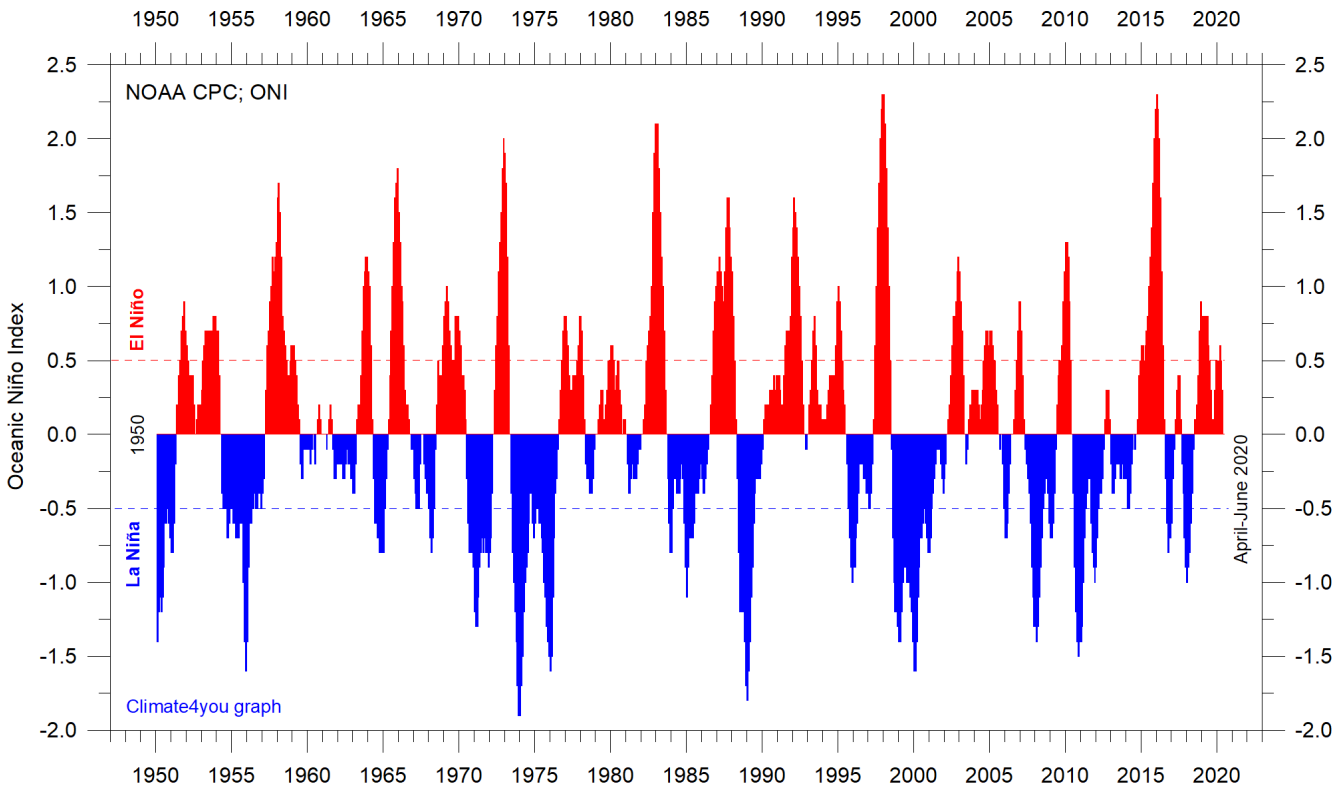

Warm (>+0.5°C) and cold (<0.5°C) episodes for the Oceanic Niño Index (ONI), defined as 3 month running mean of ERSSTv4 SST anomalies in the Niño 3.4 region (5°N-5°S, 120°-170°W)]. For historical purposes cold and warm episodes are defined when the threshold is met for a minimum of 5 consecutive over-lapping seasons. Anomalies are centred on 30-yr base periods updated every 5 years.

The recent 2015-16 El Niño episode is among the strongest since the beginning of the record in 1950. Considering the entire record, however, recent variations between El Niño and La Niña episodes do not appear abnormal in any way.

Troposphere and stratosphere temperatures from satellites, updated to June 2020

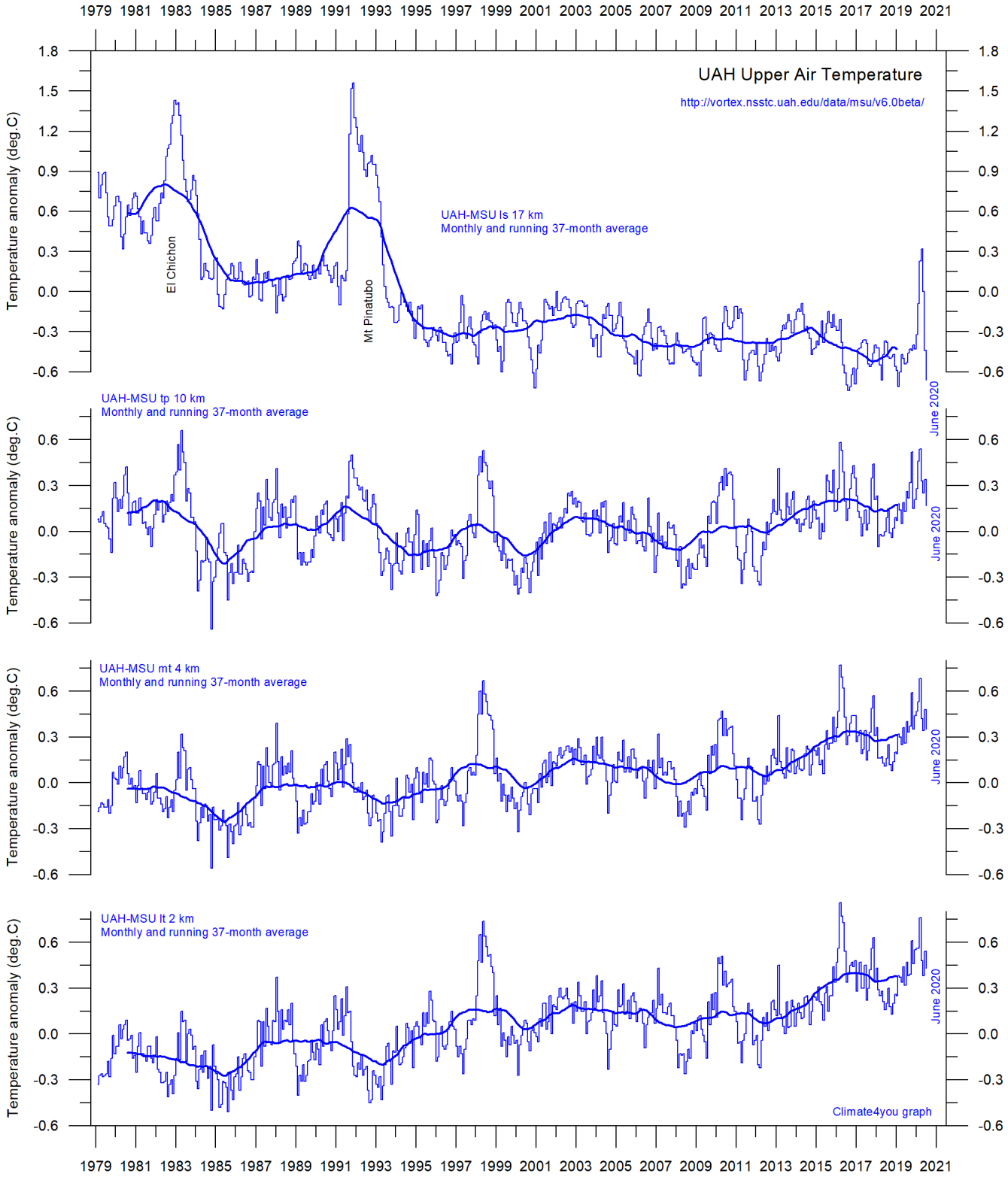

Global monthly average temperature in different according to University of Alabama at Huntsville, USA. The thin lines represent the monthly average, and the thick line the simple running 37-month average, nearly corresponding to a running 3-year average.

Zonal lower troposphere temperatures from satellites, updated to June 2020

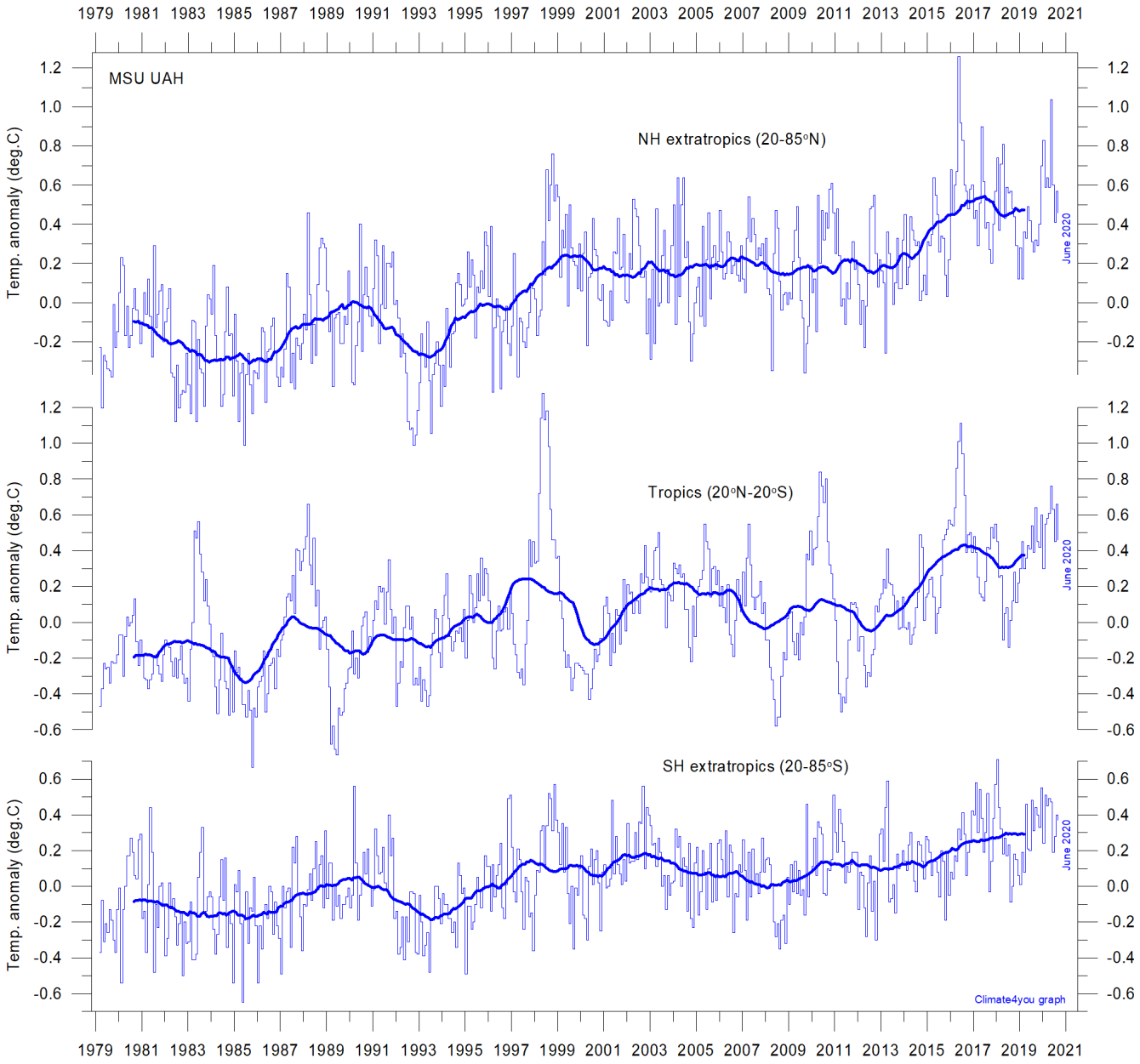

Global monthly average lower troposphere temperature since 1979 for the tropics and the northern and southern extratropics, according to University of Alabama at Huntsville, USA. Thin lines show the monthly temperature. Thick lines represent the simple running 37-month average, nearly corresponding to a running 3-year average. Reference period 1981-2010.

The overall warming since 1980 has dominantly been a northern hemisphere phenomenon, and mainly played out as a marked change between 1994 and 1999. However, this rather rapid temperature change is influenced by the Mt. Pinatubo eruption 1992-93 and the subsequent 1997 El Niño episode. The diagram also shows the temperature effects of the strong Equatorial El Niño's in 1997 and 2015-16, as well as the moderate El Niño in 2019, apparently were spreading to higher latitudes in both hemispheres with some delay.

Arctic and Antarctic lower troposphere temperature, updated to June 2020

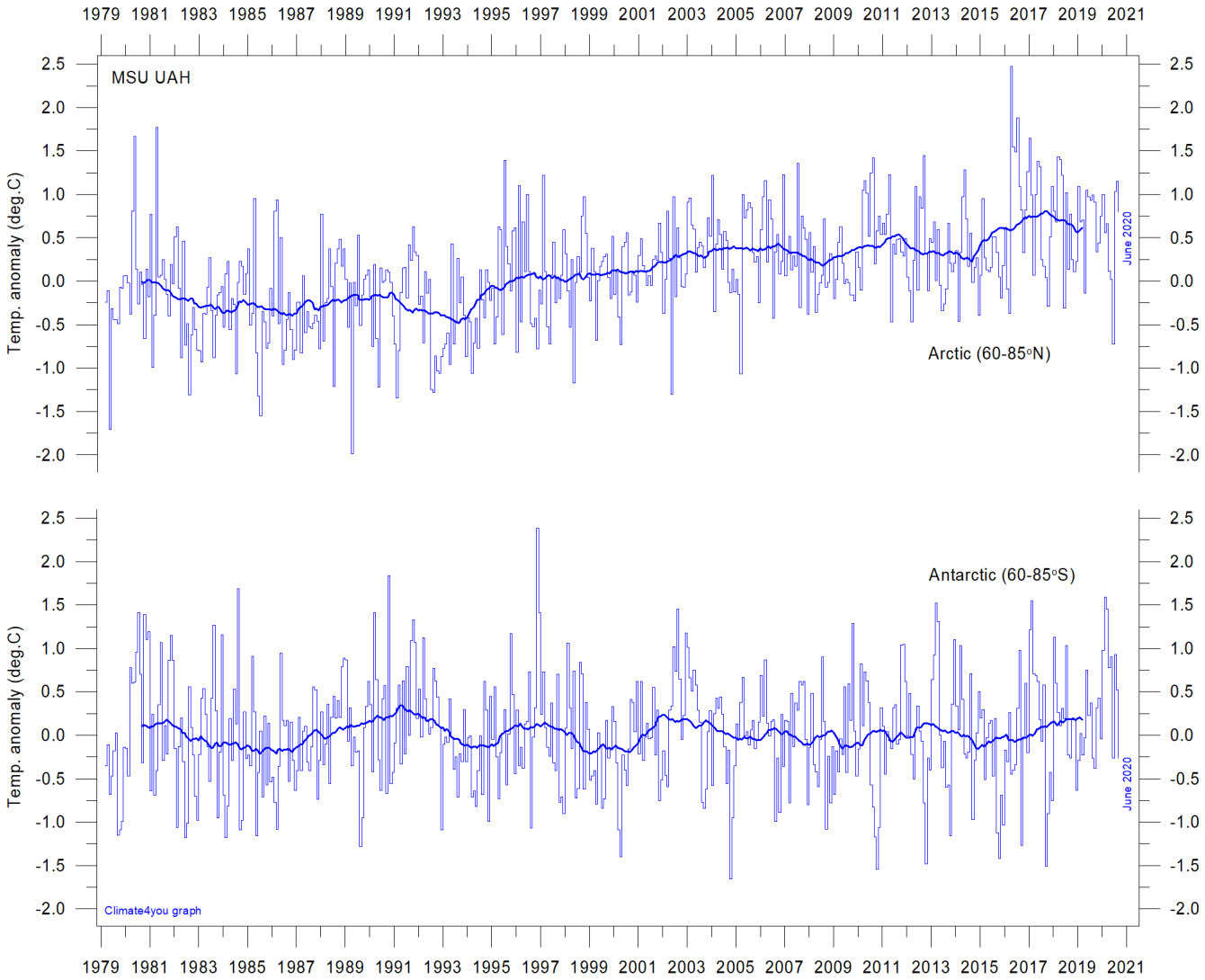

Global monthly average lower troposphere temperature since 1979 for the North Pole and South Pole regions, based on satellite observations (University of Alabama at Huntsville, USA). Thin lines show the monthly temperature. The thick line is the simple running 37-month average, nearly corresponding to a running 3-year average. Reference period 1981-2010.

In the Arctic region, warming mainly took place 1994-96, and less so subsequently. In 2016, however, temperatures peaked for several months, presumably because of oceanic heat given off to the atmosphere during the recent El Niño 2015-16 (see also figure on page 23) and then advected to higher latitudes.

This underscores how Arctic air temperatures may be affected not only by variations in local conditions but also by variations playing out in geographically remote regions. An overall temperature decrease has characterised the Arctic since 2016 (see also diagrams on page 28-30).

In the Antarctic region, temperatures have remained almost stable since the onset of the satellite record in 1979. In 2016-17 a small temperature peak visible in the monthly record may be interpreted as the subdued effect of the recent El Niño episode.

Temperature over land versus over oceans, updated to June 2020

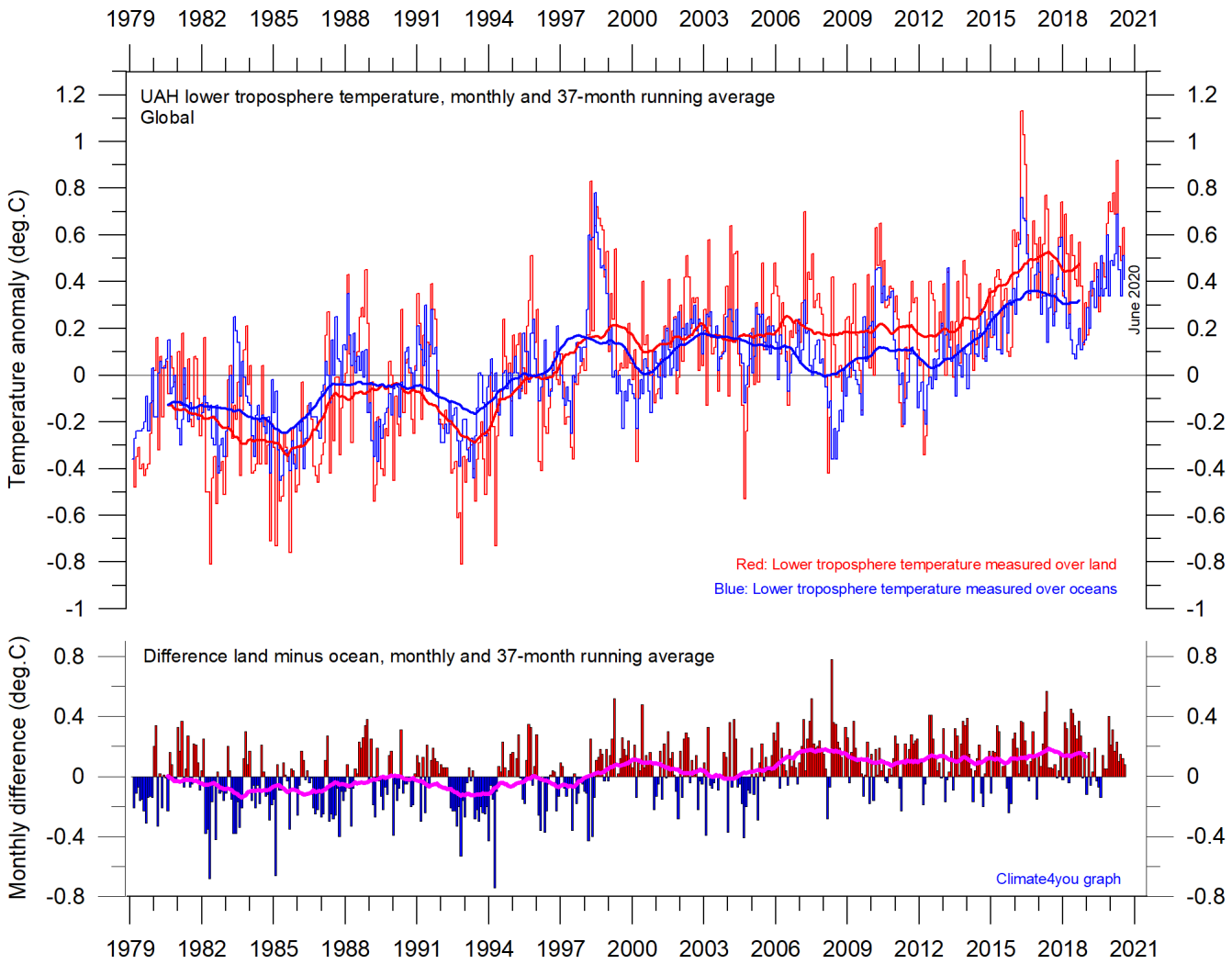

Global monthly average lower troposphere temperature since 1979 measured over land and oceans, respectively, according to University of Alabama at Huntsville, USA. Thick lines are the simple running 37-month average, nearly corresponding to a running 3-year average. Reference period 1981-2010.

Since 1979, the lower troposphere over land has warmed much more than over oceans, suggesting that the overall warming is derived mainly from incoming solar radiation.

In addition, there may be other reasons for this divergence, such as, e.g., variations in cloud cover and land use.

Arctic and Antarctic surface air temperature, updated to May 2020

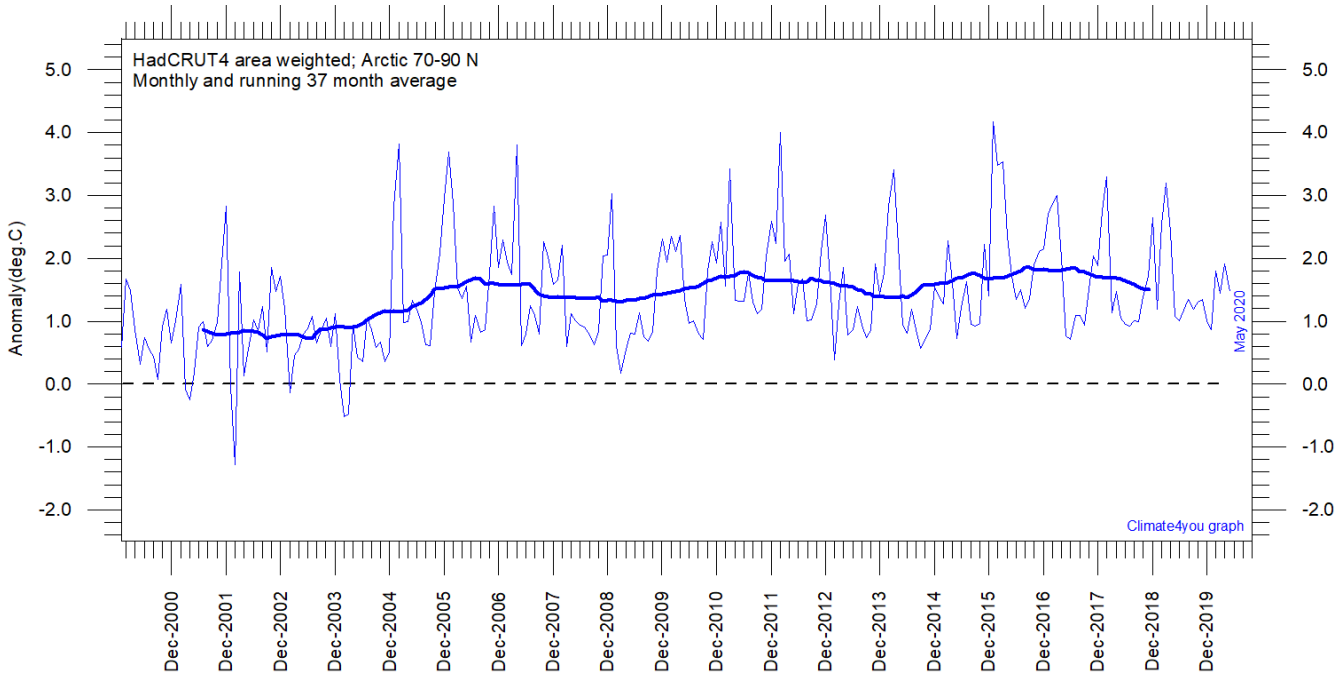

Diagram showing area weighted Arctic (70-90°N) monthly surface air temperature anomalies (HadCRUT4) since January 2000, in relation to the WMO normal period 1961-1990. The thin line shows the monthly temperature anomaly, while the thicker line shows the running 37-month (c. 3 year) average.

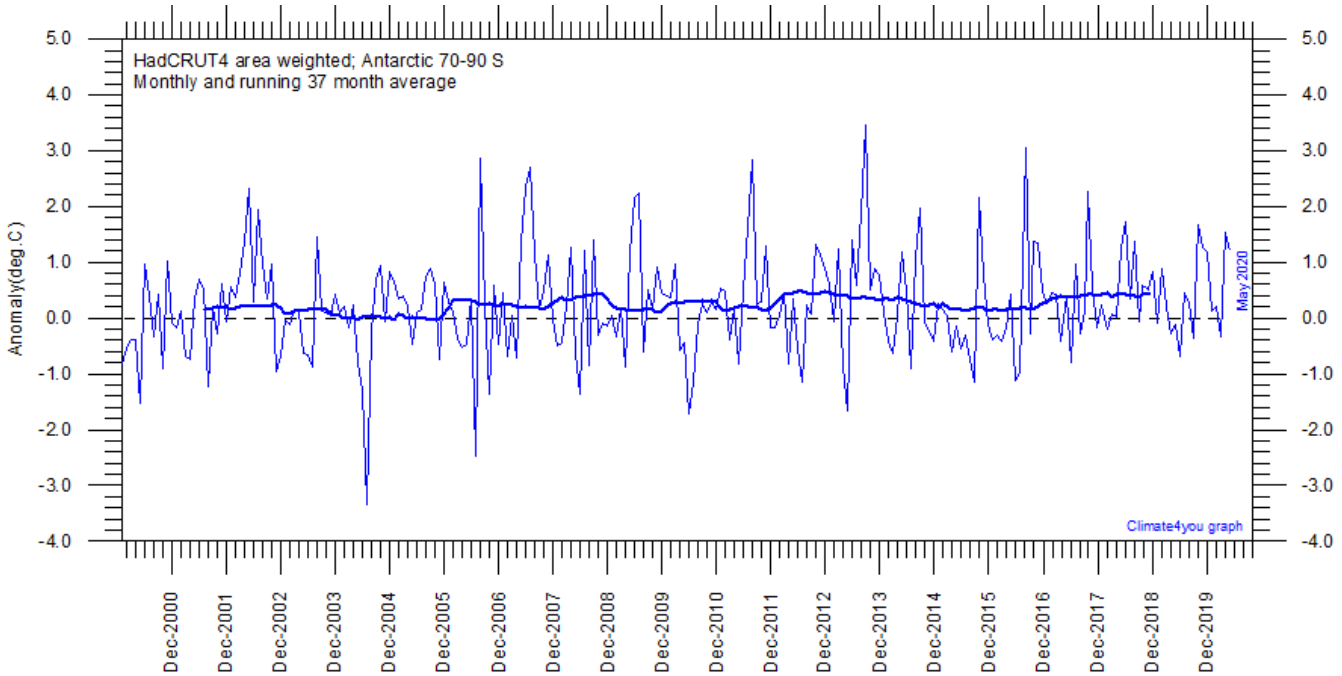

Diagram showing area weighted Antarctic (70-90°S) monthly surface air temperature anomalies (HadCRUT4) since January 2000, in relation to the WMO normal period 1961-1990. The thin line shows the monthly temperature anomaly, while the thicker line shows the running 37-month (c. 3 year) average.

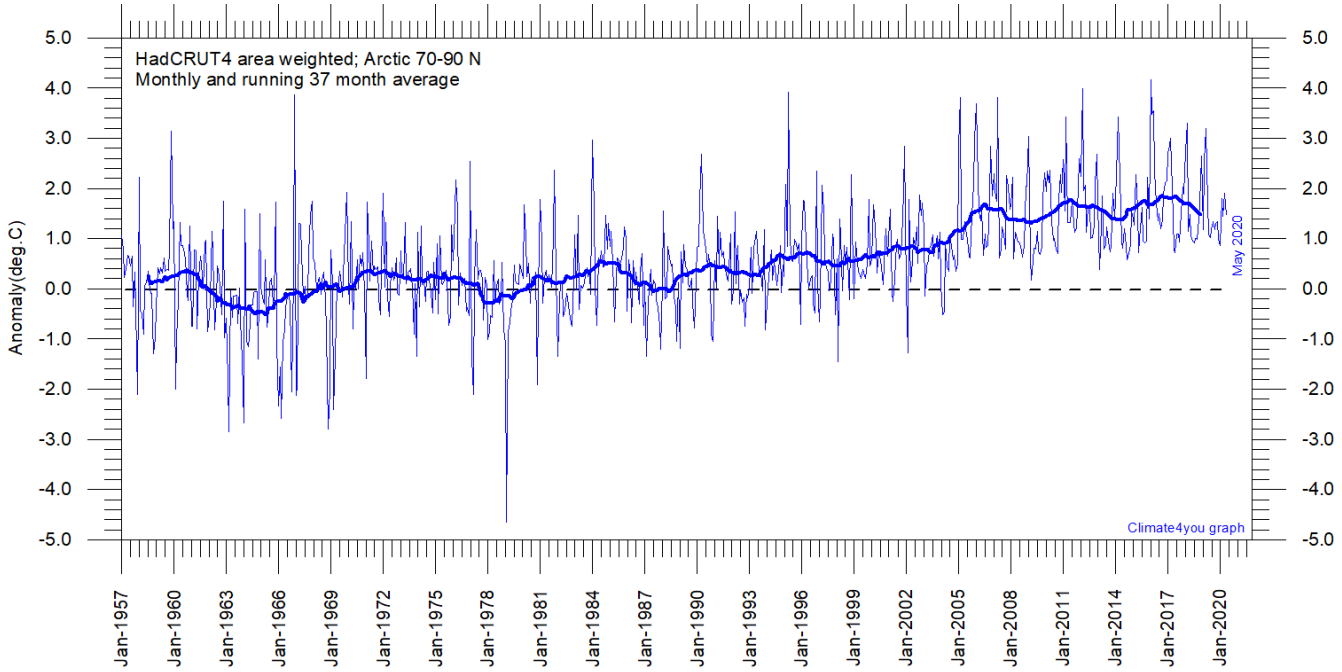

Diagram showing area weighted Arctic (70-90°N) monthly surface air temperature anomalies (HadCRUT4) since January 1957, in relation to the WMO normal period 1961-1990. The thin line shows the monthly temperature anomaly, while the thicker line shows the running 37-month (c. 3 year) average.

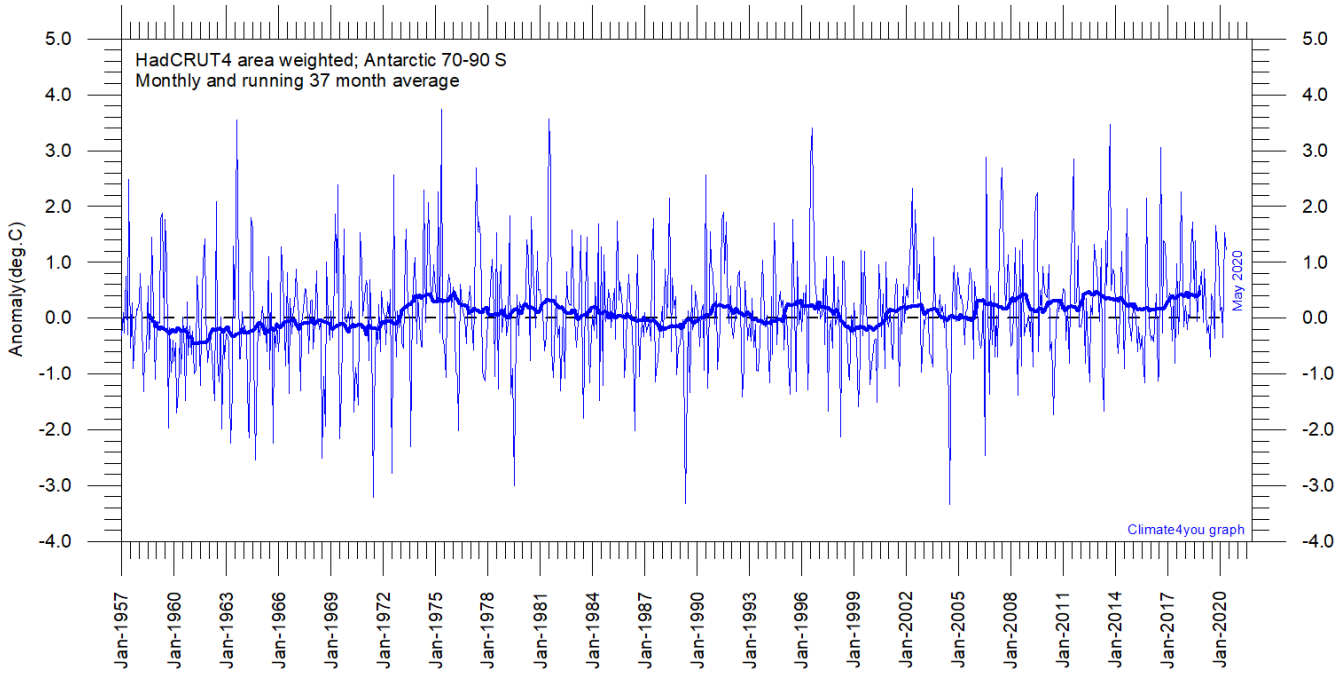

Diagram showing area weighted Antarctic (70-90°S) monthly surface air temperature anomalies (HadCRUT4) since January 1957, in relation to the WMO normal period 1961-1990. The thin line shows the monthly temperature anomaly, while the thicker line shows the running 37-month (c. 3 year) average.

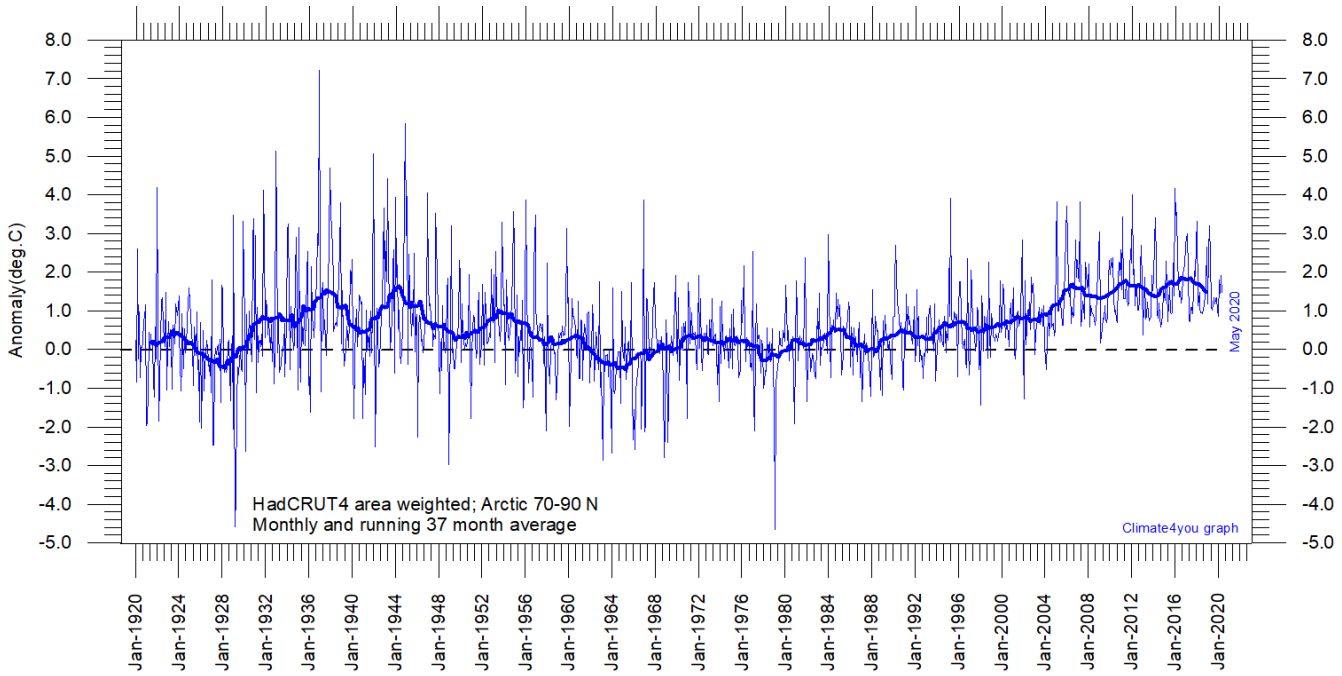

Diagram showing area-weighted Arctic (70-90°N) monthly surface air temperature anomalies (HadCRUT4) since January 1920, in relation to the WMO normal period 1961-1990. The thin line shows the monthly temperature anomaly, while the thicker line shows the running 37-month (c. 3 year) average.

Because of the relatively small number of Arctic stations before 1930, month-to-month variations in the early part of the Arctic temperature record 1920-2018 are bigger than later (diagram above).

The period from about 1930 saw the establishment of many new Arctic meteorological stations, first in Russia and Siberia, and following the 2nd World War, also in North America. The period since 2005 is warm, about as warm as the period 1930-1940.

As the HadCRUT4 data series has improved high latitude coverage data coverage (compared to the HadCRUT3 series), the individual 5°x5° grid cells have been weighted according to their surface area. This area correction is especially important for polar regions. This approach differs from the approach used by Gillet et al. 2008, which calculated a simple average, without any correction for the substantial surface area effect of latitude in polar regions.

Literature:

Gillett, N.P., Stone, D.A., Stott, P.A., Nozawa, T., Karpechko, A.Y.U., Hegerl, G.C., Wehner, M.F. and Jones, P.D. 2008. Attribution of polar warming to human influence. *Nature Geoscience* 1, 750-754.

Arctic and Antarctic sea ice, updated to June 2020

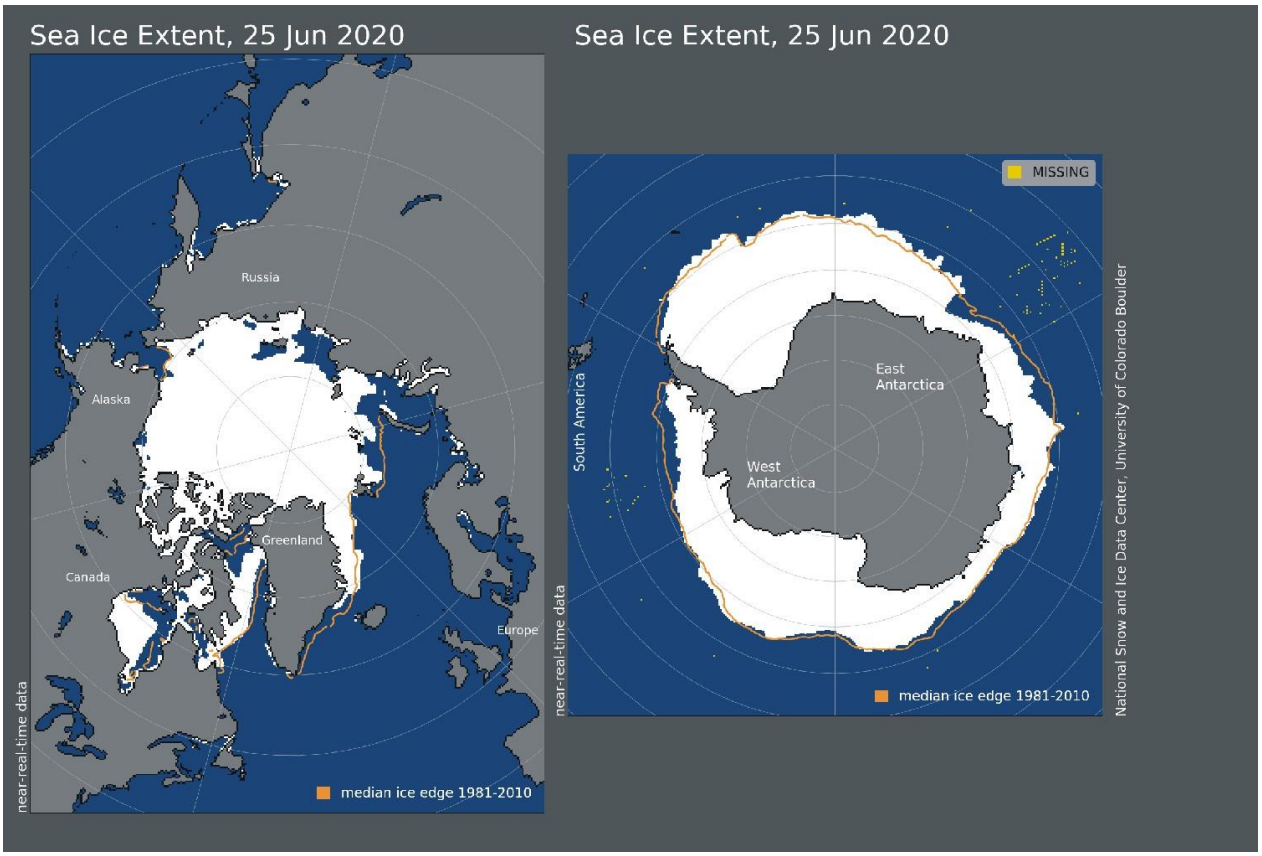

Sea ice extent 25 June 2020. The median limit of sea ice (orange line) is defined as 15% sea ice cover, according to the average of satellite observations 1981-2010 (both years included). Sea ice may therefore well be encountered outside and open water areas inside the limit shown in the diagrams above. Map source: National Snow and Ice Data Center (NSIDC).

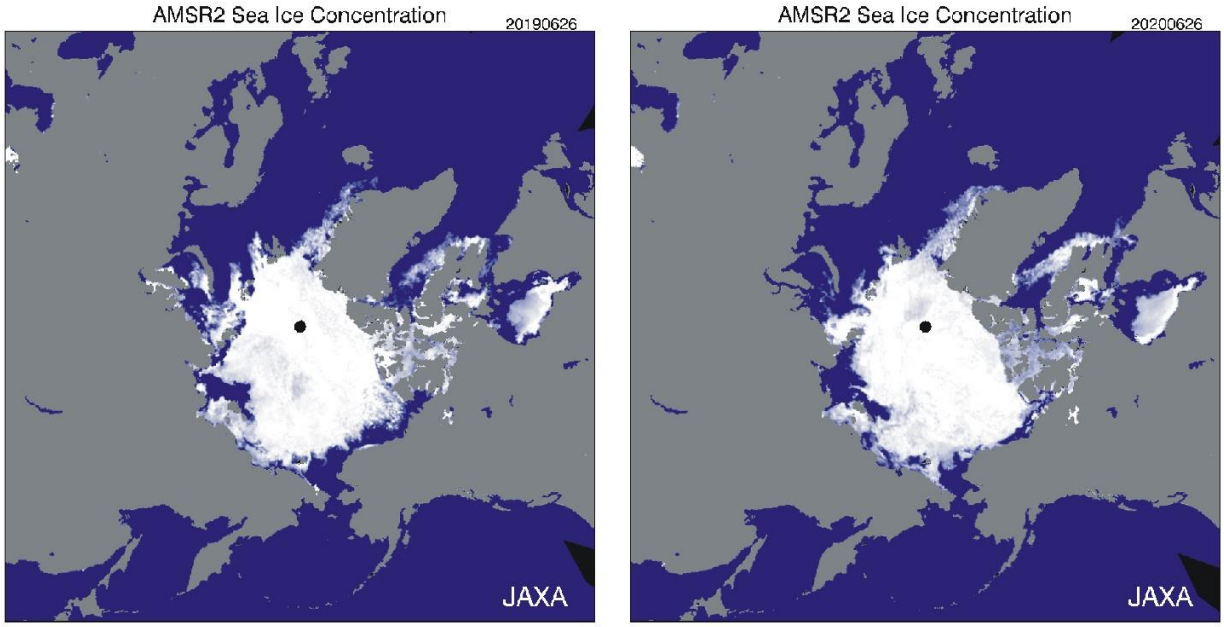

Diagrams showing Arctic sea ice extent and concentration 26 June 2019 (left) and 2020 (right), according to the Japan Aerospace Exploration Agency (JAXA).

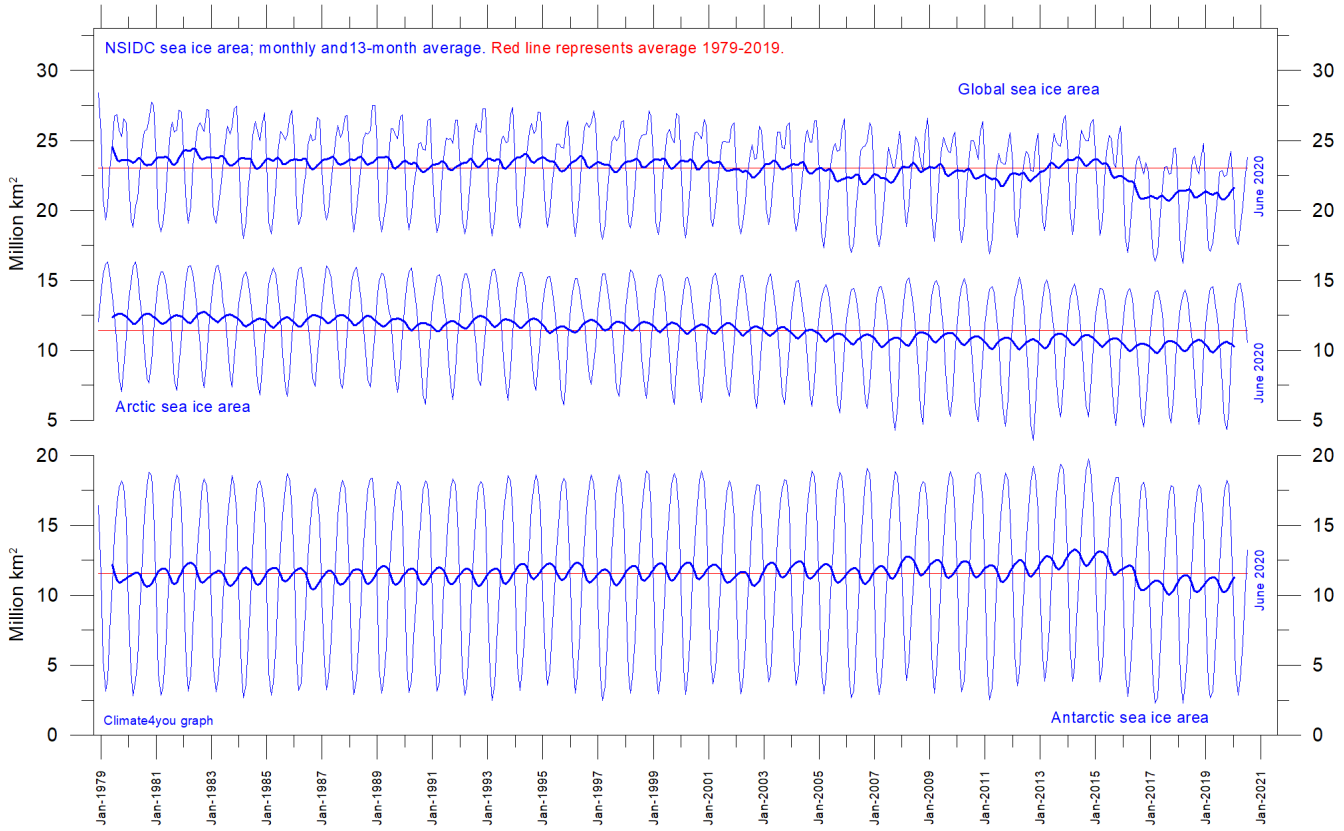

Graphs showing monthly Antarctic, Arctic and global sea ice extent since November 1978, according to the National Snow and Ice data Center (NSIDC).

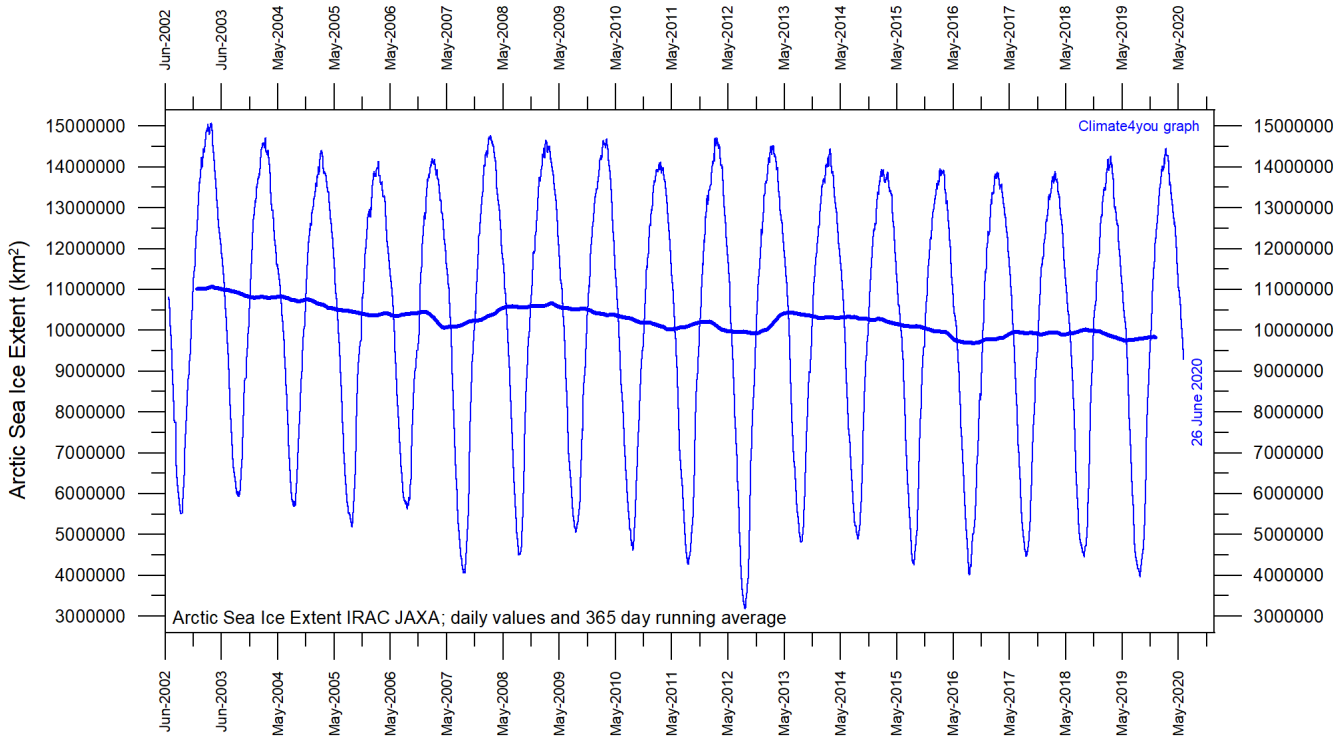

Diagram showing daily Arctic sea ice extent since June 2002, to 26 June 2020, by courtesy of Japan Aerospace Exploration Agency (JAXA).

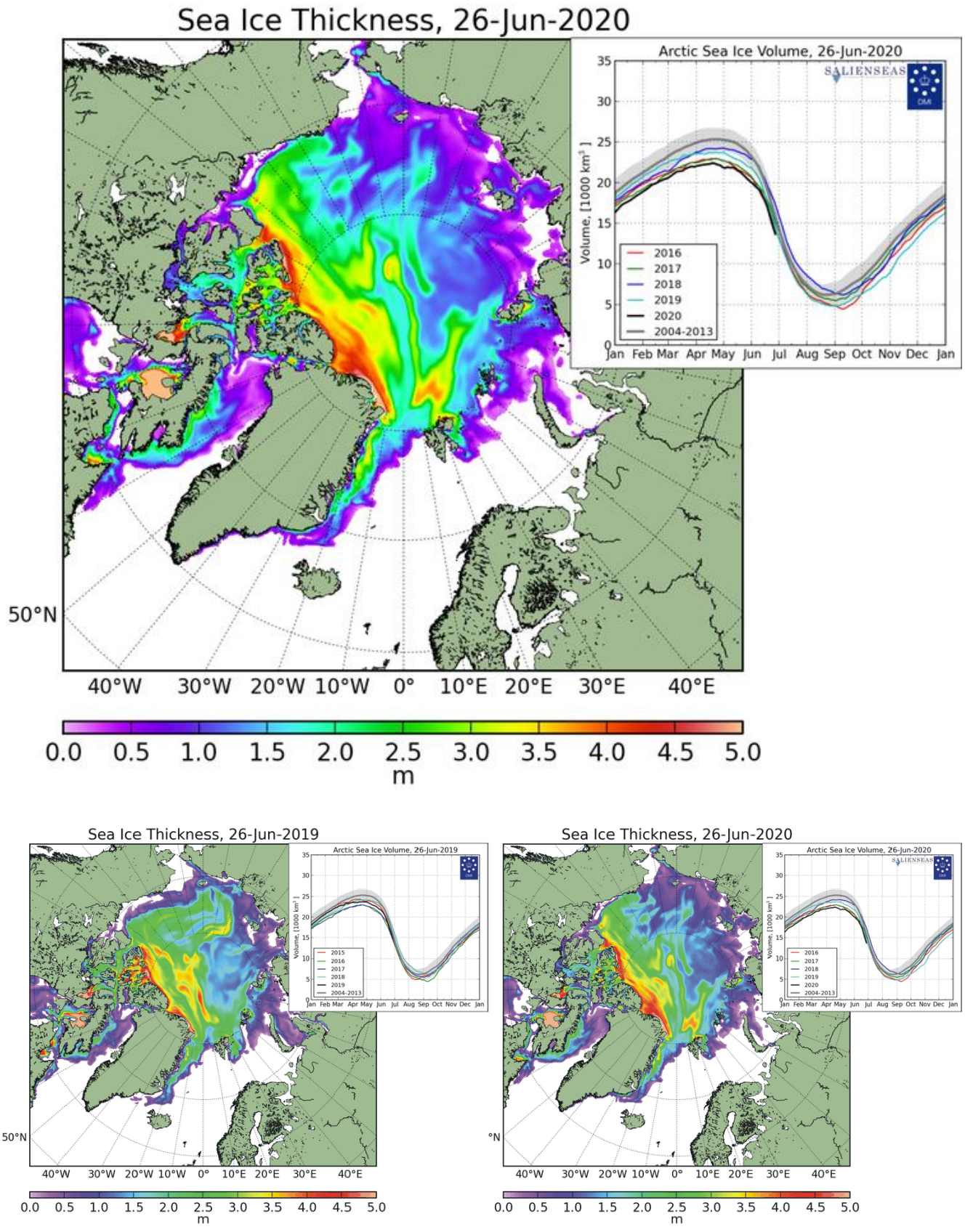

Diagrams showing Arctic sea ice extent and thickness 26 June 2019 (left) and 2020 (right and above) and the seasonal cycles of the calculated total arctic sea ice volume, according to [The Danish Meteorological Institute (DMI)](). The mean sea ice volume and standard deviation for the period 2004-2013 are shown by grey shading.

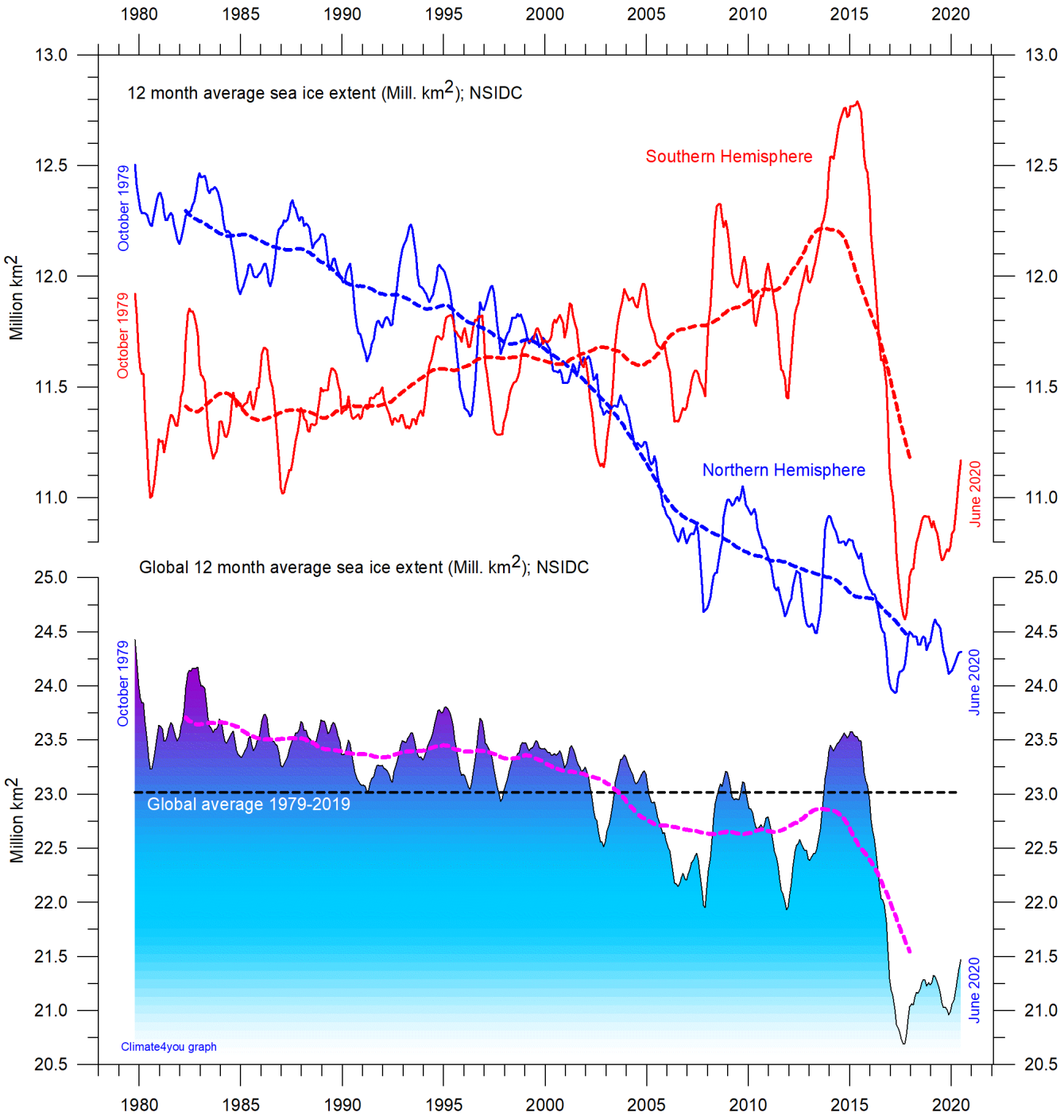

12 month running average sea ice extension, global and in both hemispheres since 1979, the satellite-era. The October 1979 value represents the monthly 12-month average of November 1978 - October 1979, the November 1979 value represents the average of December 1978 - November 1979, etc. The stippled lines represent a 61-month (ca. 5 years) average. Data source: National Snow and Ice Data Center (NSIDC).

Sea level in general

Global (or eustatic) sea-level change is measured relative to an idealised reference level, the geoid, which is a mathematical model of planet Earth's surface (Carter et al. 2014). Global sea-level is a function of the volume of the ocean basins and the volume of water they contain. Changes in global sea-level are caused by – but not limited to - four main mechanisms:

1. Changes in local and regional air pressure and wind, and tidal changes introduced by the Moon.
2. Changes in ocean basin volume by tectonic (geological) forces.
3. Changes in ocean water density caused by variations in currents, water temperature and salinity.
4. Changes in the volume of water caused by changes in the mass balance of terrestrial glaciers.

In addition to these there are other mechanisms influencing sea-level; such as storage of ground water, storage in lakes and rivers, evaporation, etc.

Mechanism 1 is controlling sea-level at many sites on a time scale from months to several years. As an example, many coastal stations show a pronounced annual variation reflecting seasonal changes in air pressures and wind speed. Longer-term climatic changes playing out over decades or centuries will also affect measurements of sea-level changes. Hansen et al. (2011, 2015) provide excellent analyses of sea-level changes caused by recurrent changes of the orbit of the Moon and other phenomena.

Mechanism 2 – with the important exception of earthquakes and tsunamis - typically operates over long (geological) time scales and is not significant on human time scales. It may relate to variations in the seafloor spreading rate, causing volume changes in mid-ocean mountain ridges, and to the slowly changing configuration of land and oceans. Another effect may be the slow rise of basins due to isostatic offloading by deglaciation after an ice age. The floor of the Baltic Sea and the Hudson Bay are presently rising, causing a slow net transfer of water from these basins into the adjoining oceans. Slow changes of very big glaciers (ice sheets) and movements in the mantle will affect the gravity field and thereby the vertical position of the ocean surface. Any increase of the total water mass as well as sediment deposition into oceans increase the load on their bottom, generating sinking by viscoelastic flow in the mantle below. The mantle flow is directed towards the surrounding land areas, which will rise, thereby partly compensating for the initial sea level increase induced by the increased water mass in the ocean.

Mechanism 3 (temperature-driven expansion) only affects the uppermost part of the oceans on human time scales. Usually, temperature-driven changes in density are more important than salinity-driven changes. Seawater is characterised by a relatively small coefficient of expansion, but the effect should however not be overlooked, especially when interpreting satellite altimetry data. Temperature-driven expansion of a column of seawater will not affect the total mass of water within the column considered and will therefore not affect the potential at the top of the water column. Temperature-driven ocean water expansion will therefore not in itself lead to any lateral displacement of water, but only locally lift the ocean surface. Near the coast, where people are living, the depth of water approaches zero, so no measurable temperature-driven expansion will take place here (Mörner 2015). Mechanism 3 is for that reason not important for coastal regions.

Mechanism 4 (changes in glacier mass balance) is an important driver for global sea-level changes along coasts, for human time scales. Volume changes of floating glaciers – ice shelves – has no influence on the global sea-level, just like volume changes of floating sea ice has no influence. Only the mass-balance of grounded or land-based glaciers is important for the global sea-level along coasts.

Summing up: Presumably, mechanism 1 and 4 are the most important for understanding sea-level changes along coasts.

References:

Carter R.M., de Lange W., Hansen, J.M., Humlum O., Idso C., Kear, D., Legates, D., Mörner, N.A., Ollier C., Singer F. & Soon W. 2014. Commentary and Analysis on the Whitehead& Associates 2014 NSW Sea-Level Report. Policy Brief, NIPCC, 24. September 2014, 44 pp. http://climatechangereconsidered.org/wp-content/uploads/2014/09/NIPCC-Report-on-NSW-Coastal-SL-9z-corrected.pdf

Hansen, J.-M., Aagaard, T. and Binderup, M. 2011. Absolute sea levels and isostatic changes of the eastern North Sea to central Baltic region during the last 900 years. Boreas, 10.1111/j.1502-3885.2011.00229.x. ISSN 0300–9483.

Hansen, J.-M., Aagaard, T. and Huijpers, A. 2015. Sea-Level Forcing by Synchronization of 56- and 74-YearOscillations with the Moon's Nodal Tide on the Northwest European Shelf (Eastern North Sea to Central Baltic Sea). Journ. Coastal Research, 16 pp.

Mörner, Nils-Axel 2015. Sea Level Changes as recorded in nature itself. Journal of Engineering Research and Applications, Vol.5, 1, 124-129.

Global sea level from satellite altimetry, updated to January 2018

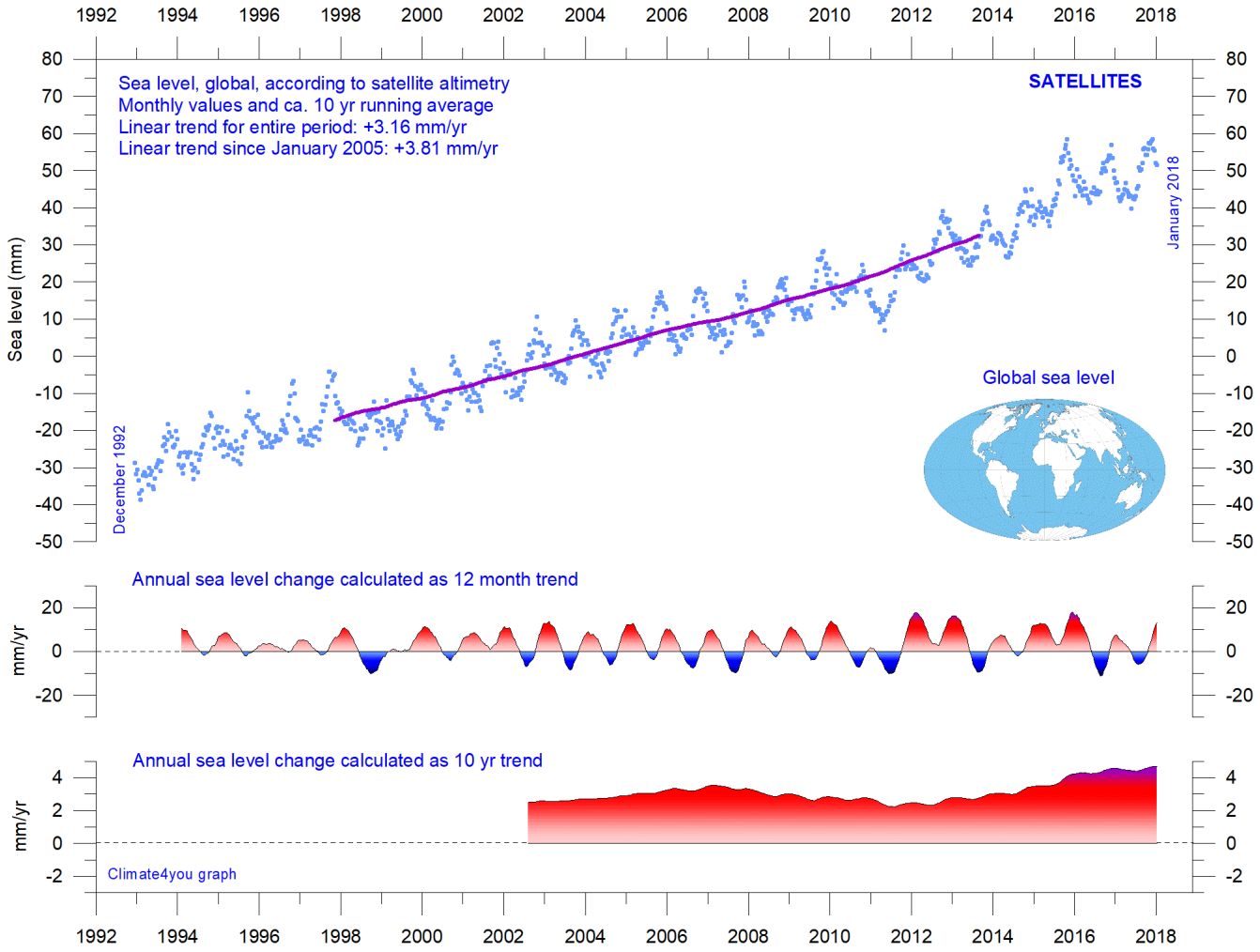

Global sea level since December 1992 according to the Colorado Center for Astrodynamics Research at University of Colorado at Boulder. The blue dots are the individual observations, and the purple line represents the running 121-month (ca. 10 year) average. The two lower panels show the annual sea level change, calculated for 1 and 10-year time windows, respectively. These values are plotted at the end of the interval considered. Data from the TOPEX/Poseidon mission have been used before 2002, and data from the Jason-1 mission (satellite launched December 2001) after 2002.

Ground truth is a term used in various fields to refer to information provided by direct observation as opposed to information provided by inference, such as, e.g., by satellite observations.

In remote sensing using satellite observations, ground truth data refers to information collected on location. Ground truth allows the satellite data to be related to real features observed on the planet surface. The collection of ground truth data enables calibration of remote-sensing data, and aids in the interpretation and analysis of what is being sensed or recorded by satellites. Ground truth sites allow the remote sensor operator to correct and improve the interpretation of satellite data.

For satellite observations on sea level ground true data are provided by the classical tide gauges (example diagram on next page), that directly measures the local sea level many places distributed along the coastlines on the surface of the planet.

Global sea level from tide-gauges, updated to December 2018

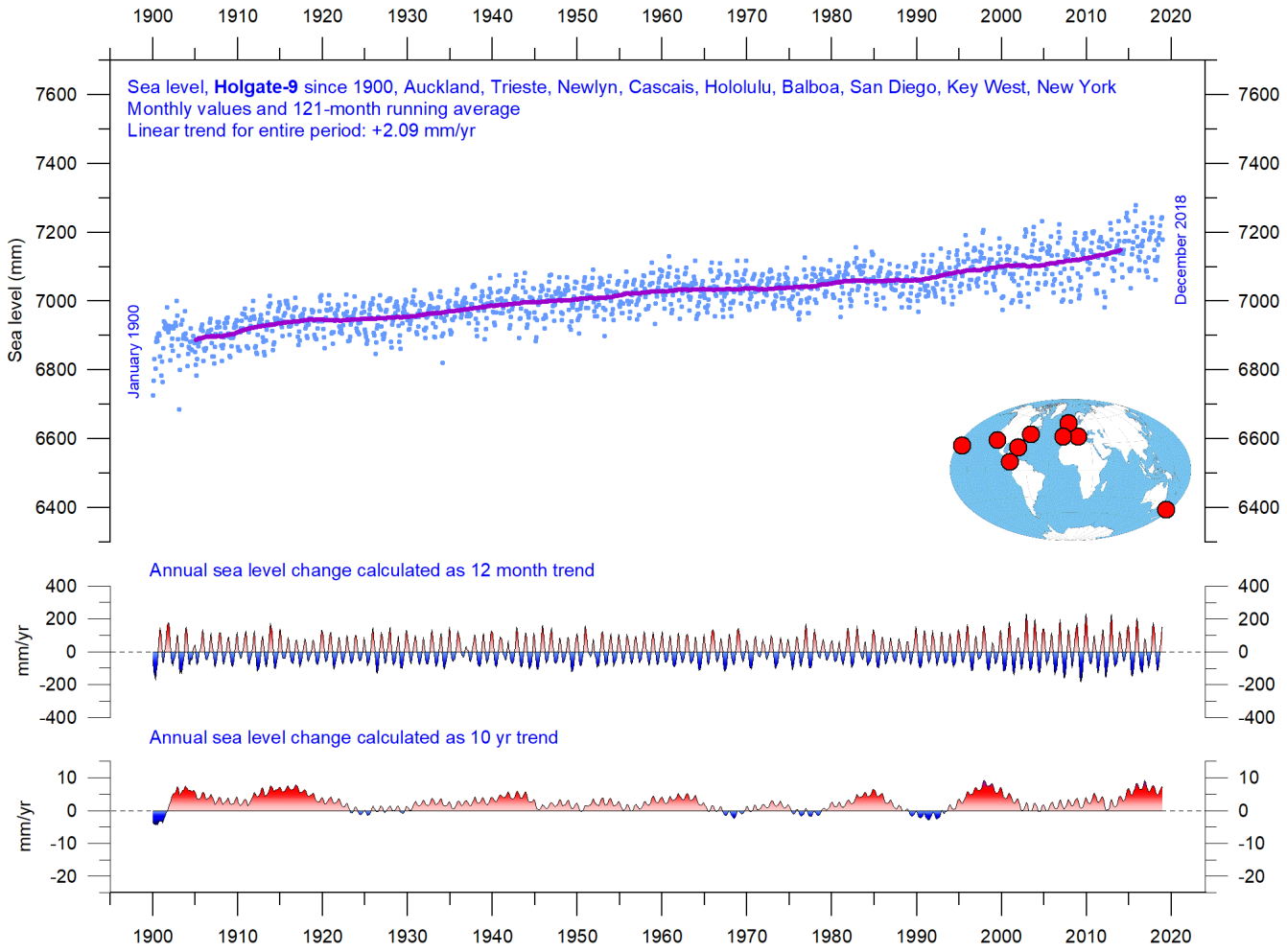

Holgate-9 monthly tide gauge data from PSMSL Data Explorer. Holgate (2007) suggested the nine stations listed in the diagram to capture the variability found in a larger number of stations over the last half century studied previously. For that reason, average values of the Holgate-9 group of tide gauge stations are interesting to follow, even though Auckland (New Zealand) has not reported data since 2000, and Cascais (Portugal) not since 1993. Unfortunately, by this data loss the Holgate-9 series since 2000 is underrepresented with respect to the southern hemisphere. The blue dots are the individual average monthly observations, and the purple line represents the running 121-month (ca. 10 year) average. The two lower panels show the annual sea level change, calculated for 1 and 10-year windows, respectively. These values are plotted at the end of the interval considered.

Data from tide-gauges all over the world suggest an average global sea-level rise of 1-1.5 mm/year, while the satellite-derived record (page 36) suggest a rise of about 3.2 mm/year, or more. The noticeable difference (at least 1:2) between the two data sets is remarkable but has no broadly accepted explanation. It is however known that satellite observations are facing several complications in areas near the coast. Vignudelli et al. (2019) provide an updated overview of the current limitations of classical satellite altimetry in coastal regions.

References:

Holgate, S.J. 2007. On the decadal rates of sea level change during the twentieth century. Geophys. Res. Letters, 34, L01602, doi:10.1029/2006GL028492

Vignudelli et al. 2019. Satellite Altimetry Measurements of Sea Level in the Coastal Zone. *Surveys in Geophysics, Vol.* 40, p. 1319–1349. https://link.springer.com/article/10.1007/s10712-019-09569-1

Northern Hemisphere weekly and seasonal snow cover, updated to June 2020

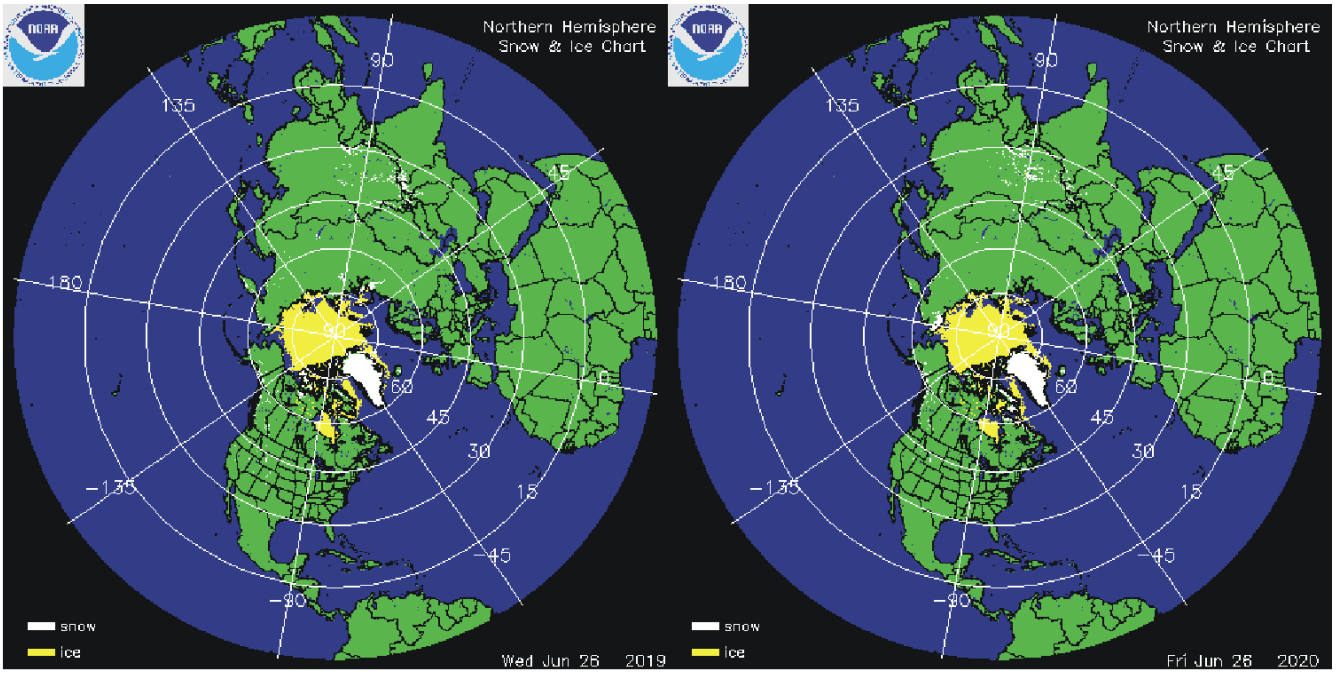

Northern hemisphere snow cover (white) and sea ice (yellow) 26 June 2019 (left) and 2020 (right). Map source: National Ice Center (NIC).

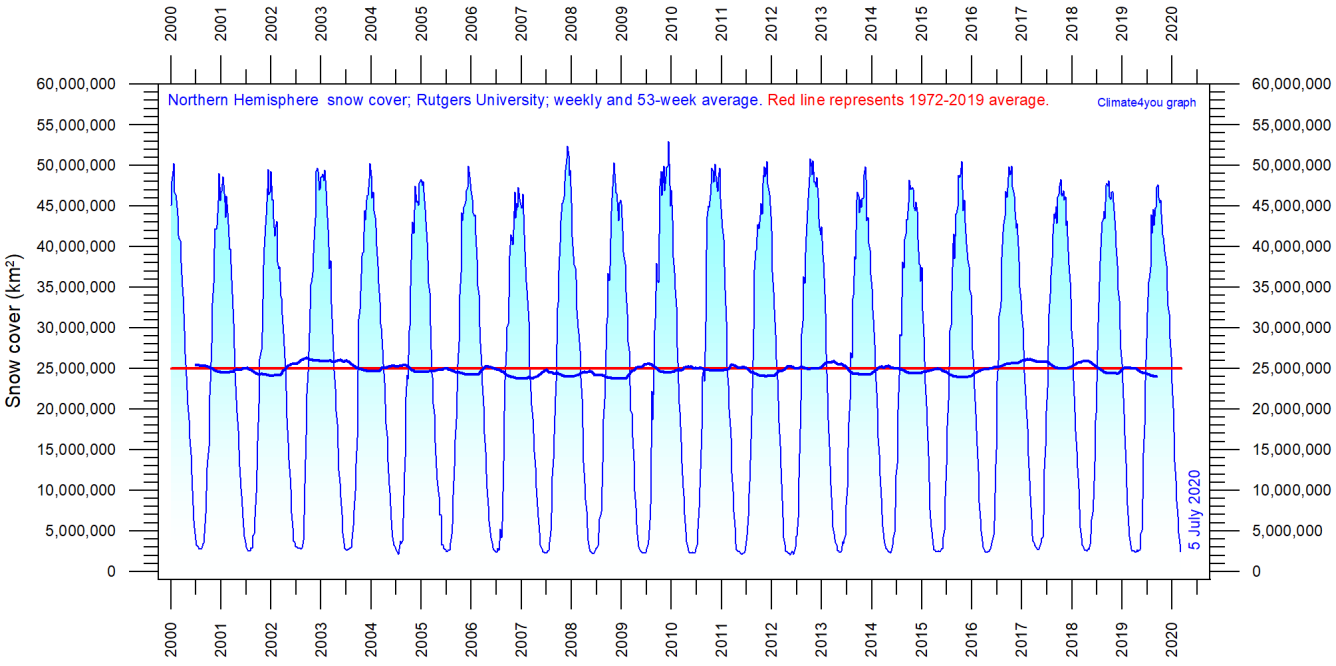

Northern hemisphere weekly snow cover since January 2000 according to Rutgers University Global Snow Laboratory. The thin blue line is the weekly data, and the thick blue line is the running 53-week average (approximately 1 year). The horizontal red line is the 1972-2019 average.

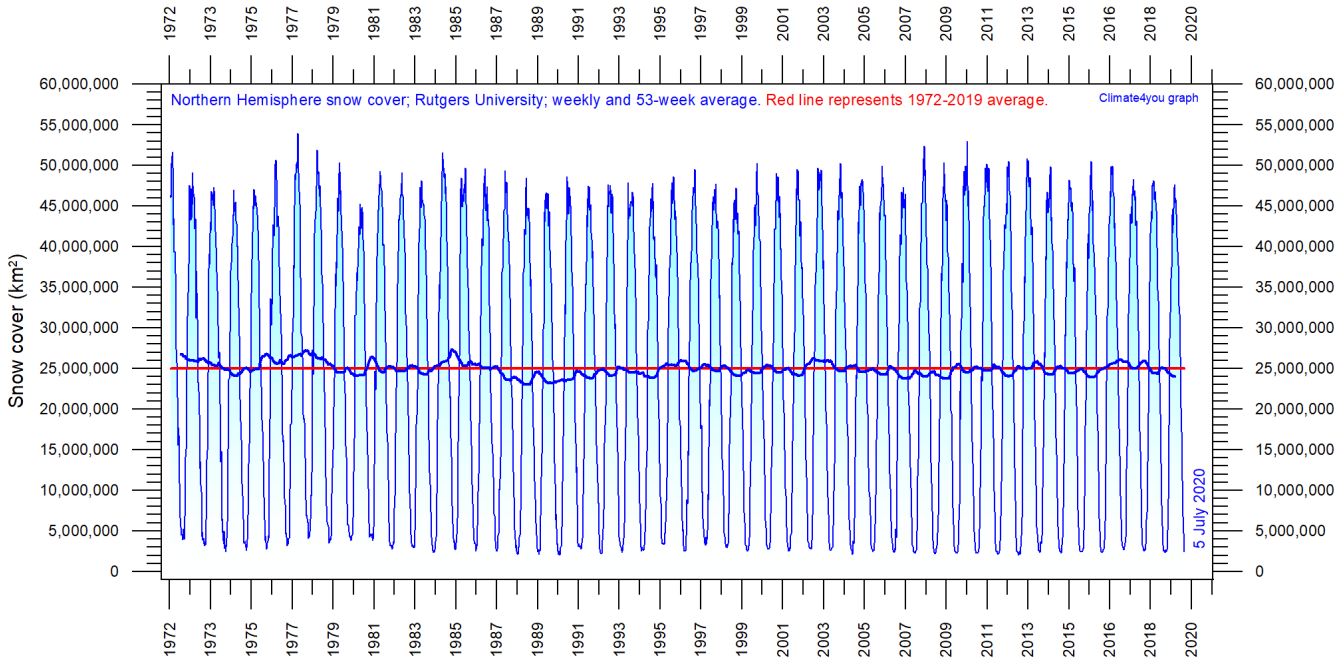

Northern hemisphere weekly snow cover since January 1972 according to Rutgers University Global Snow Laboratory. The thin blue line is the weekly data, and the thick blue line is the running 53-week average (approximately 1 year). The horizontal red line is the 1972-2019 average.

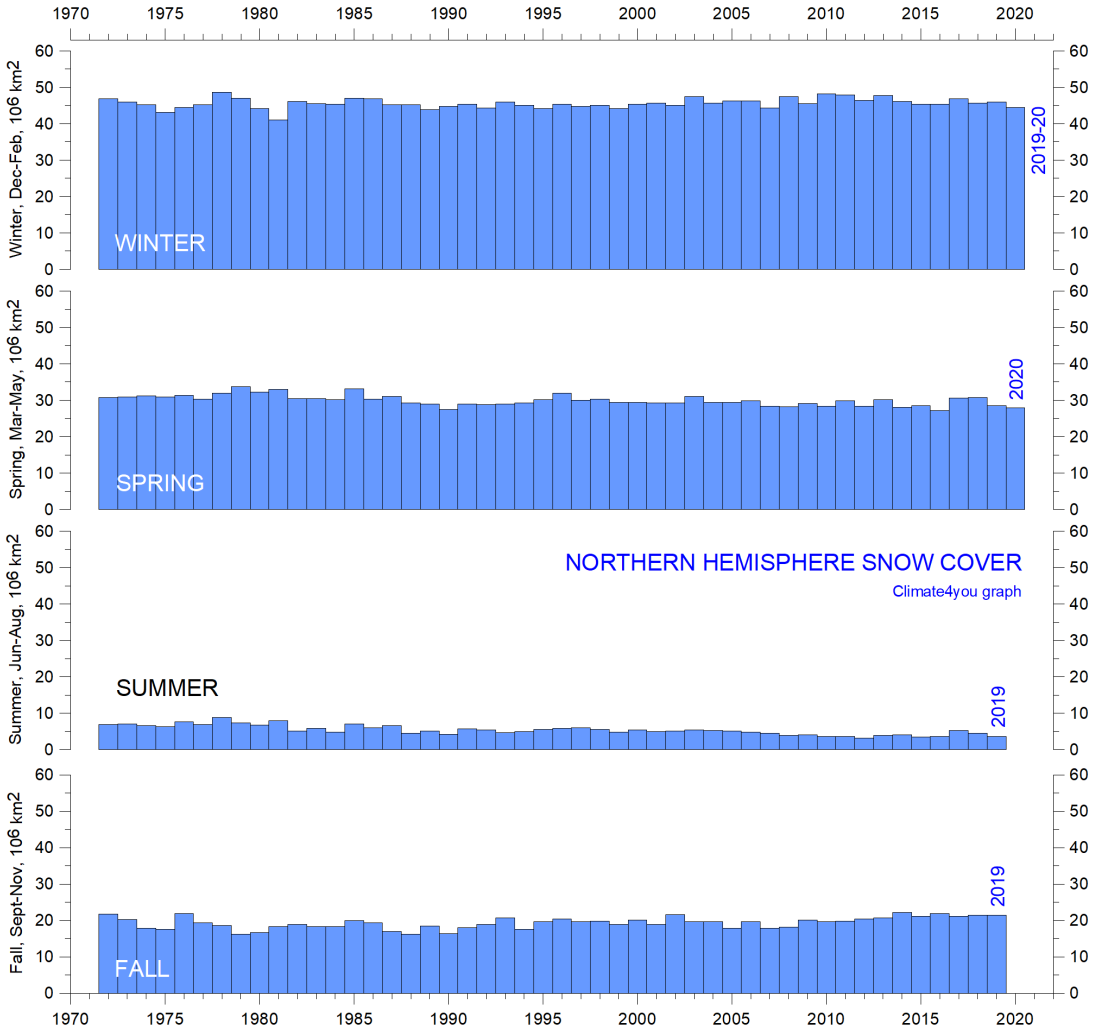

Northern hemisphere seasonal snow cover since January 1972 according to Rutgers University Global Snow Laboratory.

Atmospheric specific humidity, updated to June 2020

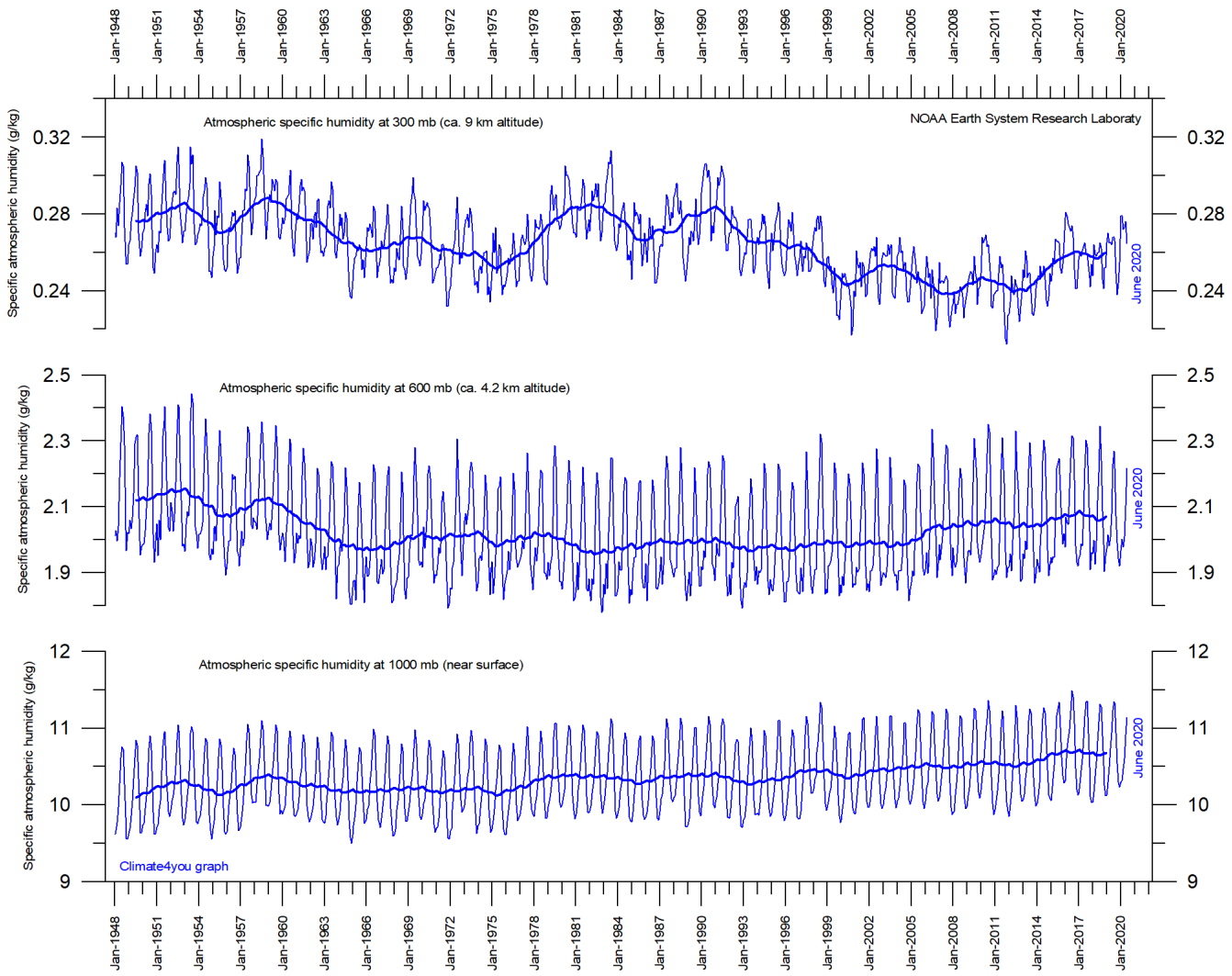

Specific atmospheric humidity (g/kg) at three different altitudes in the lower part of the atmosphere (the Troposphere) since January 1948 (Kalnay et al. 1996). The thin blue lines show monthly values, while the thick blue lines show the running 37-month average (about 3 years). Data source: Earth System Research Laboratory (NOAA).

Water vapor is the most important greenhouse gas in the Troposphere. The highest concentration is found within a latitudinal range from 50°N to 60°S. The two polar regions of the Troposphere are comparatively dry.

The diagram above shows the specific atmospheric humidity to be stable or slightly increasing up to about 4-5 km altitude. At higher levels in the Troposphere (about 9 km), the specific humidity has been decreasing for the duration of the record (since 1948), but with shorter variations superimposed on the falling trend. A Fourier frequency analysis (not shown here) shows these variations to be influenced especially by a periodic variation of about 3.7-year duration.

The persistent decrease in specific humidity at about 9 km altitude is particularly noteworthy, as this altitude roughly corresponds to the level where the theoretical temperature effect of increased atmospheric CO_2 is expected initially to play out.

Atmospheric CO_2, updated to June 2020

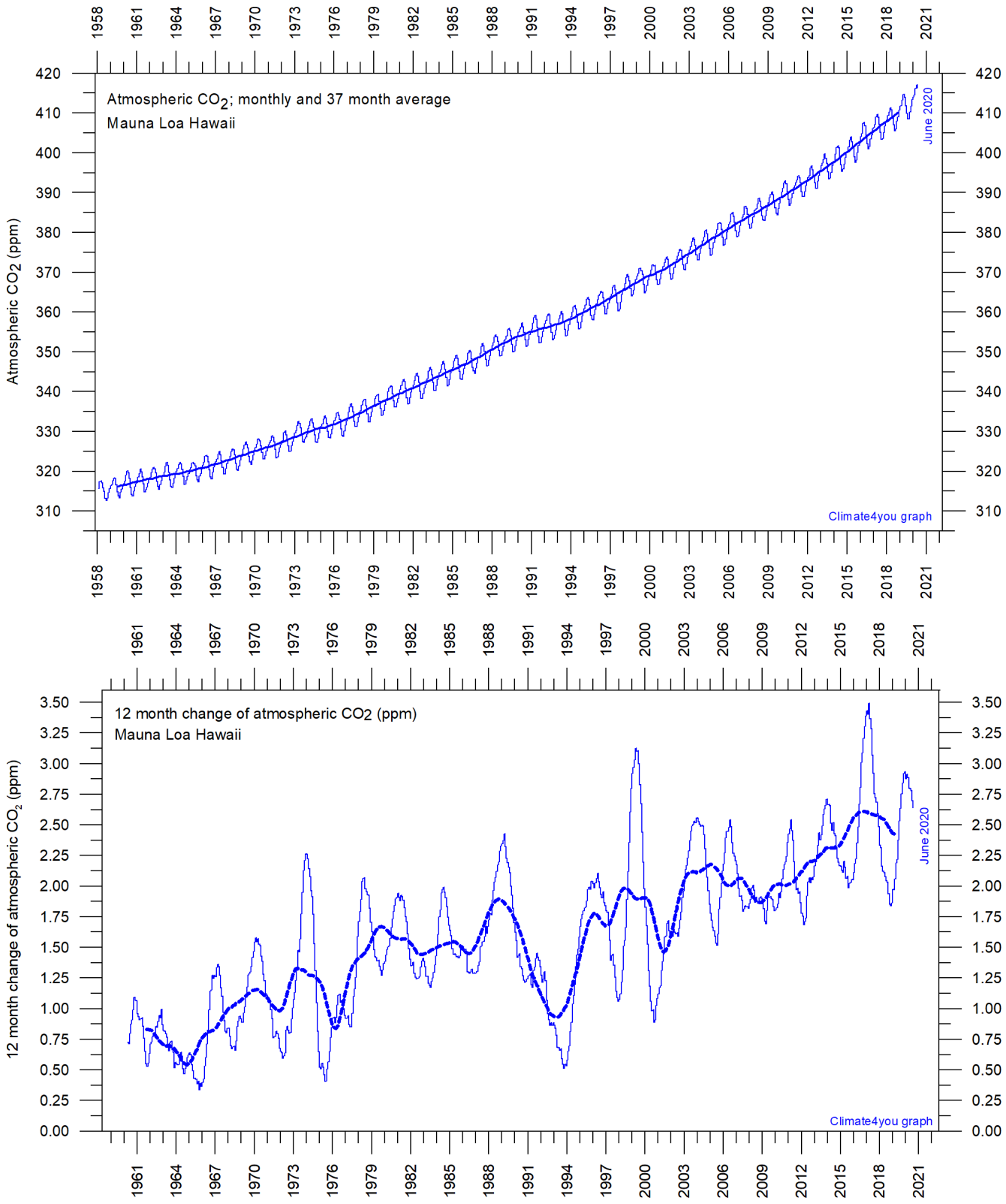

Monthly amount of atmospheric CO_2 (upper diagram) and annual growth rate (lower diagram); average last 12 months minus average preceding 12 months, thin line) of atmospheric CO_2 since 1959, according to data provided by the Mauna Loa Observatory, Hawaii, USA. The thick, stippled line is the simple running 37-observation average, nearly corresponding to a running 3-year average

The relation between annual change of atmospheric CO_2 and La Niña and El Niño episodes, updated to June 2020

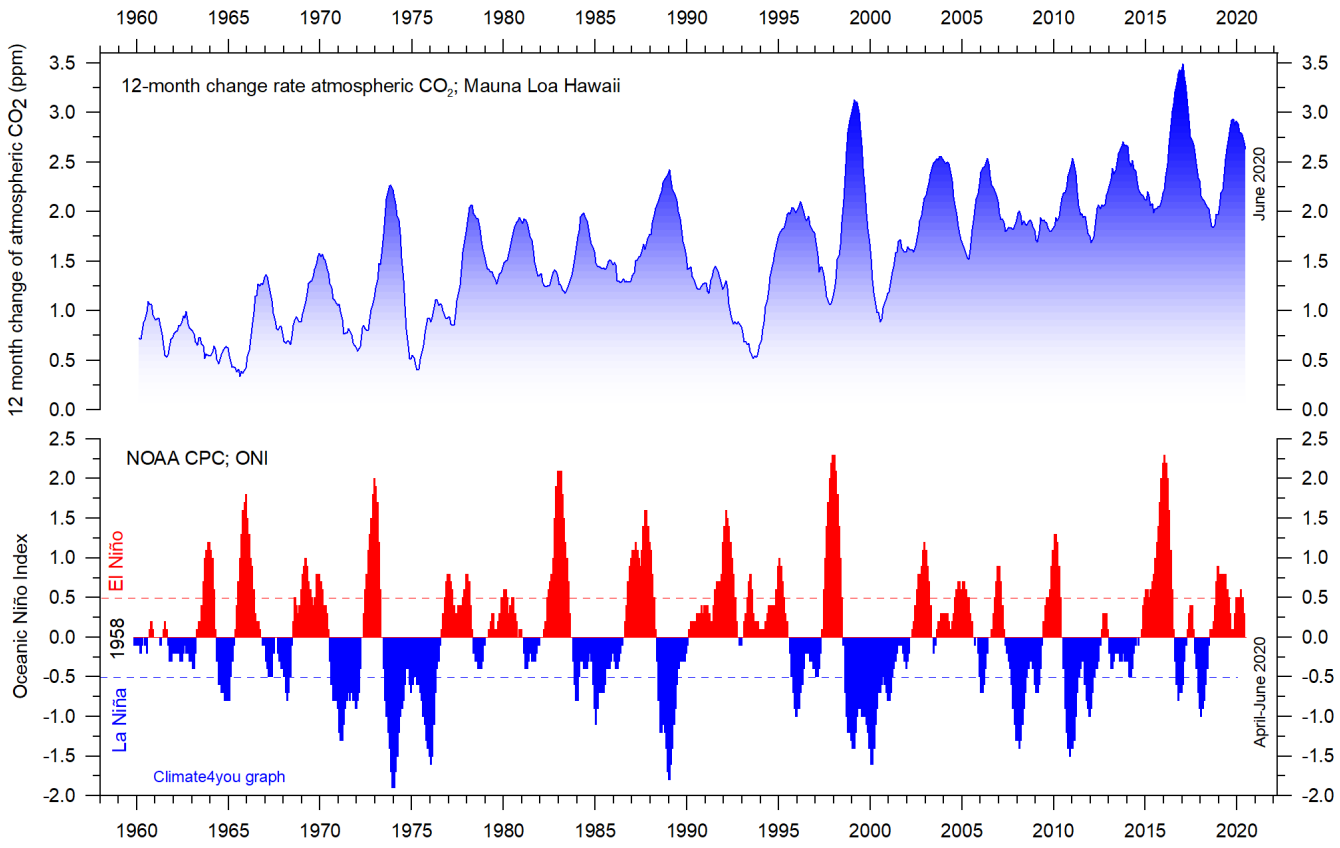

Visual association between annual growth rate of atmospheric CO_2 (upper panel) and Oceanic Niño Index (lower panel). See also diagrams on page 40 and 22, respectively.

Changes in the global atmospheric CO_2 is seen to vary roughly in concert with changes in the Oceanic Niño Index. The typical sequence of events is that changes in the global atmospheric CO_2 to a certain degree follows changes in the Oceanic Niño Index, but clearly not in all details. Many processes, natural as well as anthropogene, controls the amount of atmospheric CO_2, but oceanographic processes are clearly highly important (see also diagram on next page).

Atmospheric CO_2 and the present coronavirus pandemic

Modern political initiatives usually assume the human influence (mainly the burning of fossil fuels) to represent the core reason for the observed increase in atmospheric CO_2 since 1958 (see diagrams on page 41).

The present (since January 2020) coronavirus pandemic has resulted in a marked reduction in the global consumption of fossil fuels, as is well reflected by plummeting value of oil and gas. It is interesting to follow the effect of this on the amount of atmospheric CO_2.

By the end of June 2020 there is still no clear effect to be seen. The simplest explanation for this is that the human contribution is too small compared to the numerous natural sources and sinks for atmospheric CO_2 to appear in diagrams showing the amount of atmospheric CO_2 (diagrams on p. 41-43).

The phase relation between atmospheric CO_2 and global temperature, updated to May 2020

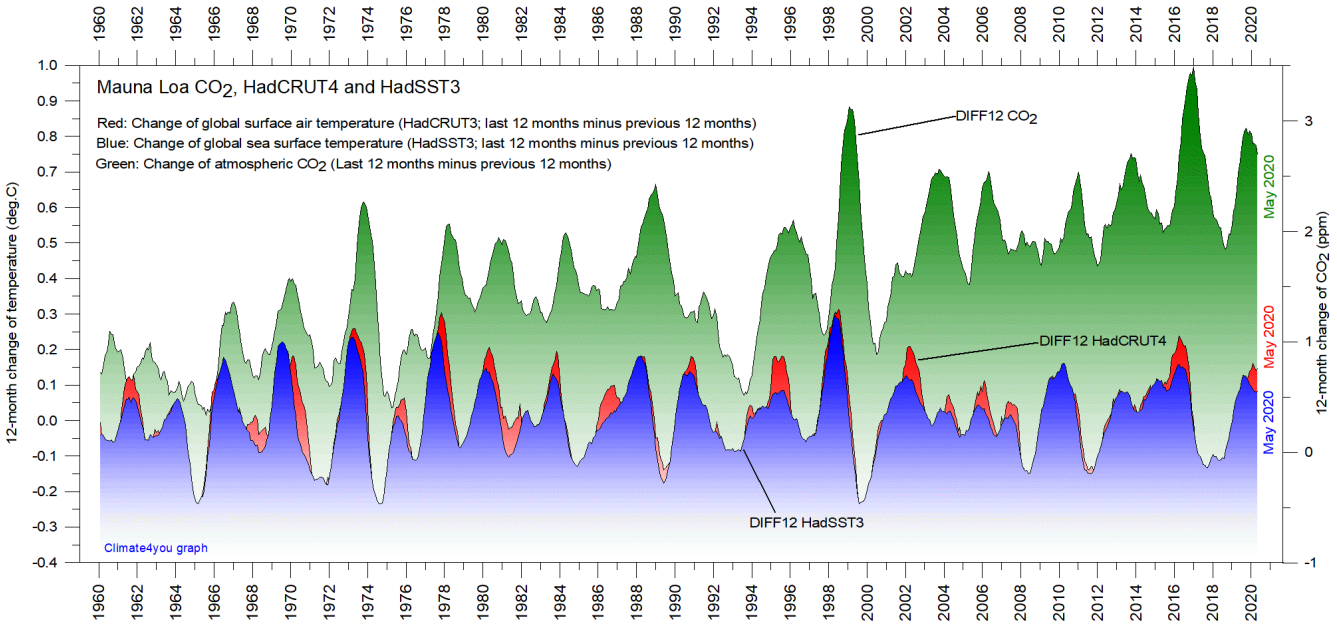

12-month change of global atmospheric CO_2 concentration (Mauna Loa; green), global sea surface temperature (HadSST3; blue) and global surface air temperature (HadCRUT4; red dotted). All graphs are showing monthly values of DIFF12, the difference between the average of the last 12 month and the average for the previous 12 months for each data series.

The typical sequence of events is seen to be that changes in the global atmospheric CO_2 follow changes in global surface air temperature, which again follow changes in global ocean surface temperatures. Thus, changes in global atmospheric CO_2 are lagging 9.5–10 months behind changes in global air surface temperature, and 11–12 months behind changes in global sea surface temperature.

References:

Humlum, O., Stordahl, K. and Solheim, J-E. 2012. The phase relation between atmospheric carbon dioxide and global temperature. Global and Planetary Change, August 30, 2012.
http://www.sciencedirect.com/science/article/pii/S0921818112001658?v=s5

Global air temperature and atmospheric CO_2, updated to June 2020

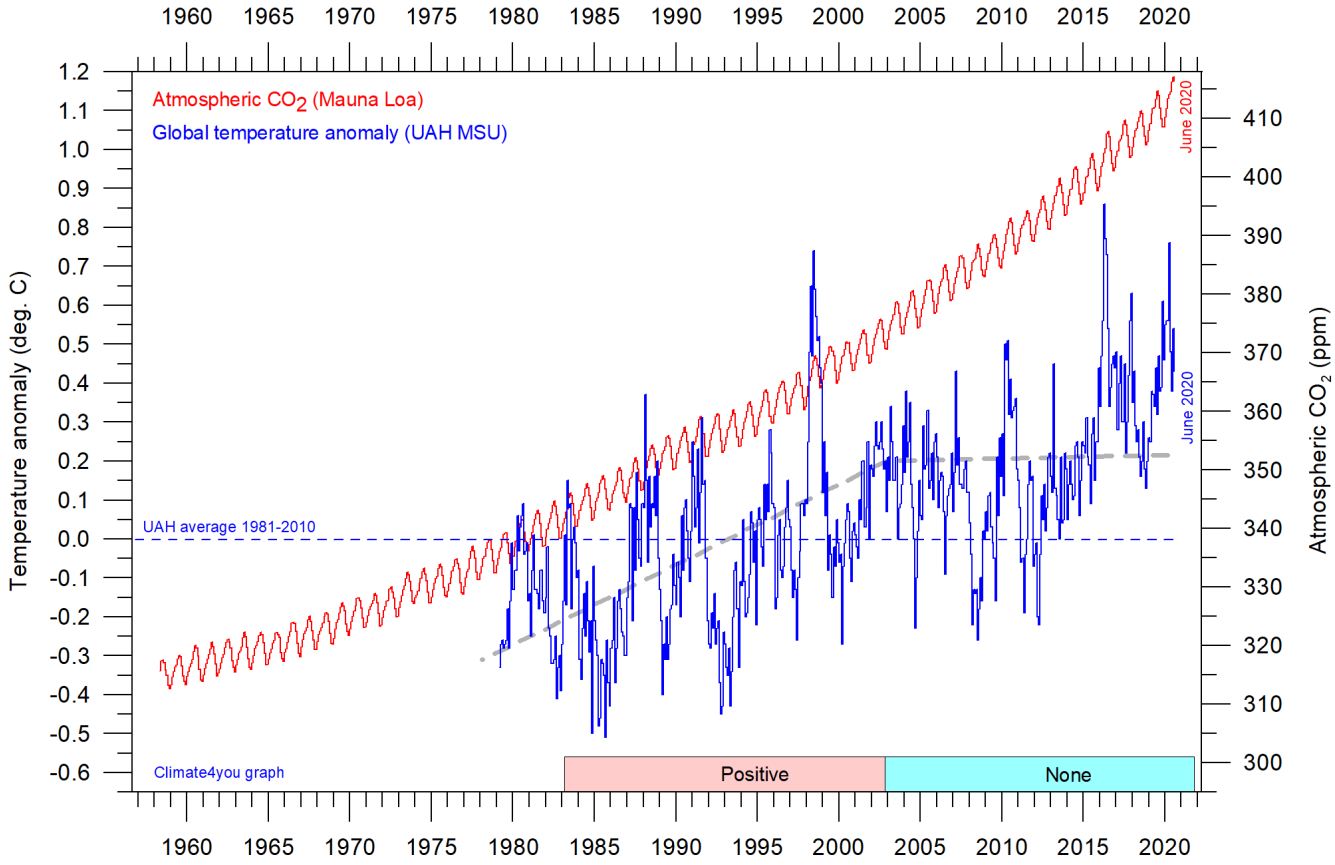

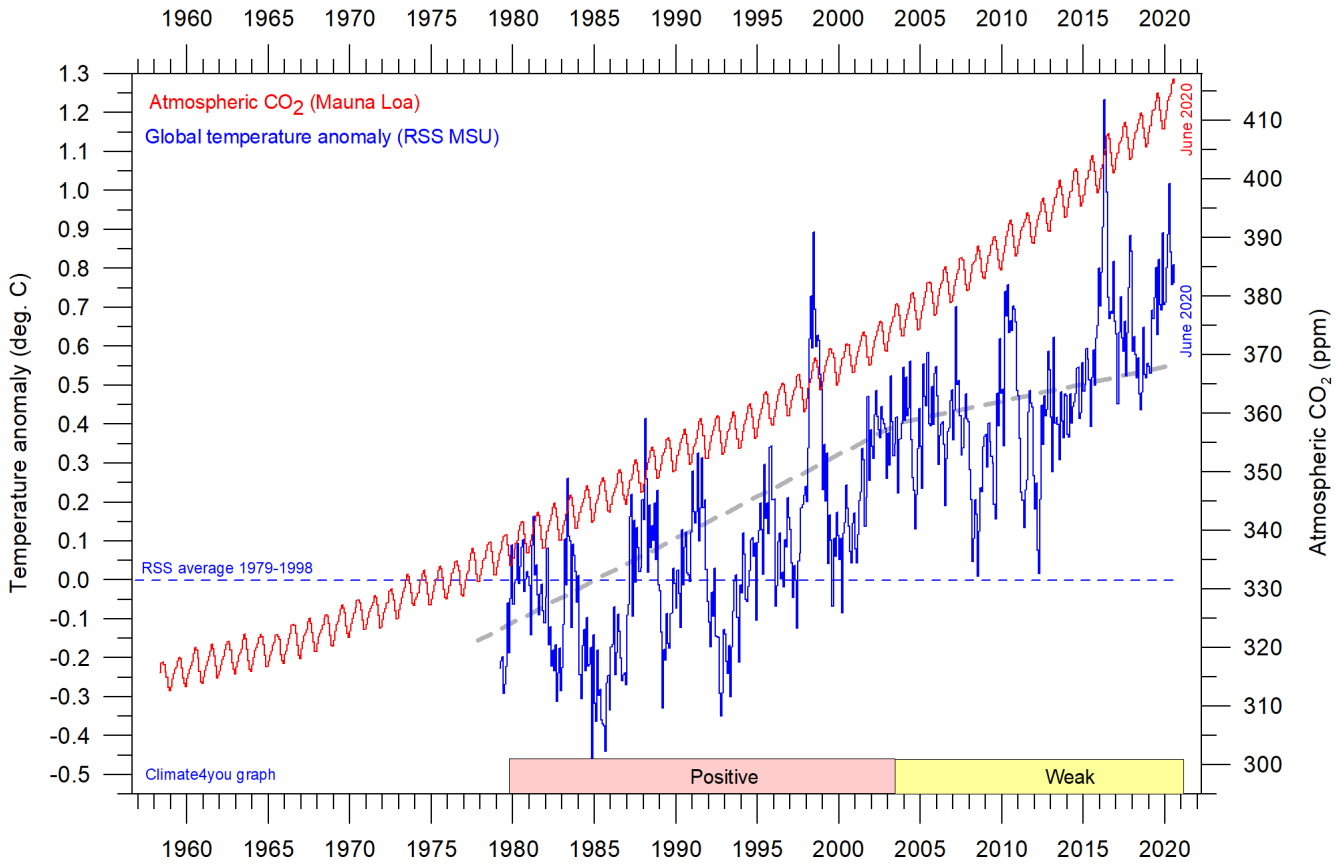

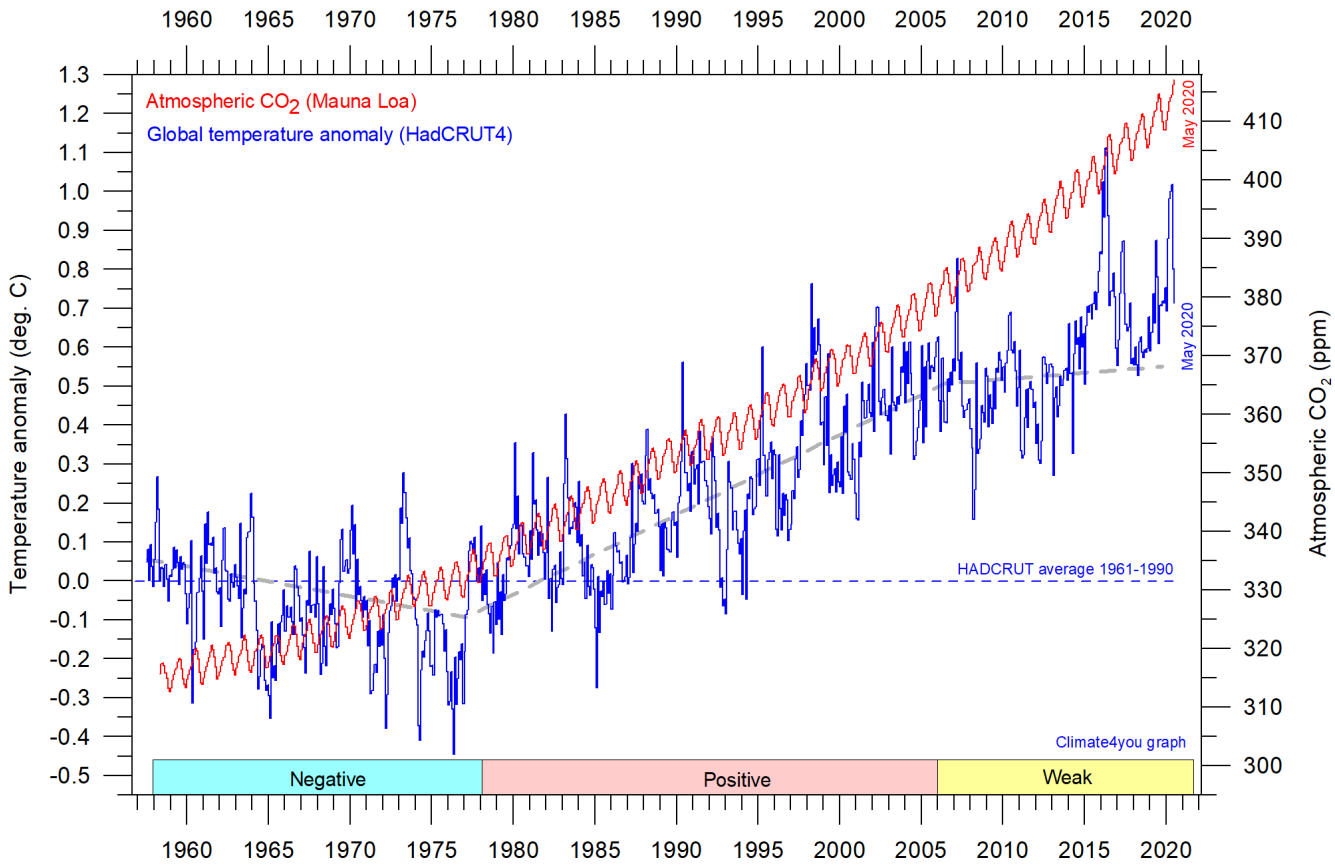
Atmospheric CO2 (Mauna Loa)
Global temperature anomaly (HadCRUT4)
May 2020
May 2020
HADCRUT average 1961-1990
Climate4you graph
Negative
Positive
Weak
Temperature anomaly (deg. C)
Atmospheric CO2 (ppm)
1960 1965 1970 1975 1980 1985 1990 1995 2000 2005 2010 2015 2020
1.3 1.2 1.1 1.0 0.9 0.8 0.7 0.6 0.5 0.4 0.3 0.2 0.1 0.0 -0.1 -0.2 -0.3 -0.4 -0.5
410 400 390 380 370 360 350 340 330 320 310 300

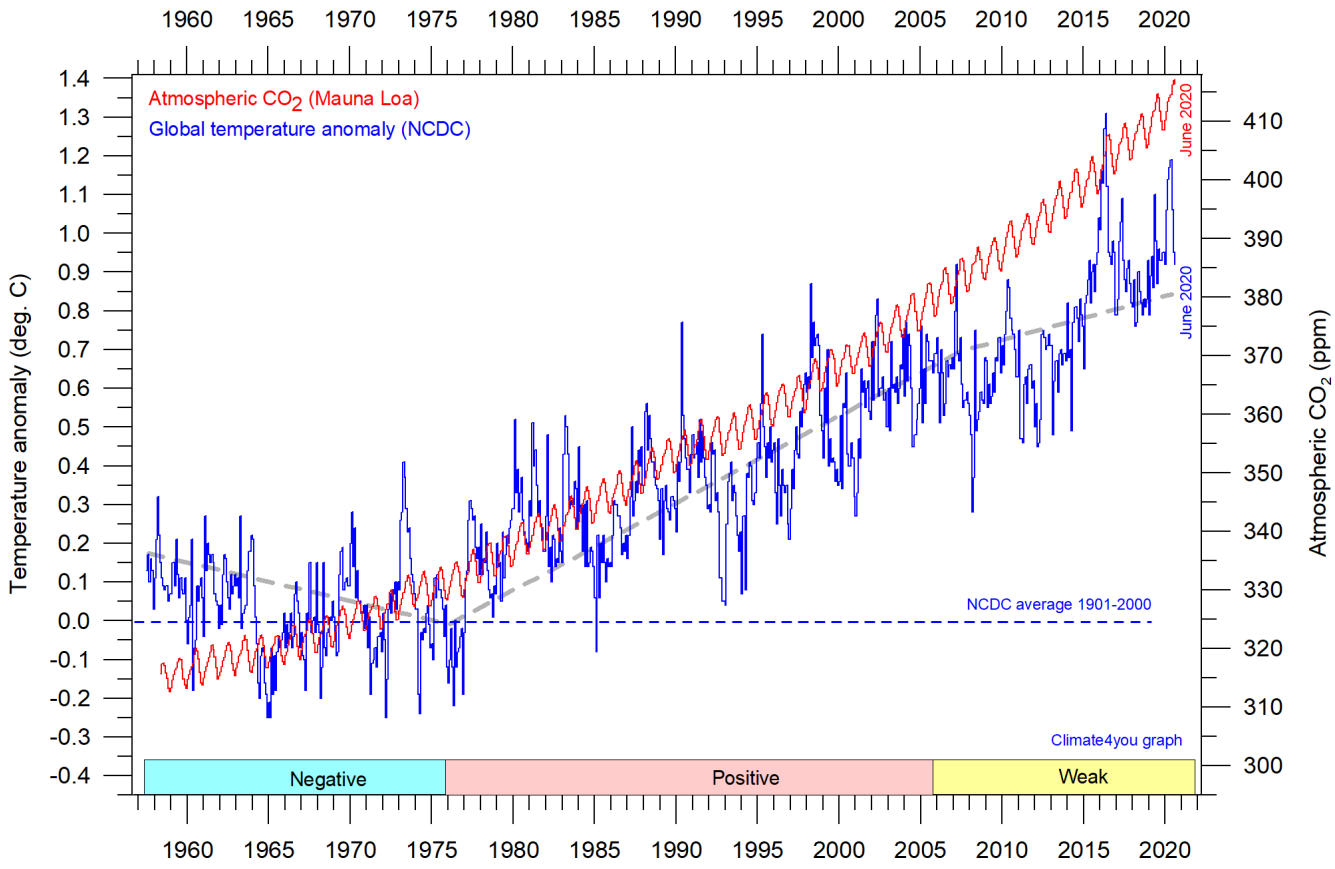
Atmospheric CO2 (Mauna Loa)
Global temperature anomaly (NCDC)
June 2020
June 2020
NCDC average 1901-2000
Climate4you graph
Negative
Positive
Weak
Temperature anomaly (deg. C)
Atmospheric CO2 (ppm)
1960 1965 1970 1975 1980 1985 1990 1995 2000 2005 2010 2015 2020
1.4 1.3 1.2 1.1 1.0 0.9 0.8 0.7 0.6 0.5 0.4 0.3 0.2 0.1 0.0 -0.1 -0.2 -0.3 -0.4
410 400 390 380 370 360 350 340 330 320 310 300

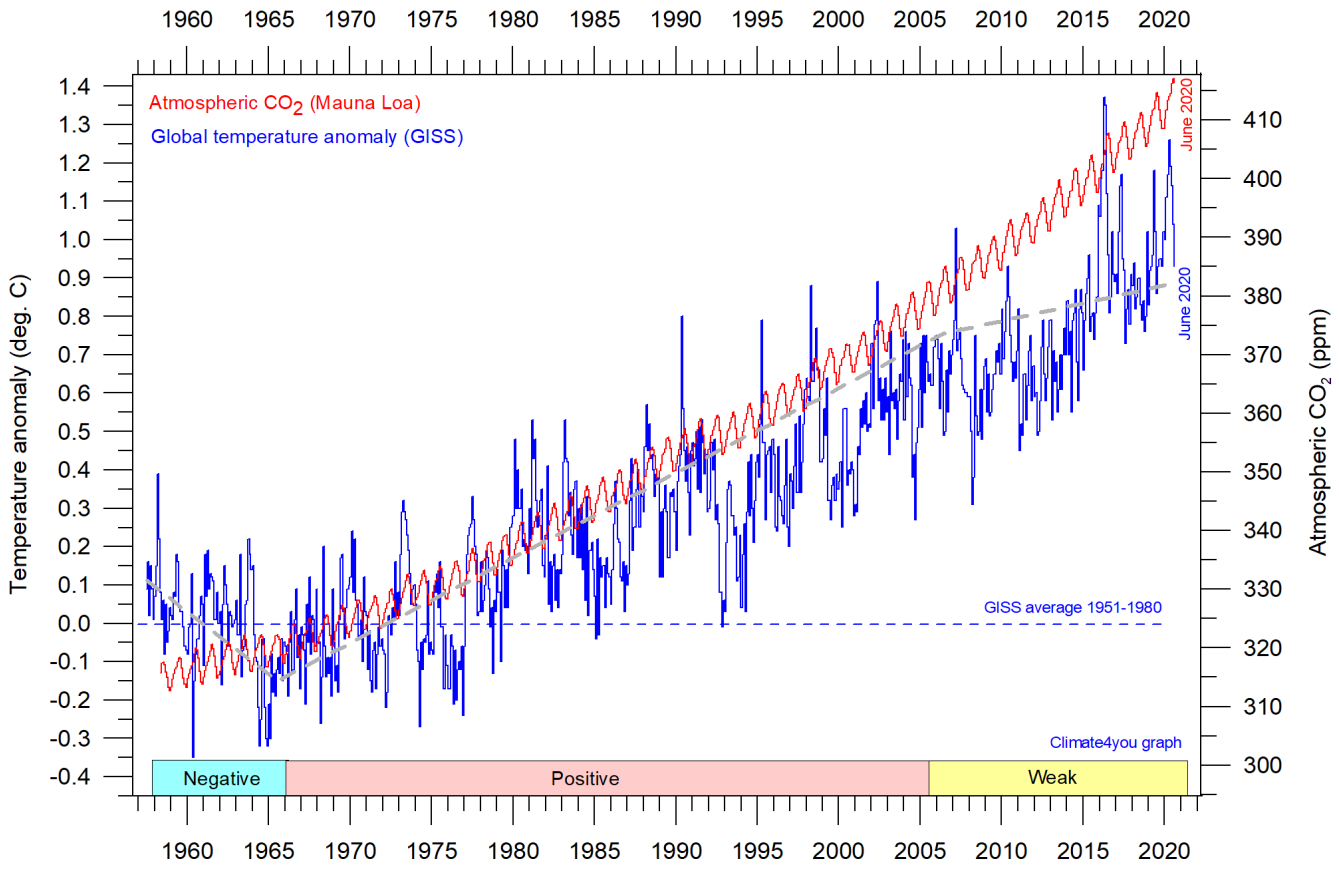

Diagrams showing UAH, RSS, HadCRUT4, NCDC and GISS monthly global air temperature estimates (blue) and the monthly atmospheric CO_2 content (red) according to the Mauna Loa Observatory, Hawaii. The Mauna Loa data series begins in March 1958, and 1958 was therefore chosen as starting year for the all diagrams above. Reconstructions of past atmospheric CO_2 concentrations (before 1958) are not incorporated in this diagram, as such past CO_2 values are derived by other means (ice cores, stomata, or older measurements using different methodology), and therefore are not directly comparable with direct atmospheric measurements. The dotted grey line indicates the approximate linear temperature trend, and the boxes in the lower part of the diagram indicate the relation between atmospheric CO_2 and global surface air temperature, negative or positive.

Most climate models are programmed to give the greenhouse gas carbon dioxide CO_2 significant influence on the modelled global temperature. It is therefore relevant to compare different temperature records with measurements of atmospheric CO_2, as shown in the diagrams above.

Any comparison, however, should not be made on a monthly or annual basis, but for a longer time, as other effects (oceanographic, cloud cover, etc.) may override the potential influence of CO_2 on short time scales such as just a few years.

It is of cause equally inappropriate to present new meteorological record values, whether daily, monthly, or annual, as demonstrating the legitimacy of the hypothesis ascribing high importance of atmospheric CO_2 for global temperatures. Any such meteorological record value may well be the result of other phenomena. Unfortunately, many news media repeatedly fall into this trap.

What exactly defines the critical length of a relevant period length to consider for evaluating the alleged importance of CO_2 remains elusive and represents a theme for discussion.

Nonetheless, the length of the critical period must be inversely proportional to the temperature sensitivity of CO_2, including feedback effects. Thus, if the net temperature effect of atmospheric CO_2 is strong, the critical period will be short, and vice versa.

However, past climate research history provides some clues as to what has traditionally been considered the relevant length of period over which to compare temperature and atmospheric CO_2.

After about 10 years of concurrent global temperature- and CO_2-increase, IPCC was established in 1988. For obtaining public and political support for the CO_2-hyphotesis the 10-year warming period leading up to 1988 most likely was considered important. Had the global temperature instead been decreasing at that time, politic support for the hypothesis would have been difficult to obtain in 1988.

Based on the previous 10 years of concurrent temperature- and CO_2-increase, many climate scientists in 1988 presumably felt that their understanding of climate dynamics was enough to conclude about the importance of CO_2 for affecting observed global temperatures.

Thus, it may safely be concluded that 10 years in 1988 was considered a period long enough to demonstrate the effect of increasing atmospheric CO_2 on global temperatures. The 10-year period is also basis for the anomality diagrams shown on page 2.

Adopting this approach as to critical time length (at least 10 years), the varying relation (positive or negative) between global temperature and atmospheric CO_2 has been indicated in the lower panels of the diagrams above.

Latest 20-year QC1 global monthly air temperature changes, updated to June 2020

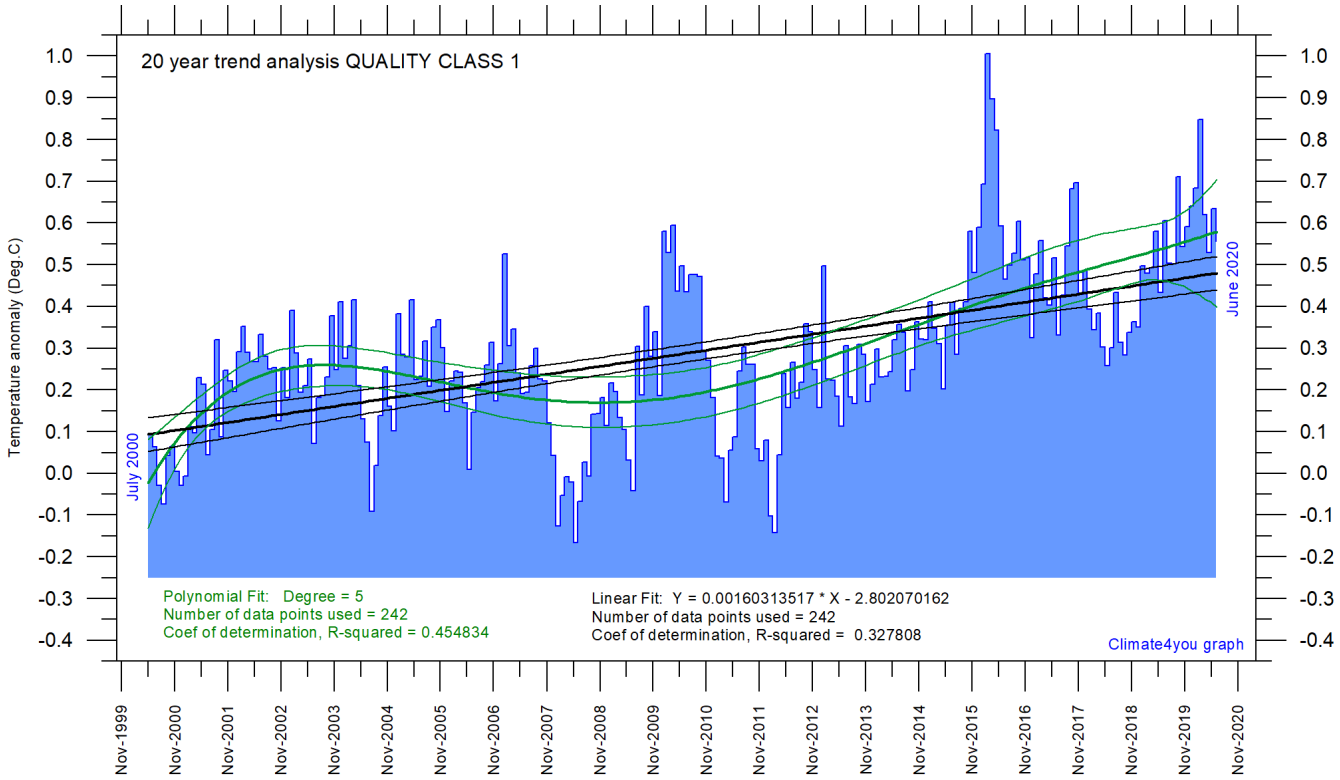

Last 20 years' global monthly average air temperature according to Quality Class 1 (UAH and RSS; see p.10) global monthly temperature estimates. The thin blue line represents the monthly values. The thick black line is the linear fit, with 95% confidence intervals indicated by the two thin black lines. The thick green line represents a 5-degree polynomial fit, with 95% confidence intervals indicated by the two thin green lines. A few key statistics are given in the lower part of the diagram (please note that the linear trend is the monthly trend).

In the enduring scientific climate debate, the following question is often put forward: Is the surface air temperature still increasing or has it basically remained without significant changes during the last 15-16 years?

The diagram above may be useful in this context and demonstrates the differences between two often used statistical approaches to determine recent temperature trends. Please also note that such fits only attempt to describe the past, and usually have small, if any, predictive power.

In addition, before using any linear trend (or other) analysis of time series a proper statistical model should be chosen, based on statistical justification.

For temperature time series, there is no *a priori* physical reason why the long-term trend should be linear in time. In fact, climatic time series often have trends for which a straight line is not a good approximation, as is clearly demonstrated by several of the diagrams shown in the present report.

For an excellent description of problems often encountered by analyses of temperature time series analyses, please see Keenan, D.J. 2014: Statistical Analyses of Surface Temperatures in the IPCC Fifth Assessment Report.

See also diagrams on page 11.

Sunspot activity and QC1 average satellite global air temperature, updated to June 2020

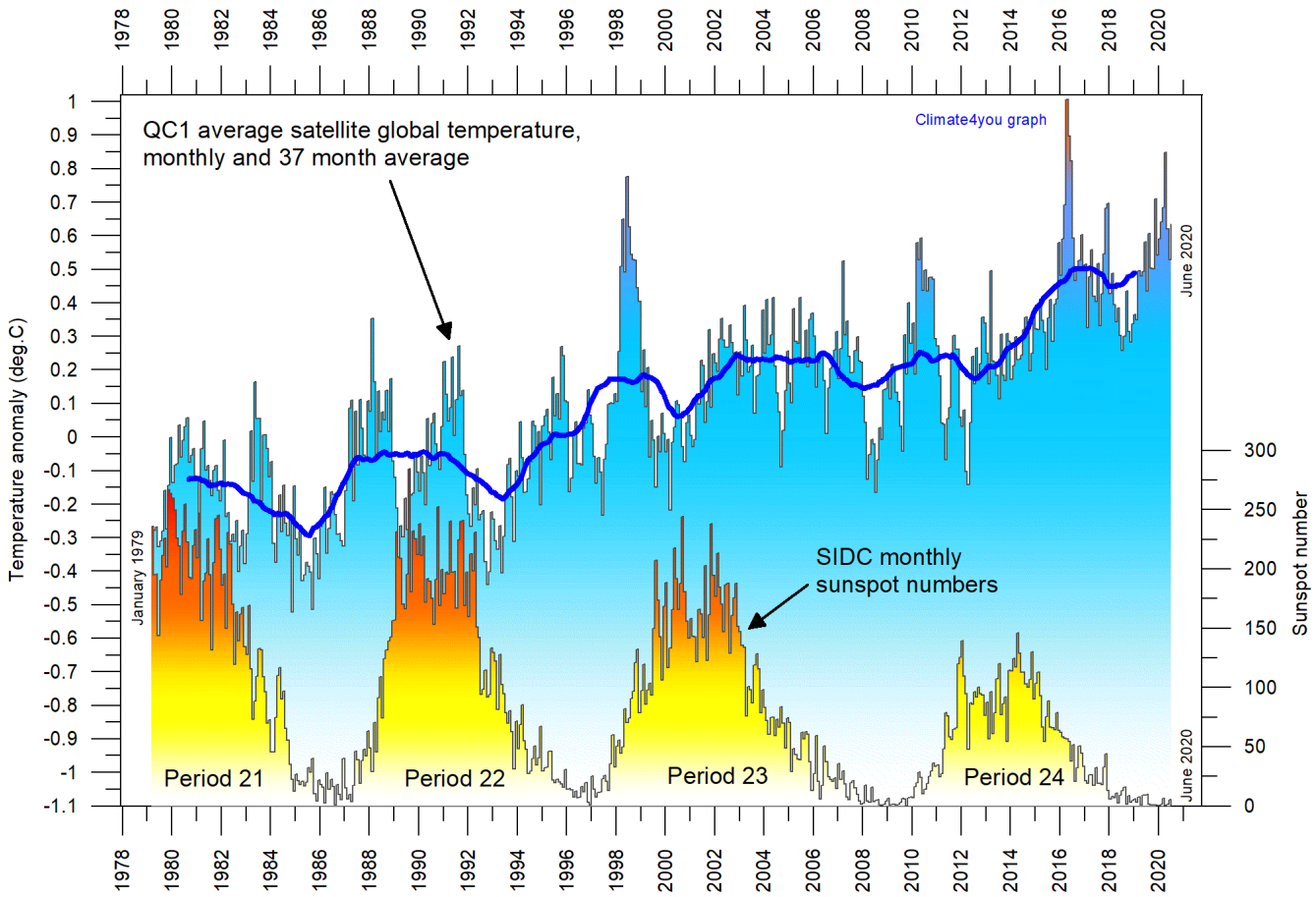

Variation of global monthly air temperature according to Quality Class 1 (UAH and RSS; see p.4) and observed sunspot number as provided by the Solar Influences Data Analysis Center (SIDC), since 1979. The thin lines represent the monthly values, while the thick line is the simple running 37-month average, nearly corresponding to a running 3-year average. The asymmetrical temperature 'bump' around 1998 is influenced by the oceanographic El Niño phenomenon in 1998, as is the case also for 2015-16. Temperatures in year 2019 was influenced by a moderate El Niño.

1959: Freighter-passenger liner "Hans Hedtoft" lost on her maiden voyage

MS Hans Hedtoft (2,857 brt) in West Greenland on her maiden voyage, shortly before setting out on the return voyage to Denmark.

On January 30, 1959, the new Danish combined freighter-passenger liner "Hans Hedtoft" was lost én route from Qaqortoq (Julianehåb), Greenland, to Copenhagen, Denmark. Besides the 40 crew members, there were 55 passengers aboard Hans Hedtoft; none of the 95 persons survived. Hans Hedtoft was on her maiden voyage and was said to be "unsinkable" due to its extraordinarily strong design, and several watertight compartments, much like what was said about the Titanic in 1912.

Hans Hedtoft was a diesel-engine ship (2,857 brt), specially designed for the Danish government to handle winter storms and sea ice in the North Atlantic Ocean near the southern tip of Greenland. She had a double steel bottom, an armored bow and stern, and was divided into seven watertight compartments, able to survive if one of these became flooded. She carried the most modern instrumentation, from radar to gyro, from Decca Navigator to radio-equipped life rafts. In addition, she was under command of the highly experienced Captain P. L. Rasmussen, who after the sea trials declared: "*This ship means a revolution in Arctic navigation*."

On 7. January 1959, the Hans Hedtoft left Copenhagen on her maiden voyage to Greenland. She arrived uneventfully at Qaqortoq in SW Greenland one week later, an unseen rapid voyage from Copenhagen to Greenland. From there she proceeded up along the west coast of Greenland, visiting Nuuk, capital of Greenland, Sisimiut and Maniitsoq. A few days later she put to sea again bound for Qaqortoq in SW Greenland. The return journey across the North Atlantic to Denmark, began on 29. January in the evening at hr. 21:15, local time. On board Hans Hedtoft were 95 persons,

including six children. Augo Lynge, one of Greenland's two Representatives in the Danish Parliament was also on board on this voyage.

Rounding Cape Farewell, the southernmost tip of Greenland in the morning of 30. January 1959, Hans Hedtoft was hit by a storm with high waves, below freezing temperatures, blizzard, and bad visibility. Following the relatively warm period in Greenland 1925-1947, in 1959 air temperatures were again declining in the Greenland region, and sea ice and icebergs was spreading further south than considered normal during the previous years.

At 13:56 Hans Hedtoft radioed weakly (by morse code) an SOS: "*Collision with iceberg*", accompanied by the ships position (59°.5 N 43° W.), about 40 km south of Cape Farwell. The collision with the iceberg must have been forceful, as Hans Hedtofts main radio antenna initially was damaged, when the emergency antenna collapsed on the main antenna by the impact and first had to be removed to reestablish clear radio communication.

Less than one hour after the first distress call came the next message from Hans Hedtoft, reporting that the engine room was filling fast from a gash in the riveted steel hull. At 15:36 came another radio message from the Hedtoft: "*Slowly sinking and in need of immediate assistance*". All electrical power (and light) was now lost on Hans Hedtoft, as the engine room and the emergency generator were completely flooded. At 17:41 the following message from Hans Hedtoft was received: "*We are slowly sinking*", and at 17:50 the final message "*we are sinking now*" was heard. At 18:06 the beginning of "*SOS*" was heard followed by a couple of radio bearing signals, but the transmission was interrupted, and no further communication was ever received from Hans Hedtoft. Most likely, Hans Hedtoft went down at this time.

A West German ocean-going trawler, the Johannes Krüss (photo next page; commanded by Kapitän Albert Sierck), and the U.S. Coast Guard cutter Campbell both were in the area near Hans Hedtoft and almost immediately turned toward Hans Hedtoft's reported position after the initial distress call at 13:56. Johannes Krüss was about 50 km southeast of Hans Hedtoft's reported position. At that time GPS was not available, and a position on sea had to be determined by other means, including radio bearing.

After the sinking of Hans Hedtoft, there remained some doubt about the real position of both Hans Hedtoft and Johannes Krüss on the tragic day in January 1959. This is demonstrated by the steering of Johannes Krüss during her rescue attempt. Following the initial distress call, Johannes Krüss from 14:18 steamed towards NW, in direction of the assumed position of Hans Hedtoft. However, at 15:04 a radio bearing made towards Hans Hedtoft prompted the skipper of Johannes Krüss to make a 90^{o} backboard turn, towards SW. This demonstrates that at least one of the two ships initial position must have been wrong, and potentially both.

However, due to the high waves, floating ice, dwindling daylight, blizzard, and generally extremely poor visibility Johannes Krüss were unable to find Hans Hedtoft before she went down. Presumably, Johannes Krüss made it to the position of Hans Hedtoft short time after her sinking, after navigating gallantly in the ice-filled stormy and dangerous waters, in blizzard, with little or no daylight. At least, the two skippers over radio had been discussing how best to transfer passengers and crew from Hans Hedtoft to Johannes Krüss. Seemingly, Hans Hedtoft was visible on the radar of Johannes Krüss shortly before she arrived at Hans Hedtofts final position. However, in the extremely difficult conditions Johannes Krüss was unable to find any survivors or wreckage from Hans Hedtoft. It also remains a possibility, that Johannes Krüss passed Hans Hedtoft in the darkness and blizzard before 18:06, without the two ships observing each other.

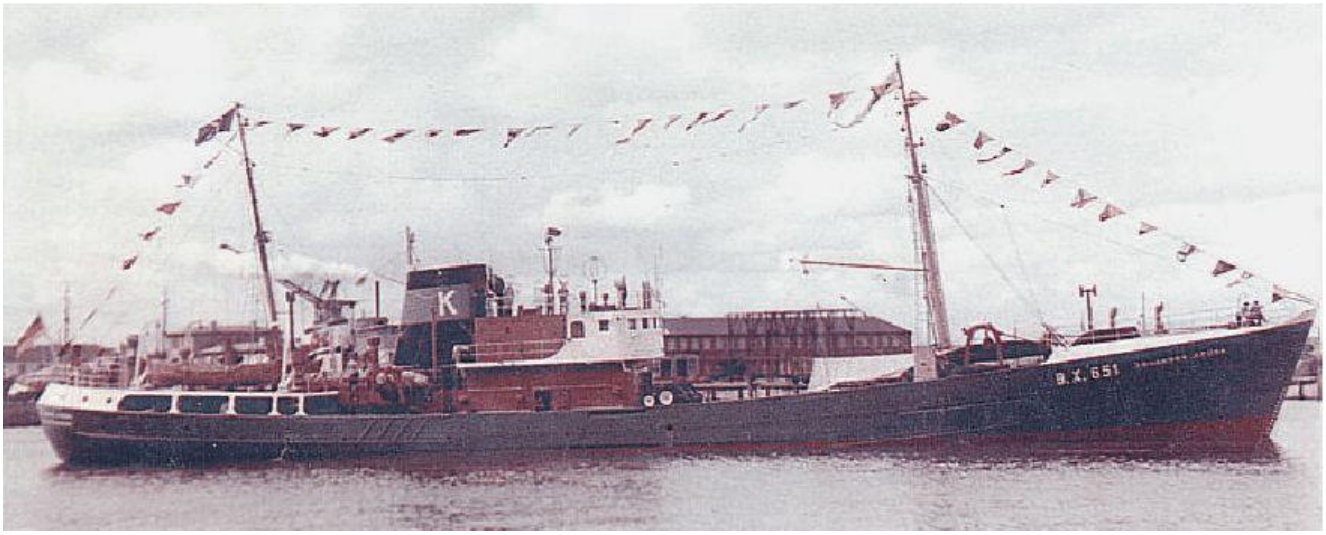

The German 60.4 m long ocean-going trawler Johannes Krüss in 1956, setting out for sea trials before her maiden voyage.

The only item ever recovered from Hans Hedtoft was a life belt that was washed ashore on the coast of Iceland, 9 months after the ship was lost. Evidently, and somewhat peculiar, all lifeboats and -rafts went down with Hans Hedtoft, and were apparently not released before the sinking.

It is conceivable, that the stormy weather with icing and darkness to the crew and passengers on Hans Hedtoft made it pointless or impossible to attempt leaving the ship in the lifeboats and life rafts. Also, any attempt of transporting people from Hans Hedtoft to Johannes Krüss would probably have been extremely difficult, should the two ships have found each other in the darkness. But clearly, an attempt would have been made.

Eight years later, in early March 1967, the trawler Johannes Krüss was itself lost in the same waters as Hans Hedtoft. The ship simply disappeared with its entire crew of 22, after last being having radio contact on 28 February, from a position about 450 km east of Cape Farewell, Greenland's southern tip. At that time, the wind strength was 10 on the Beaufort scale, and the air temperature -22°C.

Most likely the loss of Johannes Krüss was caused by a collision with an iceberg or an ice floe, or perhaps rapid icing leading to capsizing; at least something suddenly happened with the ship, preventing any distress call being made.

In 1967, when Johannes Krüss was lost, the cooling beginning around 1947 was even more pronounced, and sea ice conditions in the North Atlantic known to be more difficult than in 1959.

References:

Rockwell, T. 2013. *I de bedste hænder - Historien om MS Hans Hedtofts forlis*. Lindhardt og Ringhof, København, ISBN: 9788711357118.

Politiken 1999. Katastrofen ved Kap Farvel. Danish Newspaper 'Politiken', 24. January 1999. http://www.hanshedtoft.dk/04 Diverse/Medier/1401_001.pdf

*****

All diagrams in this report, along with any supplementary information, including links to data sources and previous issues of this newsletter, are freely available for download on www.climate4you.com

Yours sincerely,

Ole Humlum (Ole.Humlum@gmail.com)

Arctic Historical Evaluation and Research Organisation, Longyearbyen, Svalbard

20 July 2020.